

June 17, 2004

Higgs Dilepton Group Meeting

$h \rightarrow \gamma\gamma$ Update

Alex Melnitchouk
University of Mississippi

fake rates start here

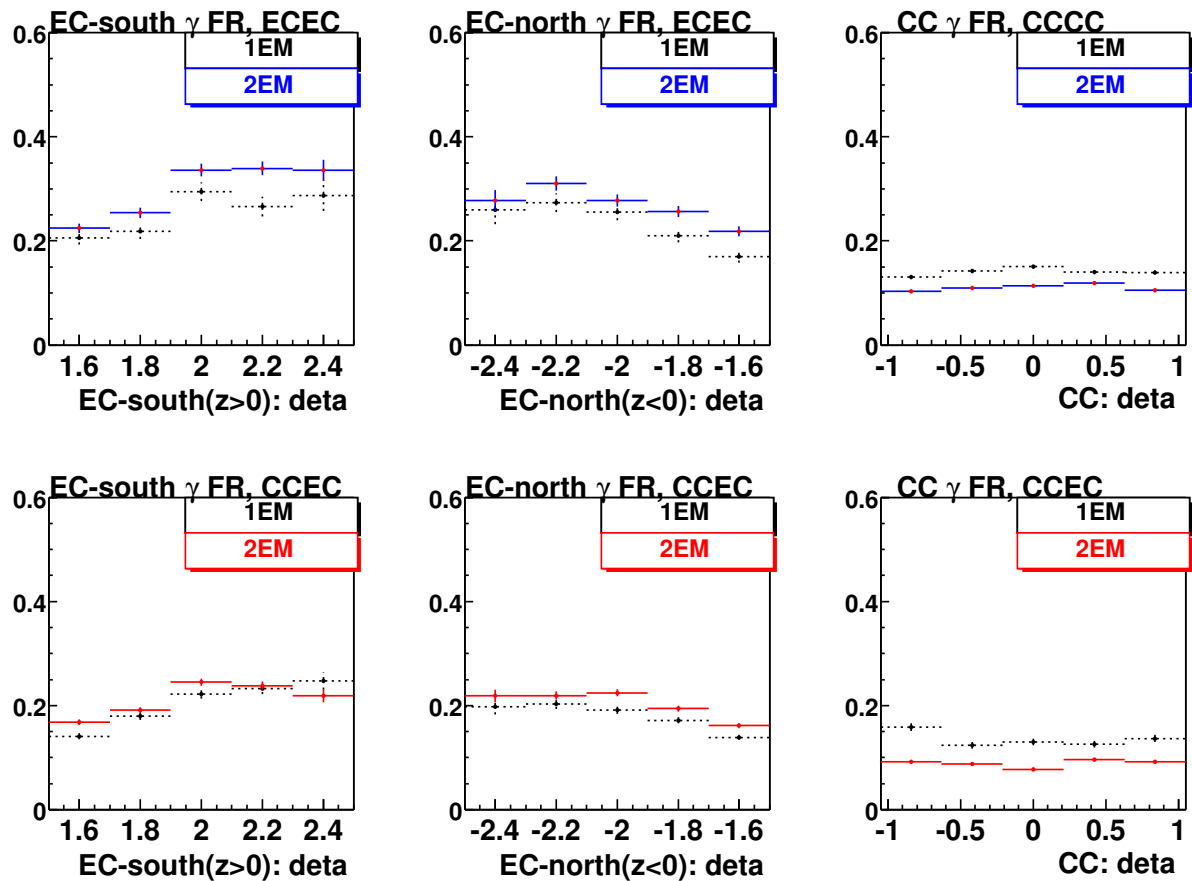


Figure 1: Photon fake rates. Tight track match is used in photon definition. More needs to be said.

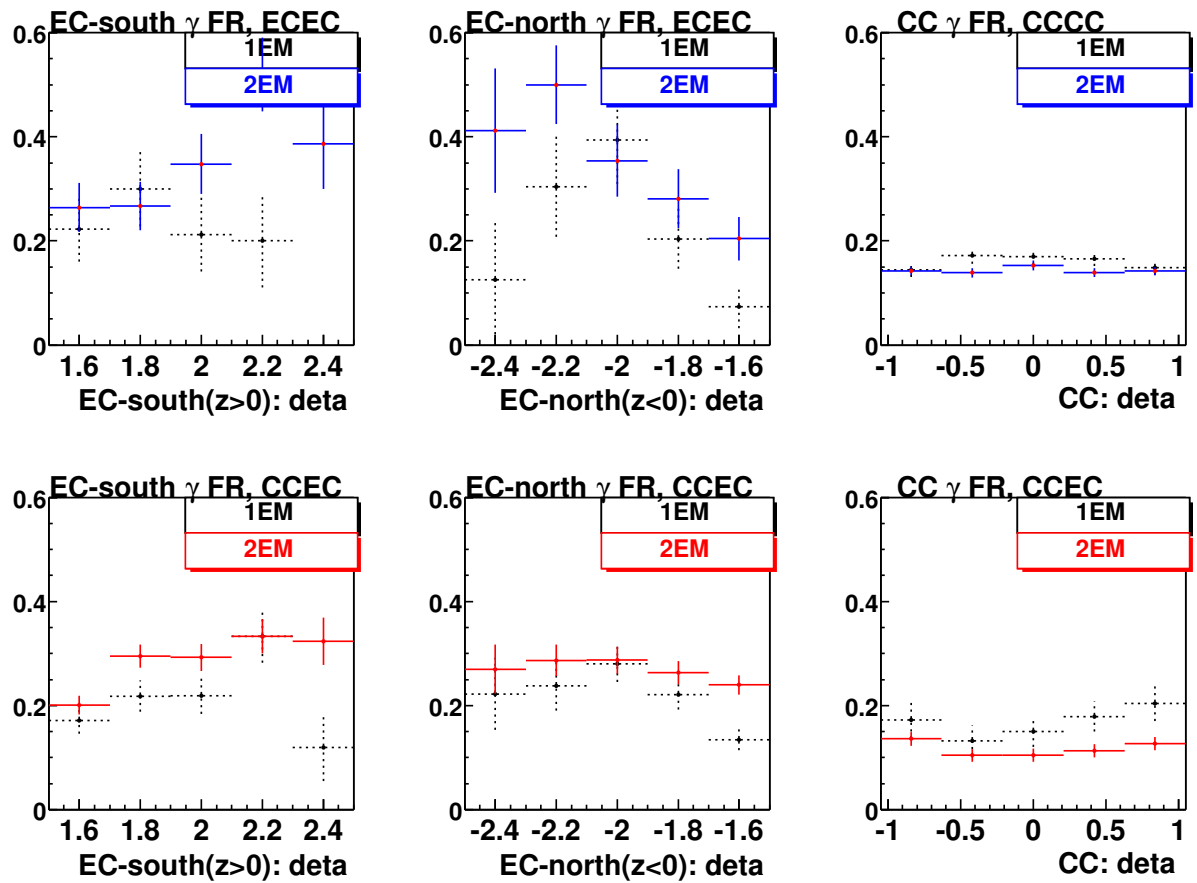


Figure 2: Photon fake rates after for $p_T^{\gamma\gamma} > 35$ GeV. Tight track match is used in photon definition. More needs to be said.

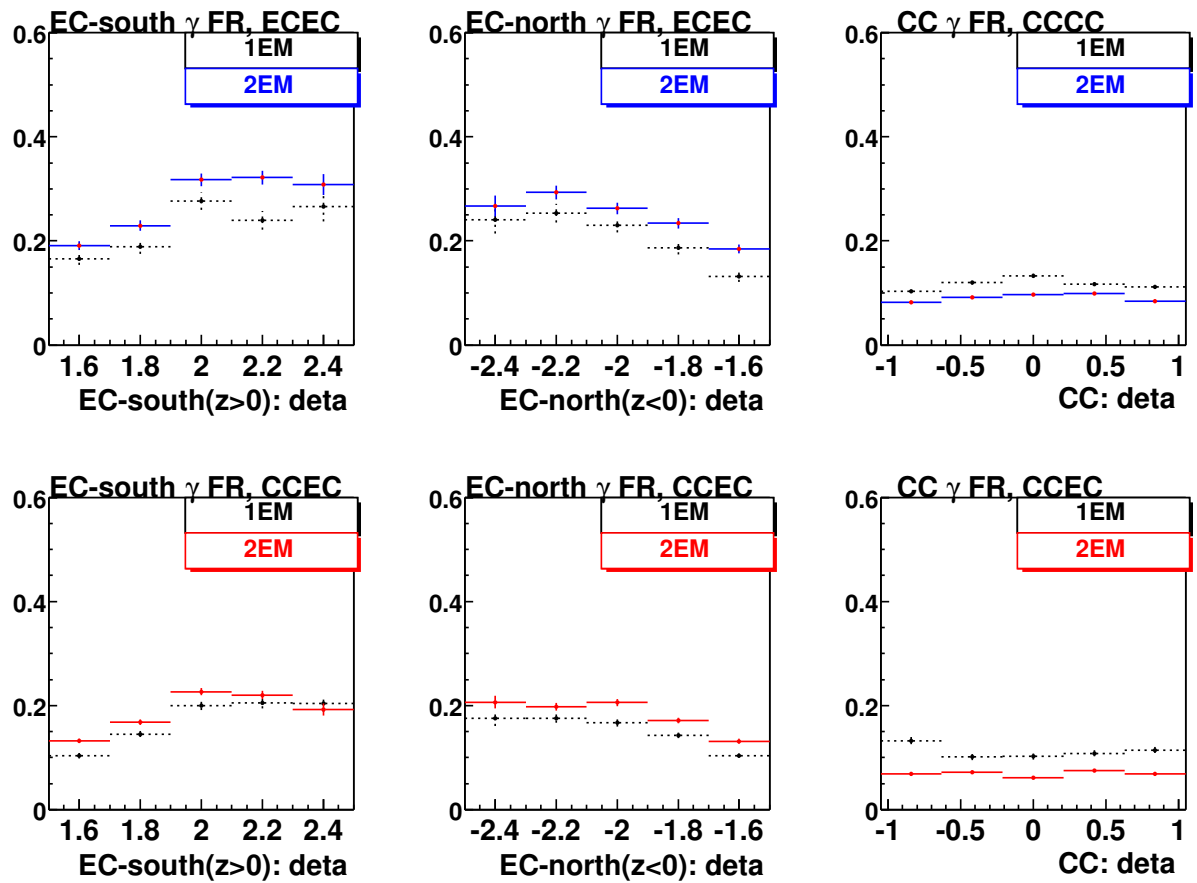


Figure 3: Photon fake rates. Tight track match is used in photon definition. More needs to be said.

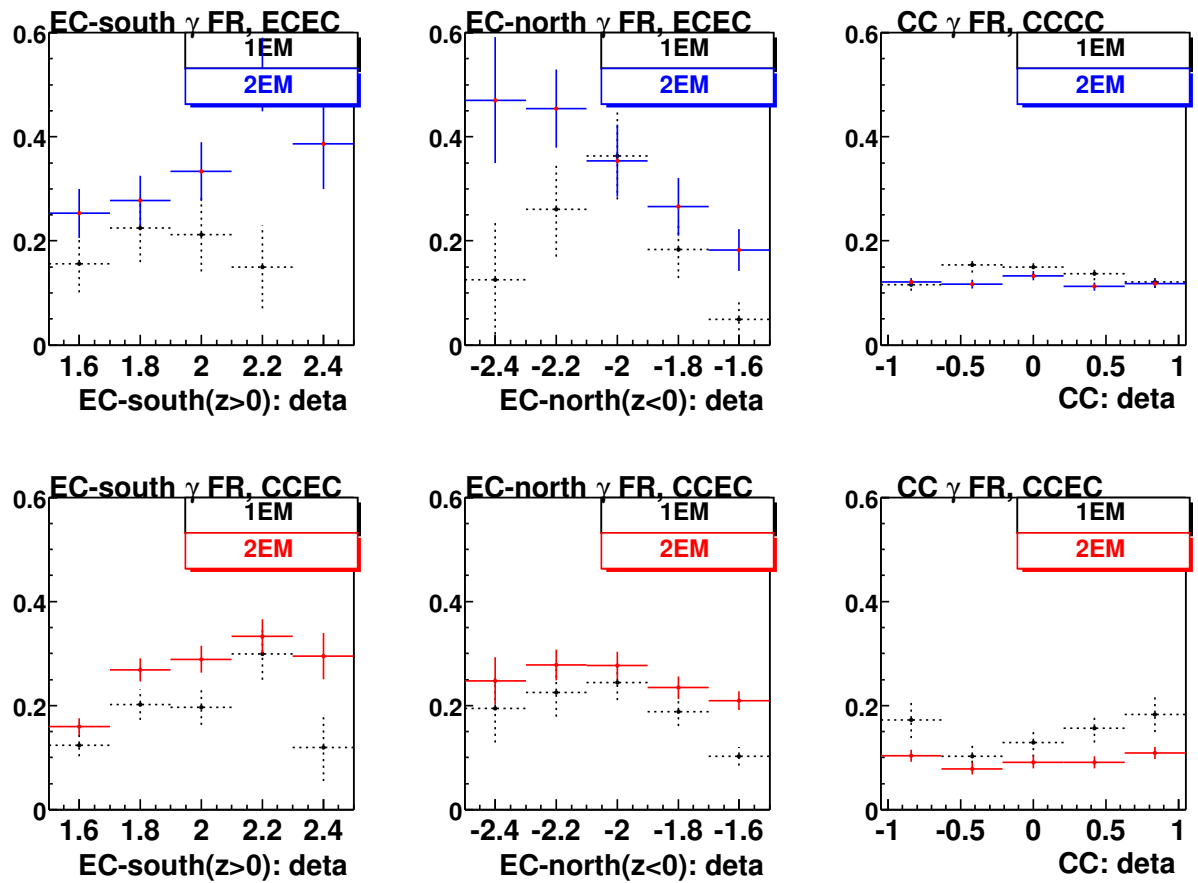
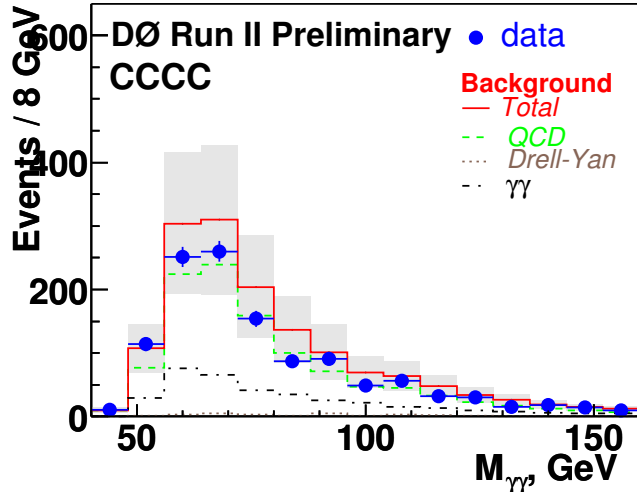
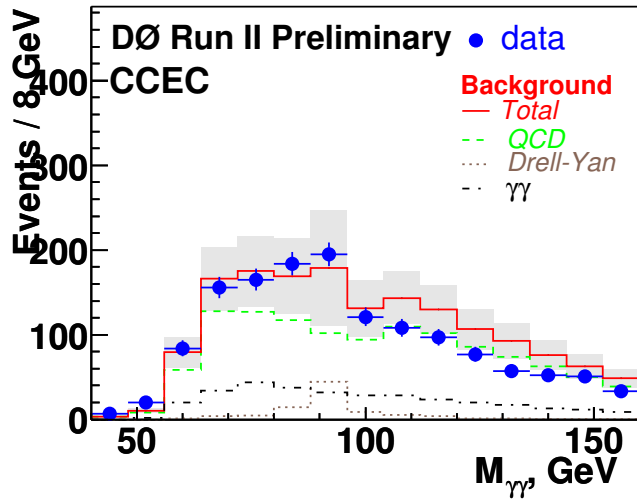


Figure 4: Photon fake rates after for $p_T^{\gamma\gamma} > 35$ GeV. Tight track match is used in photon definition. More needs to be said.

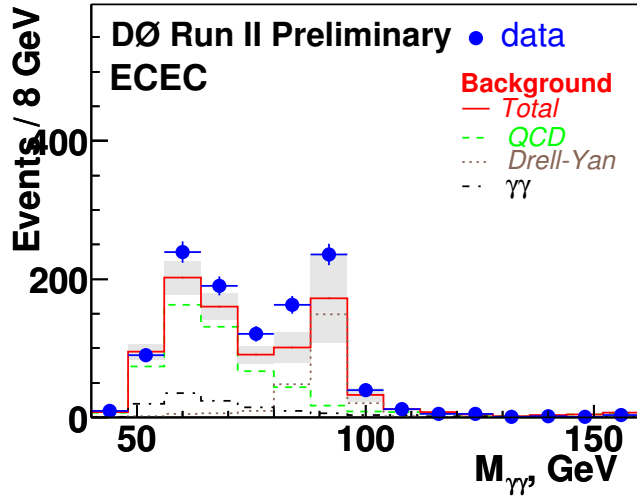
mass distributions, other variables (and comparisons with Higgs) start here



data = 1192.0
bkgd = 1462.6 +- 544.1
QCD = 1075.2 +- 532.4
DY = 28.3 +- 27.9
gamma-gamma = 359.1 +- 108.8

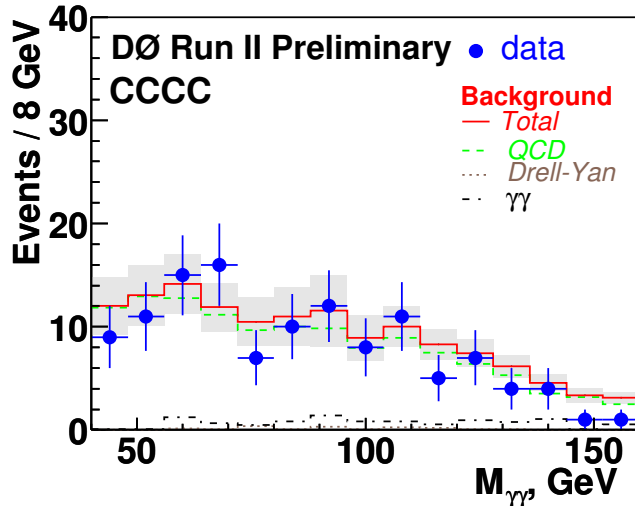


data = 1407.0
bkgd = 1574.1 +- 369.8
QCD = 1162.3 +- 345.3
DY = 91.1 +- 97.5
gamma-gamma = 320.6 +- 89.1

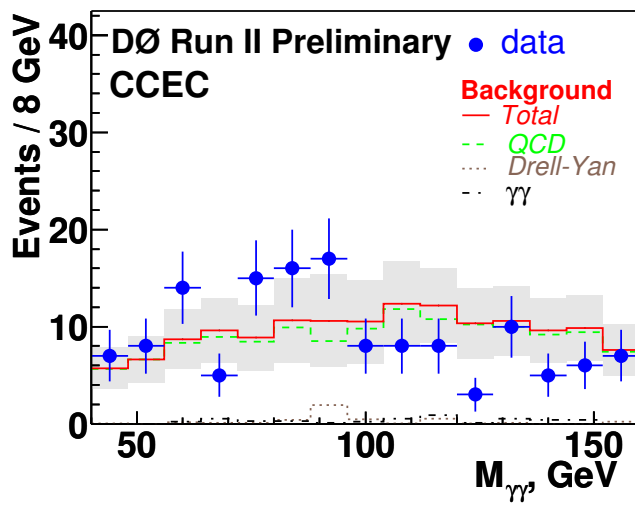


data = 1116.0
bkgd = 900.9 +- 135.5
QCD = 537.0 +- 87.6
DY = 243.2 +- 98.7
gamma-gamma = 120.7 +- 30.6

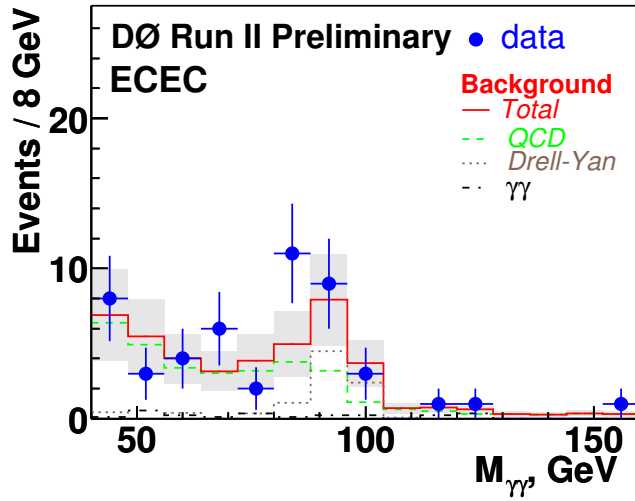
Figure 5: Distributions of the $\gamma\gamma$ invariant mass and event yields for different event topologies. Points – $\gamma\gamma$ spectrum observed in data, solid (red) line – total SM background with systematic errors shown with gray rectangles, dashed (green) line – QCD background, dotted (brown) line – Drell-Yan background, dot-dashed (black) line – direct diphoton background.



data = 121.0
bkgd = 136.0 +/- 28.3
QCD = 123.5 +/- 28.1
DY = 2.0 +/- 1.9
 $\gamma\gamma = 10.6 +/- 3.2$



data = 137.0
bkgd = 143.9 +/- 50.8
QCD = 135.1 +/- 50.6
DY = 4.3 +/- 4.3
 $\gamma\gamma = 4.5 +/- 1.3$



data = 49.0
bkgd = 43.3 +/- 16.0
QCD = 31.7 +/- 15.5
DY = 9.2 +/- 4.1
 $\gamma\gamma = 2.4 +/- 0.6$

Figure 6: Distributions of the $\gamma\gamma$ invariant mass and event yields for different event topologies after analysis optimization cut ($p_T^{\gamma\gamma} > 35$ GeV) is applied. Points – $\gamma\gamma$ spectrum observed in data, solid (red) line – total SM background with systematic errors shown with gray rectangles, dashed (green) line – QCD background, dotted (brown) line – Drell-Yan background, dot-dashed (black) line – direct diphoton background.

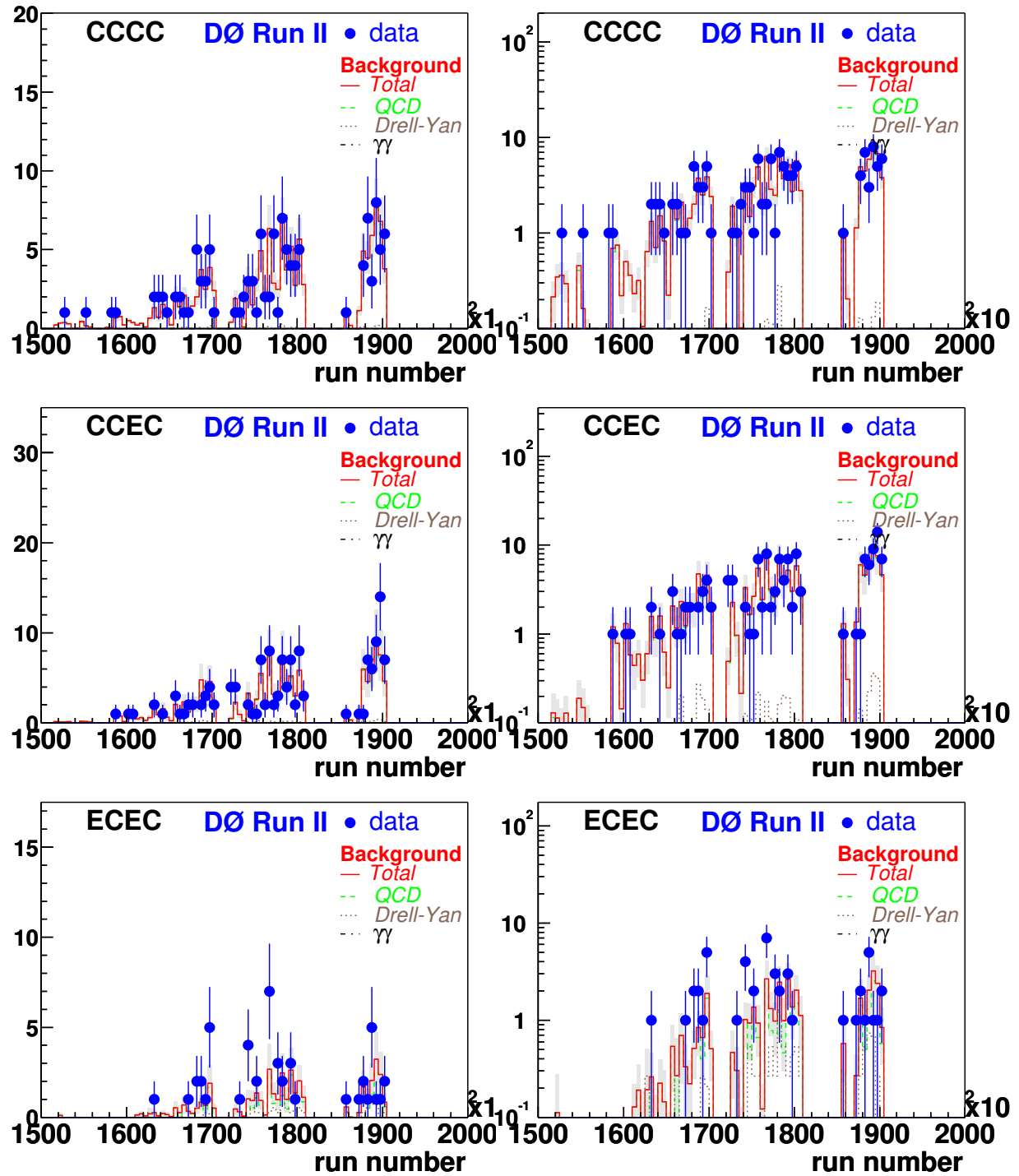


Figure 7: Run number distributions for data and estimated background. Left: linear scale. Right: logarithmic scale. Points – data, solid (red) line – total SM background with systematic errors shown with gray rectangles, dashed (green) line – QCD background, dotted (brown) line – Drell-Yan background, dot-dashed (black) line – direct diphoton background.

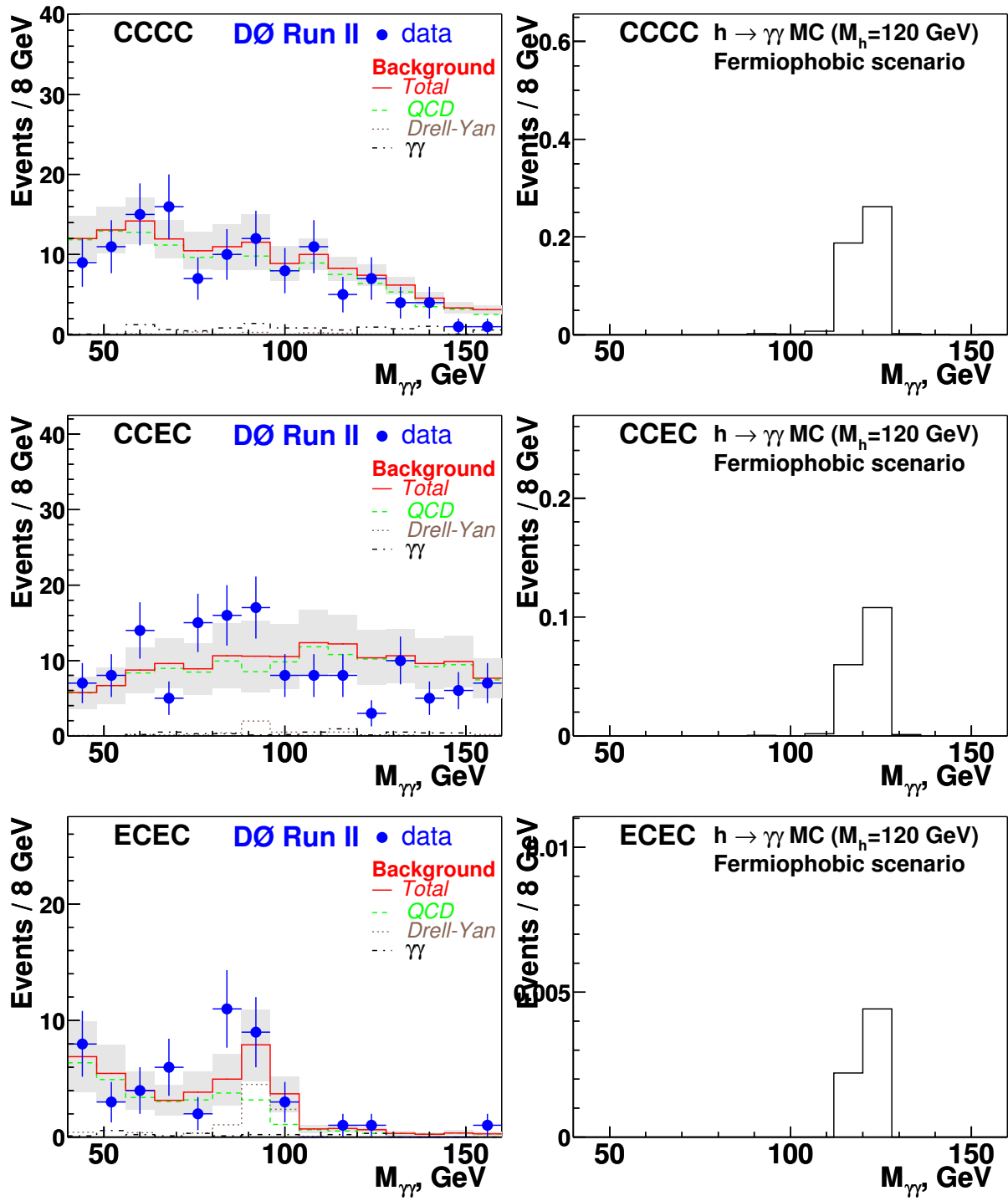


Figure 8: $\gamma\gamma$ invariant mass distributions. Left: data and estimated background, points – data, solid (red) line – total SM background with systematic errors shown with gray rectangles, dashed (green) line – QCD background, dotted (brown) line – Drell-Yan background, dot-dashed (black) line – direct diphoton background. Right: 120 GeV Fermiophobic Higgs (vertical scale corresponds to the number of expected $h \rightarrow \gamma\gamma$ events for $\approx 270 \text{ pb}^{-1}$)

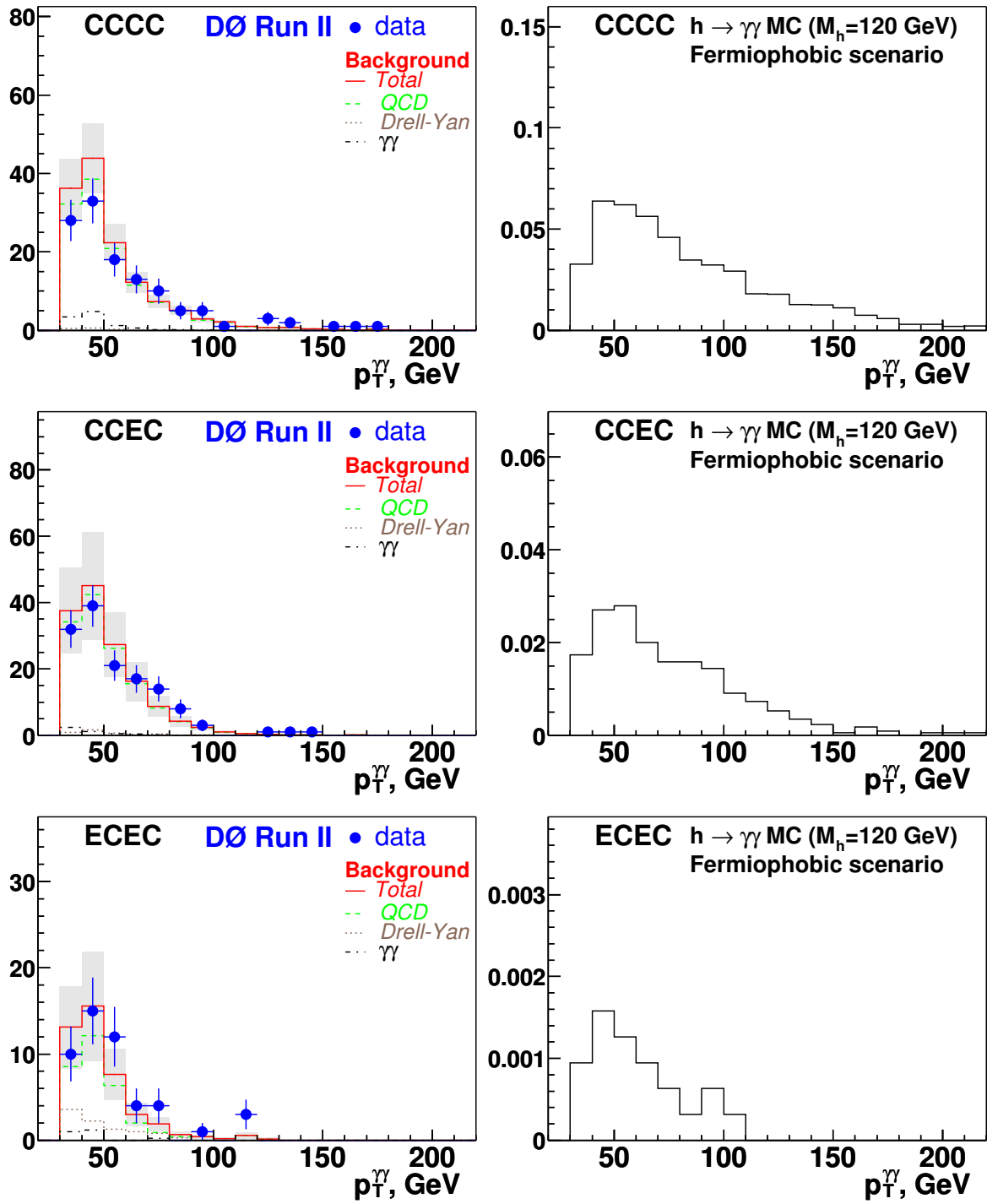


Figure 9: $p_T^{\gamma\gamma}$ distributions (linear scale). Left: data and estimated background, points – data, solid (red) line – total SM background with systematic errors shown with gray rectangles, dashed (green) line – QCD background, dotted (brown) line – Drell-Yan background, dot-dashed (black) line – direct diphoton background. Right: 120 GeV Fermiophobic Higgs (vertical scale corresponds to the number of expected $h \rightarrow \gamma\gamma$ events for $\approx 270 \text{ pb}^{-1}$)

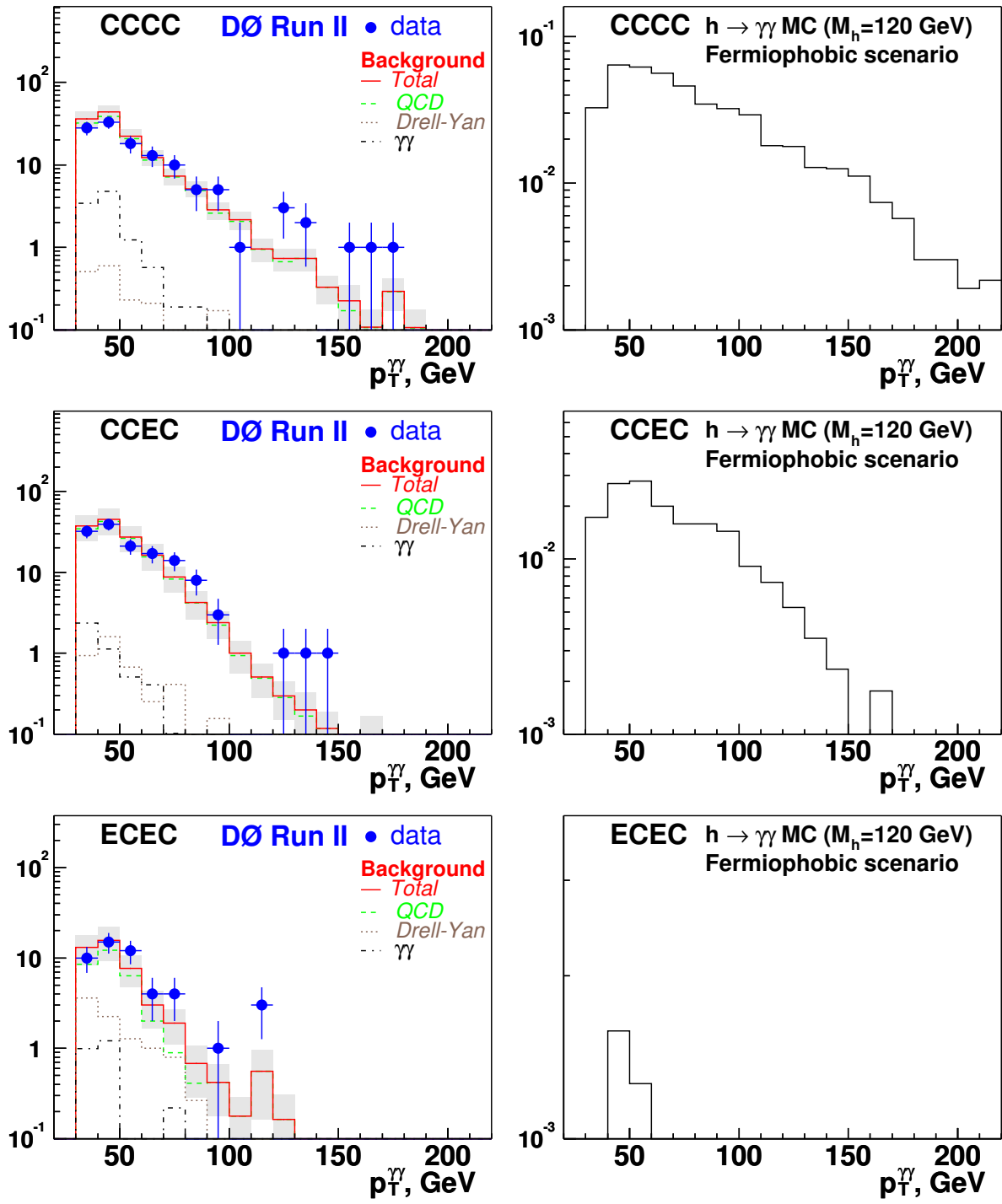


Figure 10: $p_T^{\gamma\gamma}$ distributions (logarithmic scale). Left: data and estimated background, points – data, solid (red) line – total SM background with systematic errors shown with gray rectangles, dashed (green) line – QCD background, dotted (brown) line – Drell-Yan background, dot-dashed (black) line – direct diphoton background. Right: 120 GeV Fermiophobic Higgs (vertical scale corresponds to the number of expected $h \rightarrow \gamma\gamma$ events for $\approx 270 \text{ pb}^{-1}$)

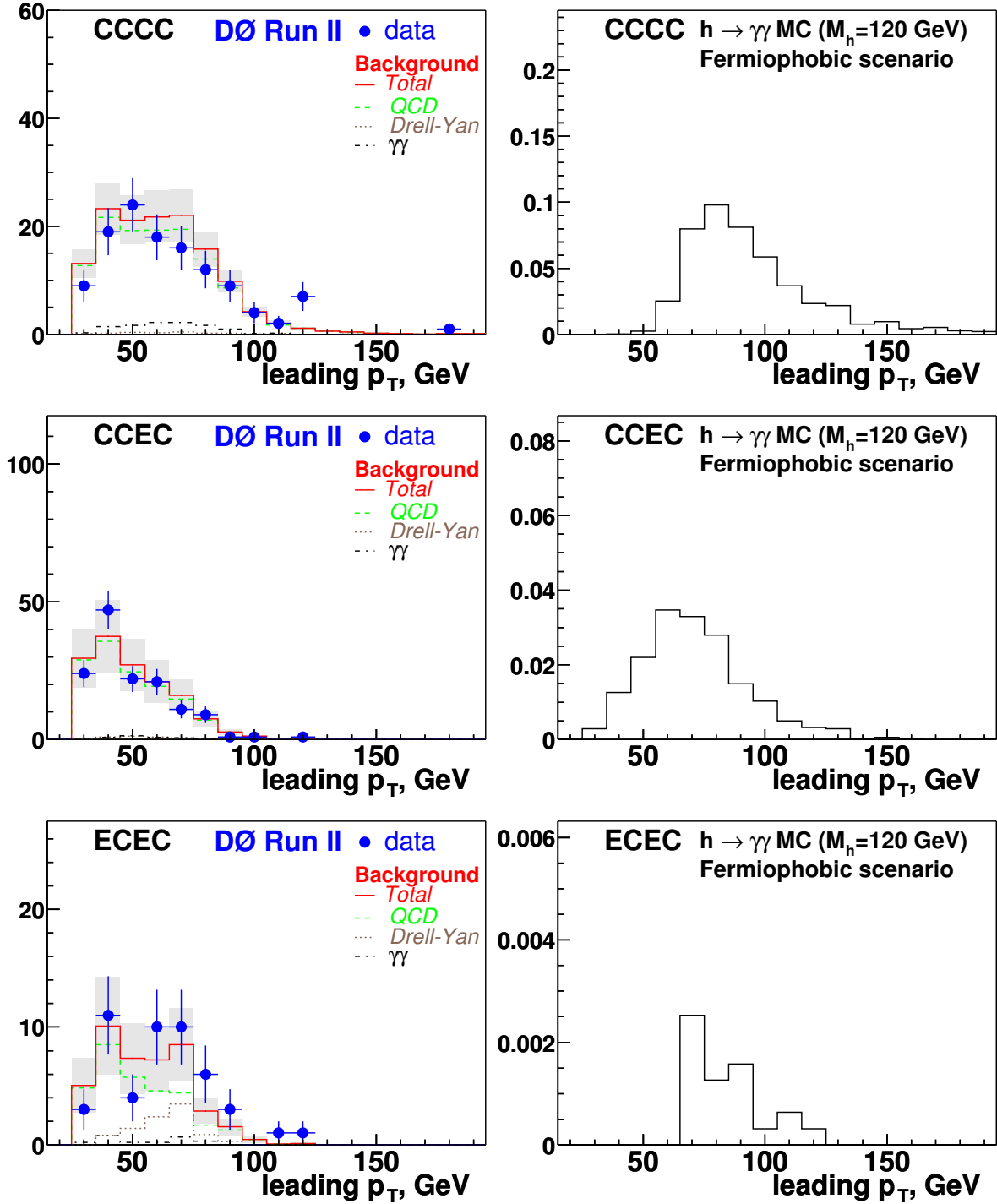


Figure 11: Leading photon p_T distributions (linear scale). Left: data and estimated background, points – data, solid (red) line – total SM background with systematic errors shown with gray rectangles, dashed (green) line – QCD background, dotted (brown) line – Drell-Yan background, dot-dashed (black) line – direct diphoton background. Right: 120 GeV Fermiophobic Higgs (vertical scale corresponds to the number of expected $h \rightarrow \gamma\gamma$ events for $\approx 270 \text{ pb}^{-1}$)

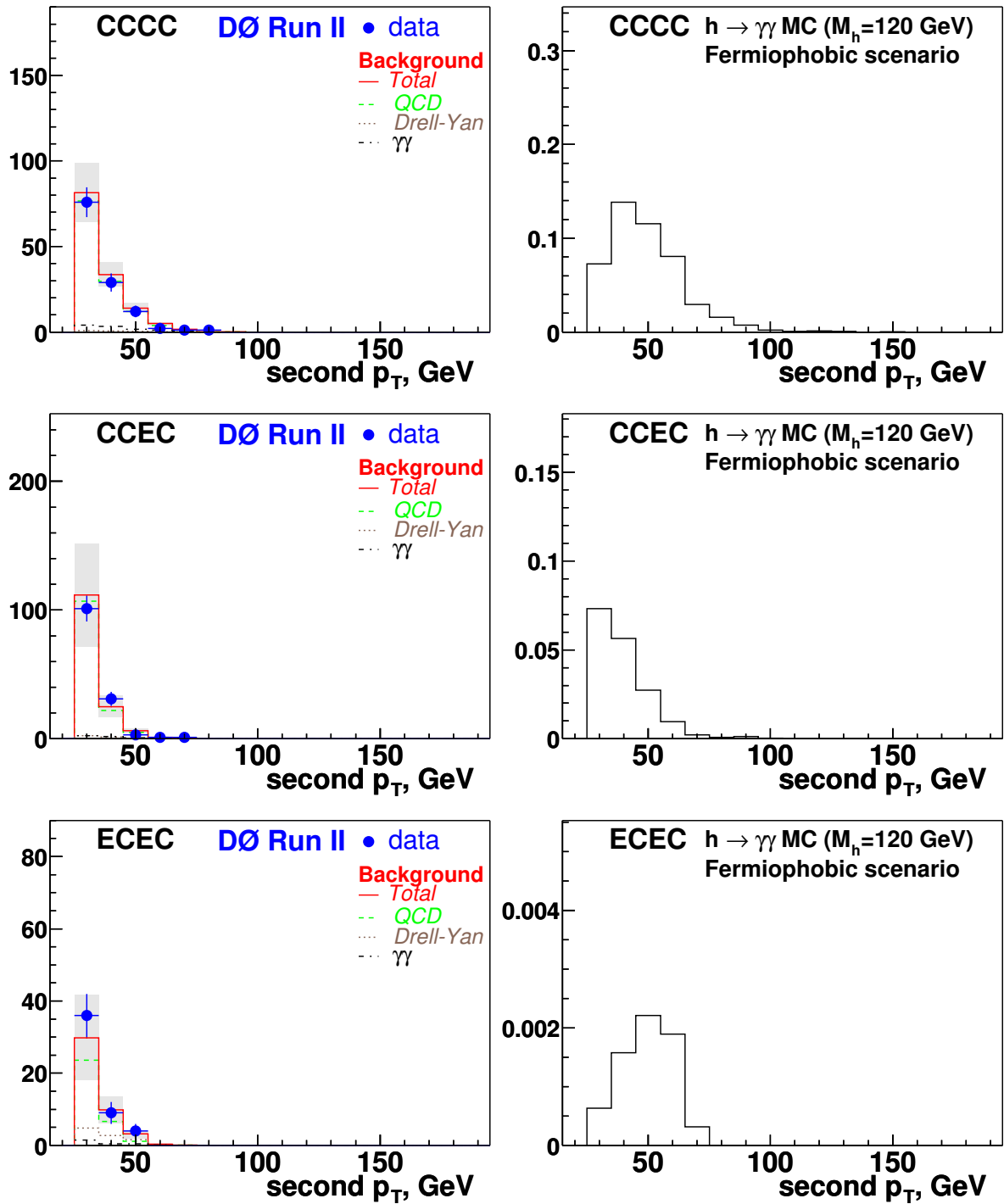


Figure 12: Second photon p_T distributions (linear scale). Left: data and estimated background, points – data, solid (red) line – total SM background with systematic errors shown with gray rectangles, dashed (green) line – QCD background, dotted (brown) line – Drell-Yan background, dot-dashed (black) line – direct diphoton background. Right: 120 GeV Fermiophobic Higgs (vertical scale corresponds to the number of expected $h \rightarrow \gamma\gamma$ events for $\approx 270 \text{ pb}^{-1}$)

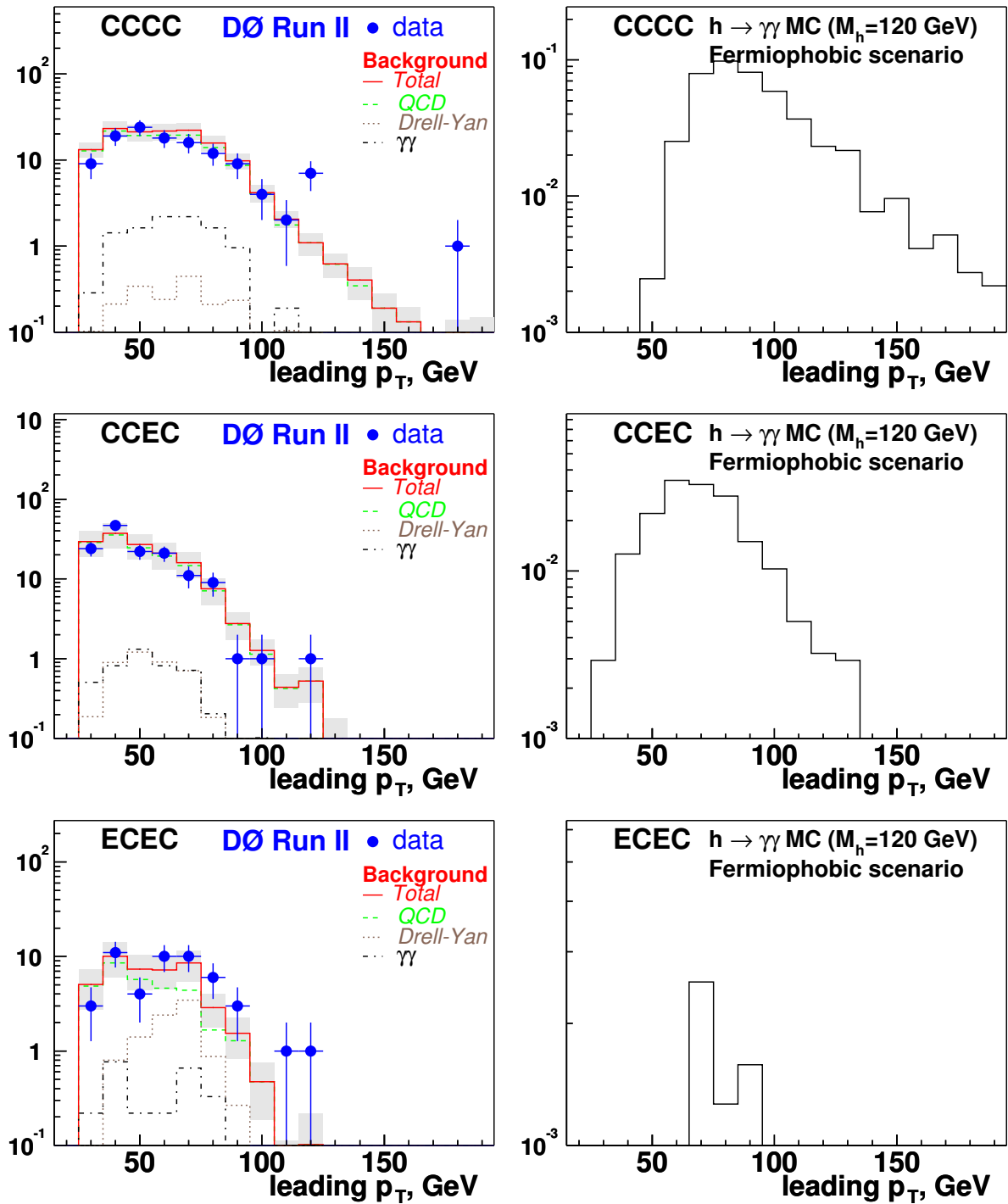


Figure 13: Leading photon p_T distributions (logarithmic scale). Left: data and estimated background, points – data, solid (red) line – total SM background with systematic errors shown with gray rectangles, dashed (green) line – QCD background, dotted (brown) line – Drell-Yan background, dot-dashed (black) line – direct diphoton background. Right: 120 GeV Fermiophobic Higgs (vertical scale corresponds to the number of expected $h \rightarrow \gamma\gamma$ events for $\approx 270 \text{ pb}^{-1}$)

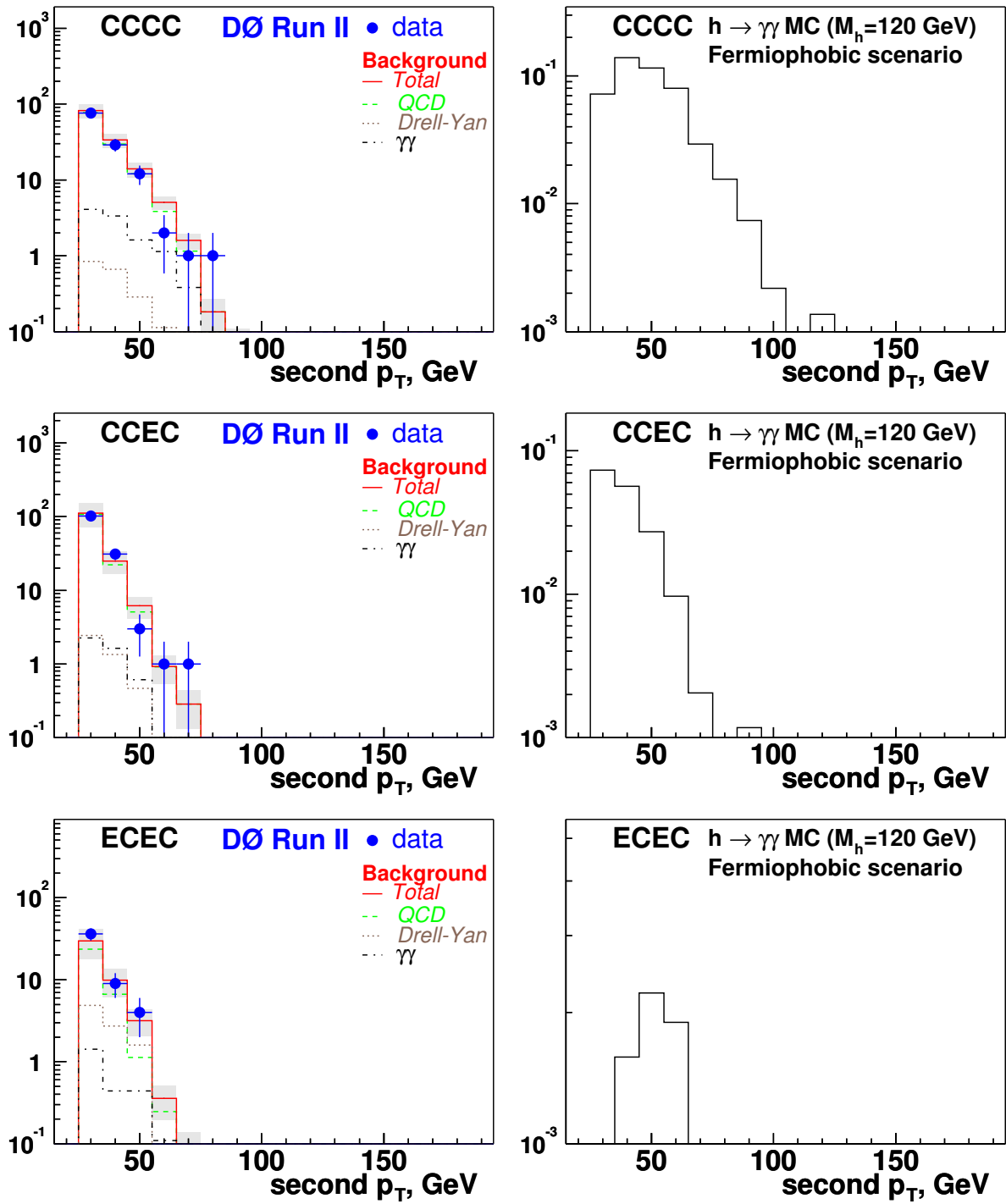


Figure 14: Second photon p_T distributions (logarithmic scale). Left: data and estimated background, points – data, solid (red) line – total SM background with systematic errors shown with gray rectangles, dashed (green) line – QCD background, dotted (brown) line – Drell-Yan background, dot-dashed (black) line – direct diphoton background. Right: 120 GeV Fermiophobic Higgs (vertical scale corresponds to the number of expected $h \rightarrow \gamma\gamma$ events for $\approx 270 \text{ pb}^{-1}$)

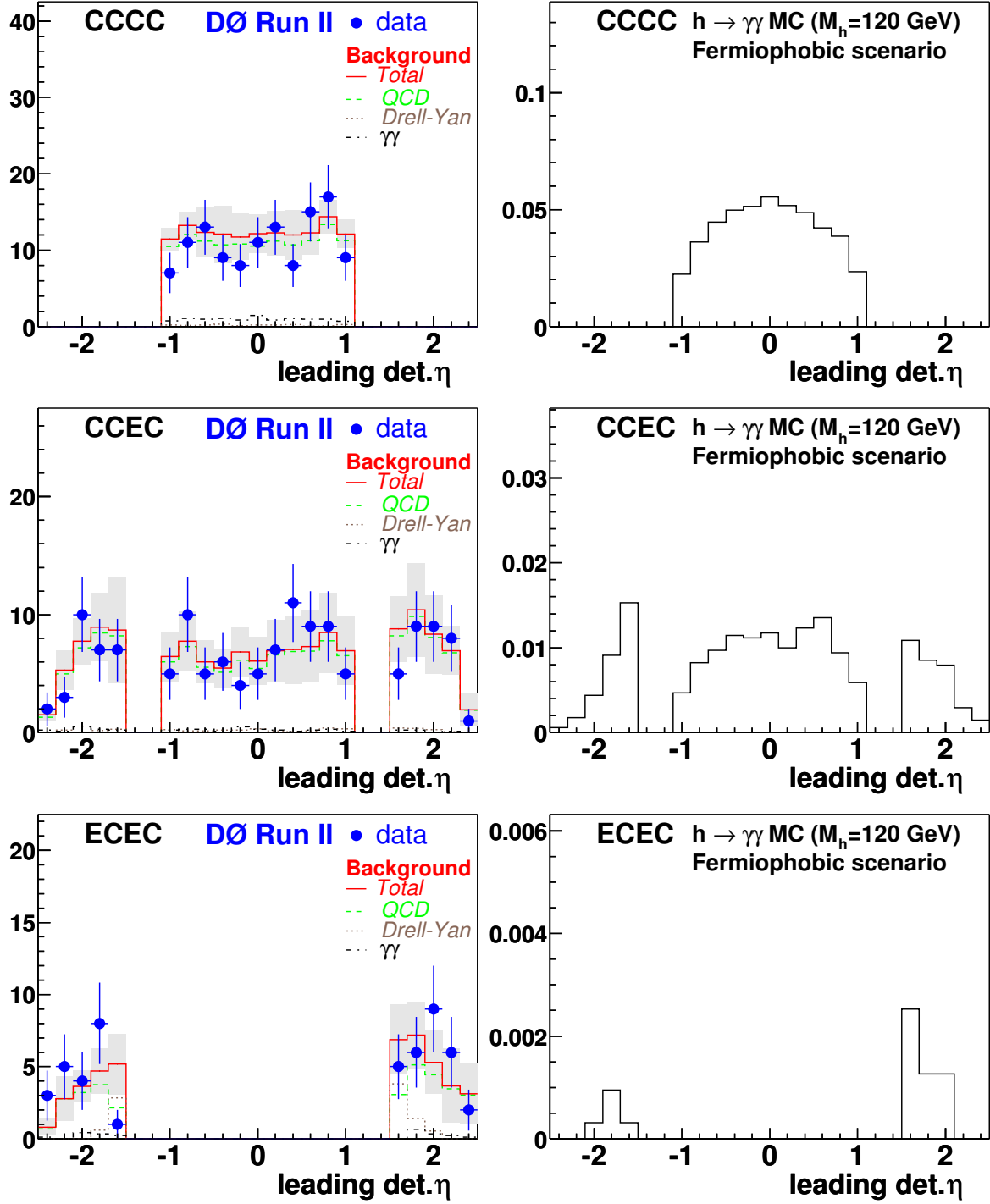


Figure 15: Leading photon detector η distributions. Left: data and estimated background, points – data, solid (red) line – total SM background with systematic errors shown with gray rectangles, dashed (green) line – QCD background, dotted (brown) line – Drell-Yan background, dot-dashed (black) line – direct diphoton background. Right: 120 GeV Fermiophobic Higgs (vertical scale corresponds to the number of expected $h \rightarrow \gamma\gamma$ events for $\approx 270 \text{ pb}^{-1}$)

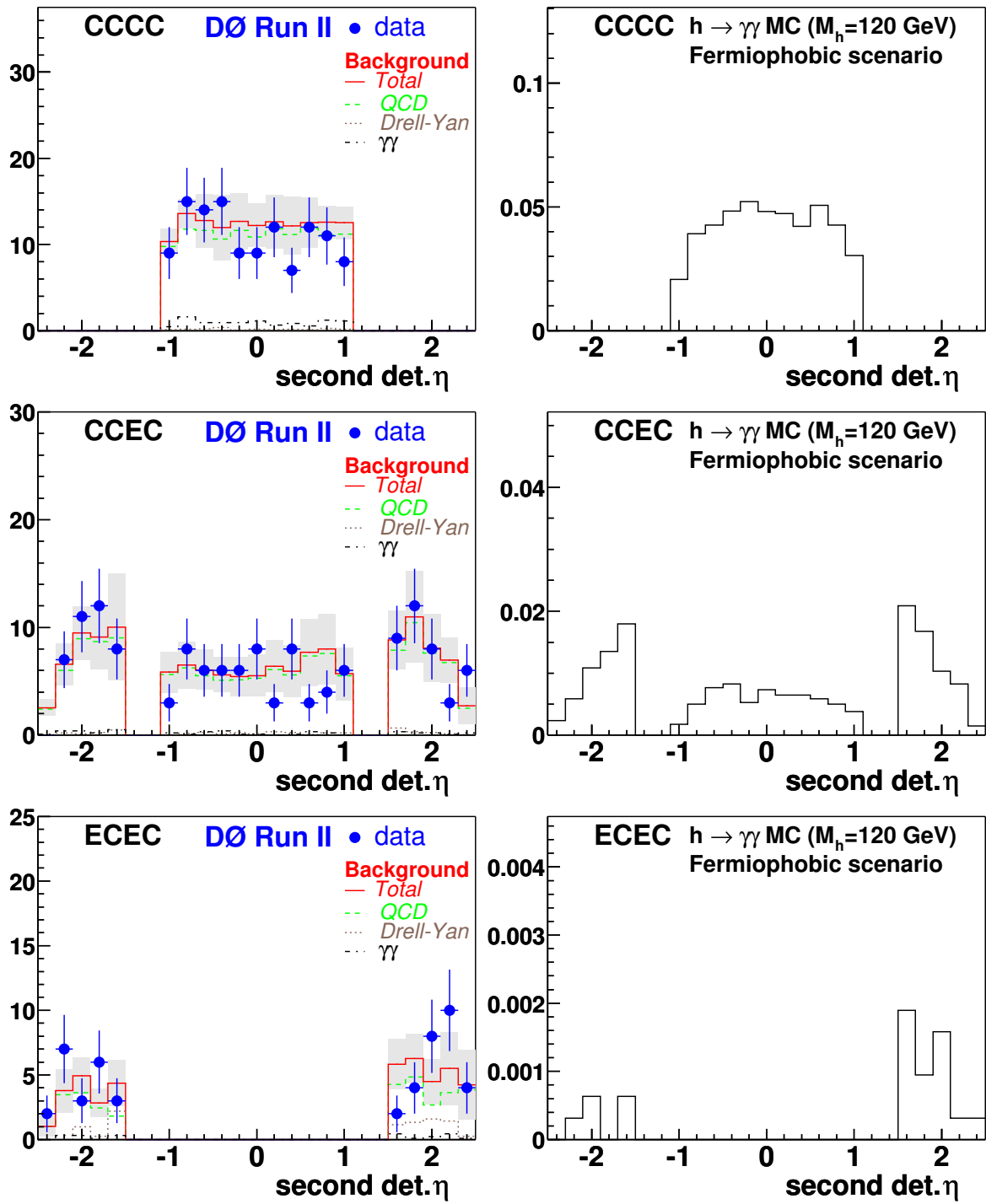


Figure 16: Second photon detector η distributions. Left: data and estimated background, points – data, solid (red) line – total SM background with systematic errors shown with gray rectangles, dashed (green) line – QCD background, dotted (brown) line – Drell-Yan background, dot-dashed (black) line – direct diphoton background. Right: 120 GeV Fermiophobic Higgs (vertical scale corresponds to the number of expected $h \rightarrow \gamma\gamma$ events for $\approx 270 \text{ pb}^{-1}$)

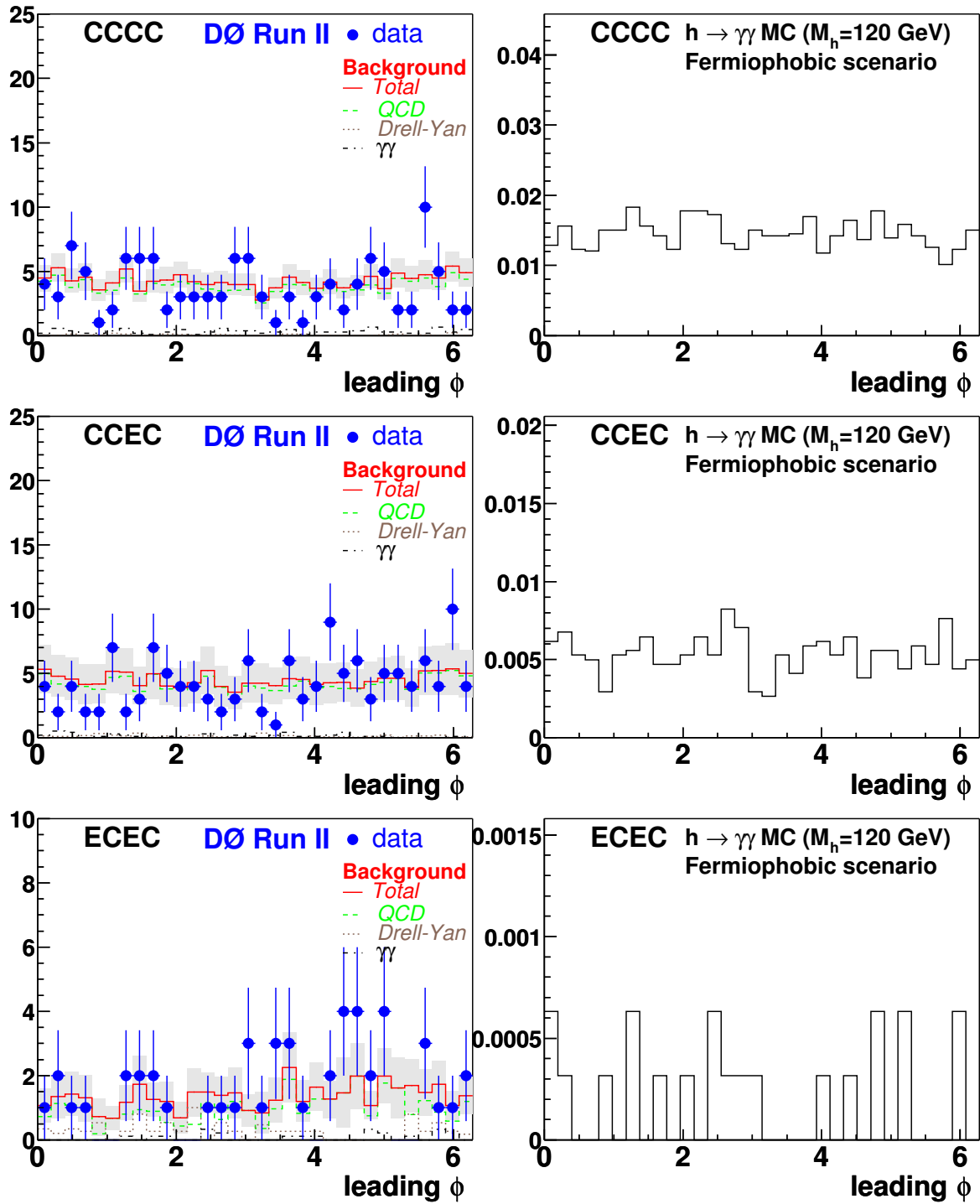


Figure 17: Leading photon detector ϕ distributions. Left: data and estimated background, points – data, solid (red) line – total SM background with systematic errors shown with gray rectangles, dashed (green) line – QCD background, dotted (brown) line – Drell-Yan background, dot-dashed (black) line – direct diphoton background. Right: 120 GeV Fermiophobic Higgs (vertical scale corresponds to the number of expected $h \rightarrow \gamma\gamma$ events for $\approx 270 \text{ pb}^{-1}$)

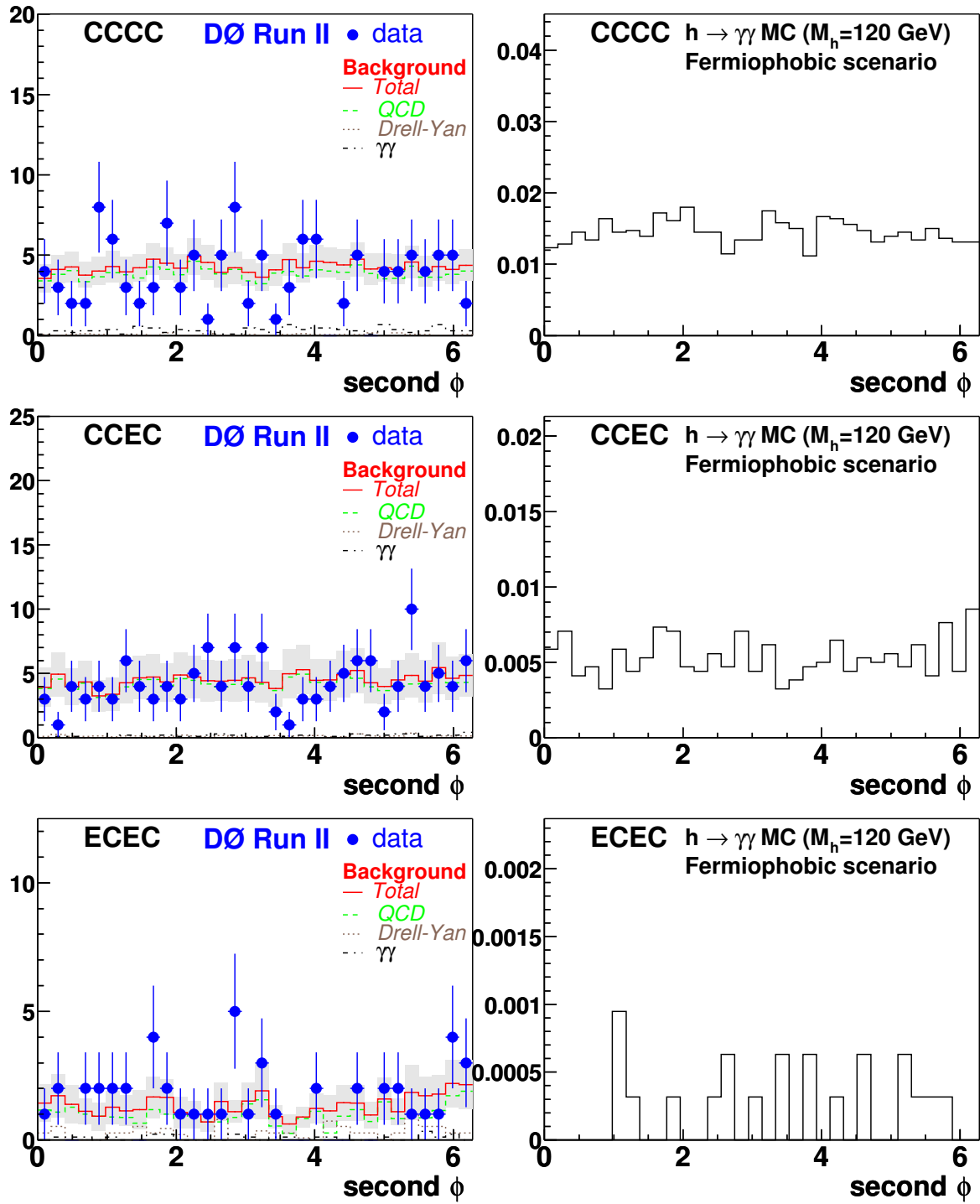


Figure 18: Second photon detector ϕ distributions. Left: data and estimated background, points – data, solid (red) line – total SM background with systematic errors shown with gray rectangles, dashed (green) line – QCD background, dotted (brown) line – Drell-Yan background, dot-dashed (black) line – direct diphoton background. Right: 120 GeV Fermiophobic Higgs (vertical scale corresponds to the number of expected $h \rightarrow \gamma\gamma$ events for $\approx 270 \text{ pb}^{-1}$)

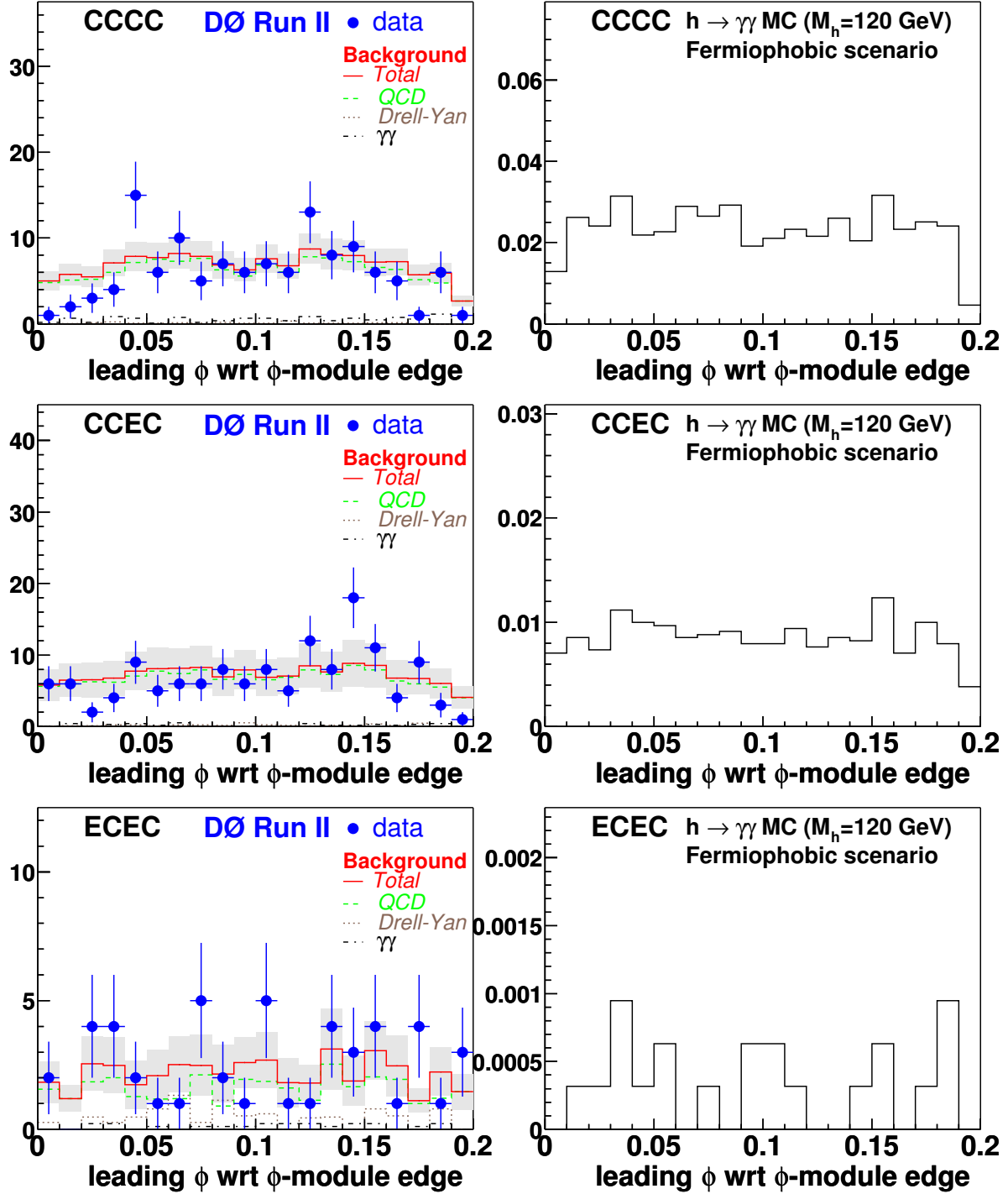


Figure 19: Distributions of leading photon detector ϕ with respect to calorimeter ϕ -module boundaries (applies only to Central Calorimeter). Left: data and estimated background, points – data, solid (red) line – total SM background with systematic errors shown with gray rectangles, dashed (green) line – QCD background, dotted (brown) line – Drell-Yan background, dot-dashed (black) line – direct diphoton background. Right: 120 GeV Fermiophobic Higgs (vertical scale corresponds to the number of expected $h \rightarrow \gamma\gamma$ events for $\approx 270 \text{ pb}^{-1}$)

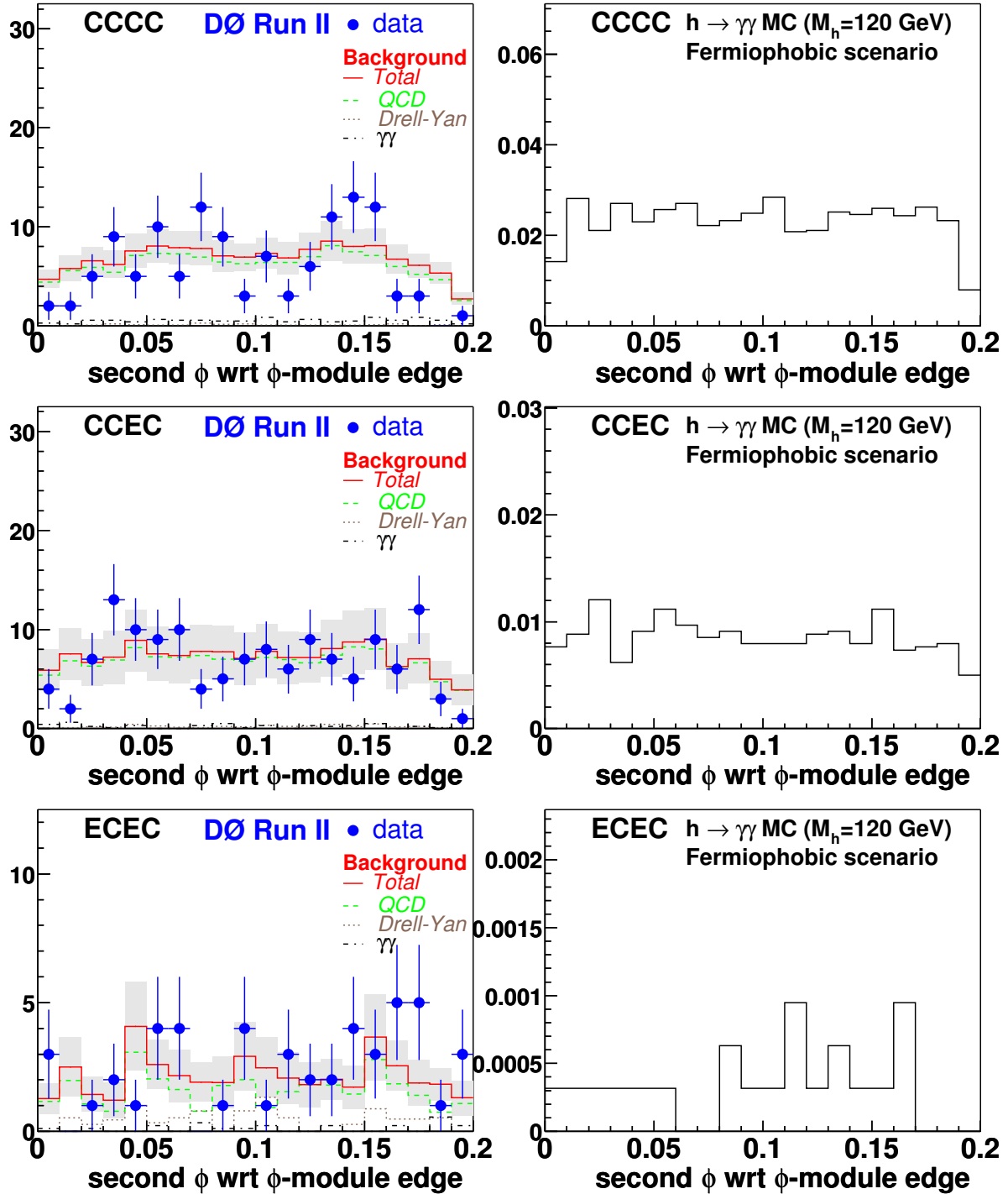


Figure 20: Distributions of second photon detector ϕ with respect to calorimeter ϕ -module boundaries (applies only to Central Calorimeter). Left: data and estimated background, points – data, solid (red) line – total SM background with systematic errors shown with gray rectangles, dashed (green) line – QCD background, dotted (brown) line – Drell-Yan background, dot-dashed (black) line – direct diphoton background. Right: 120 GeV Fermiophobic Higgs (vertical scale corresponds to the number of expected $h \rightarrow \gamma\gamma$ events for $\approx 270 \text{ pb}^{-1}$)

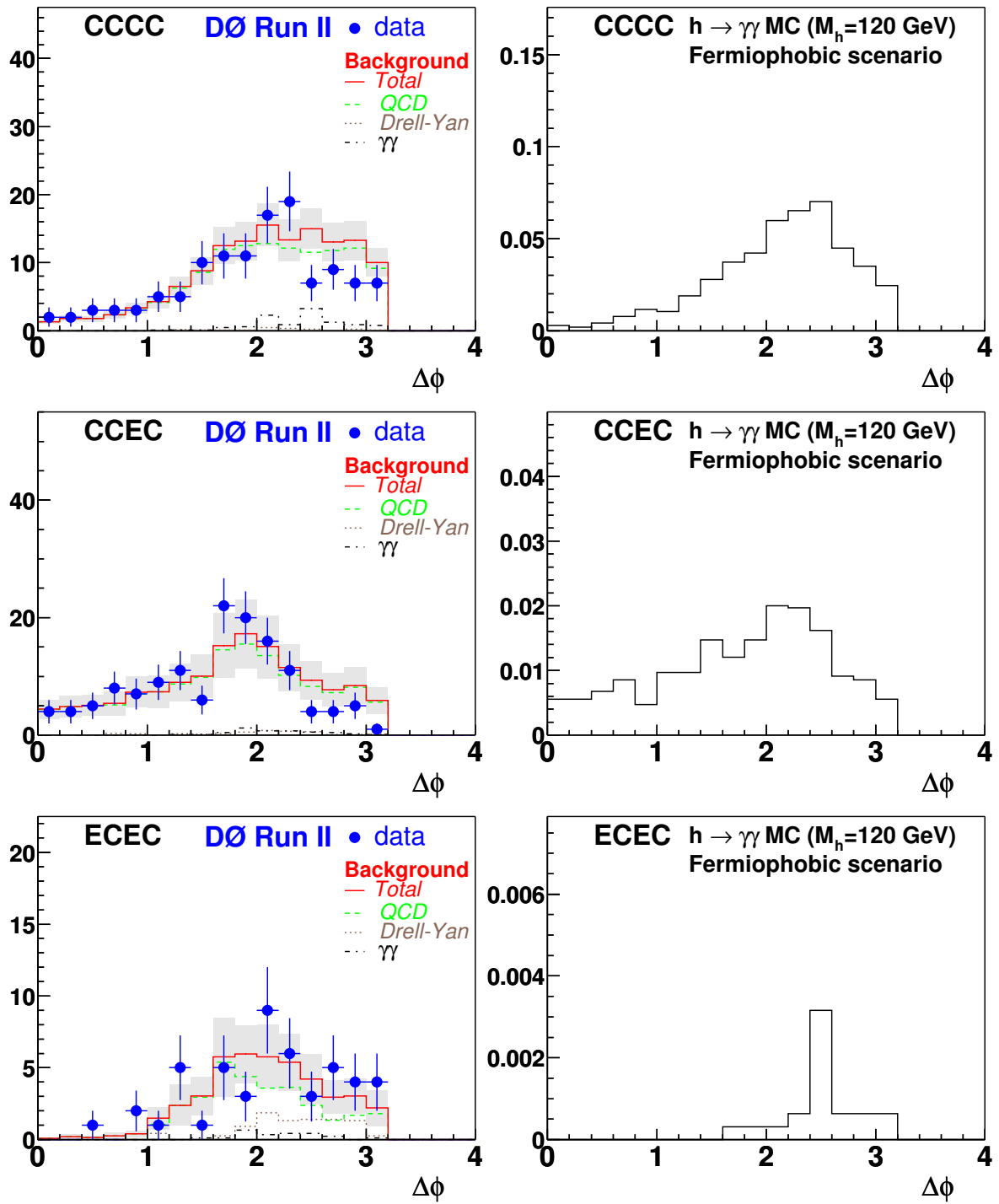


Figure 21: $\Delta\phi$ separation between two photons. Left: data and estimated background, points – data, solid (red) line – total SM background with systematic errors shown with gray rectangles, dashed (green) line – QCD background, dotted (brown) line – Drell-Yan background, dot-dashed (black) line – direct diphoton background. Right: 120 GeV Fermiophobic Higgs (vertical scale corresponds to the number of expected $h \rightarrow \gamma\gamma$ events for $\approx 270 \text{ pb}^{-1}$)

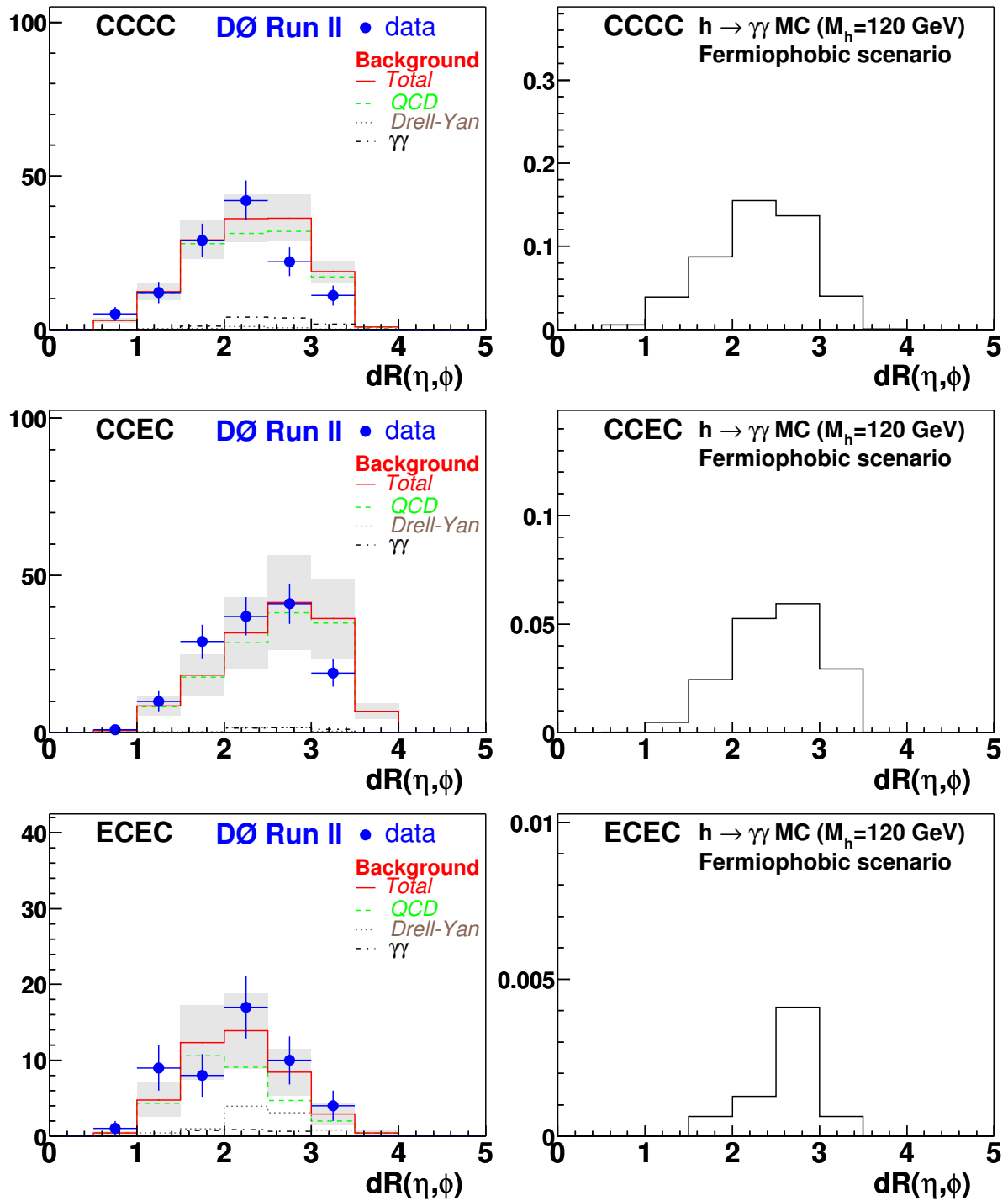


Figure 22: $dR(\eta, \phi)$ separation between two photons. Left: data and estimated background, points – data, solid (red) line – total SM background with systematic errors shown with gray rectangles, dashed (green) line – QCD background, dotted (brown) line – Drell-Yan background, dot-dashed (black) line – direct diphoton background. Right: 120 GeV Fermiophobic Higgs (vertical scale corresponds to the number of expected $h \rightarrow \gamma\gamma$ events for $\approx 270 \text{ pb}^{-1}$)

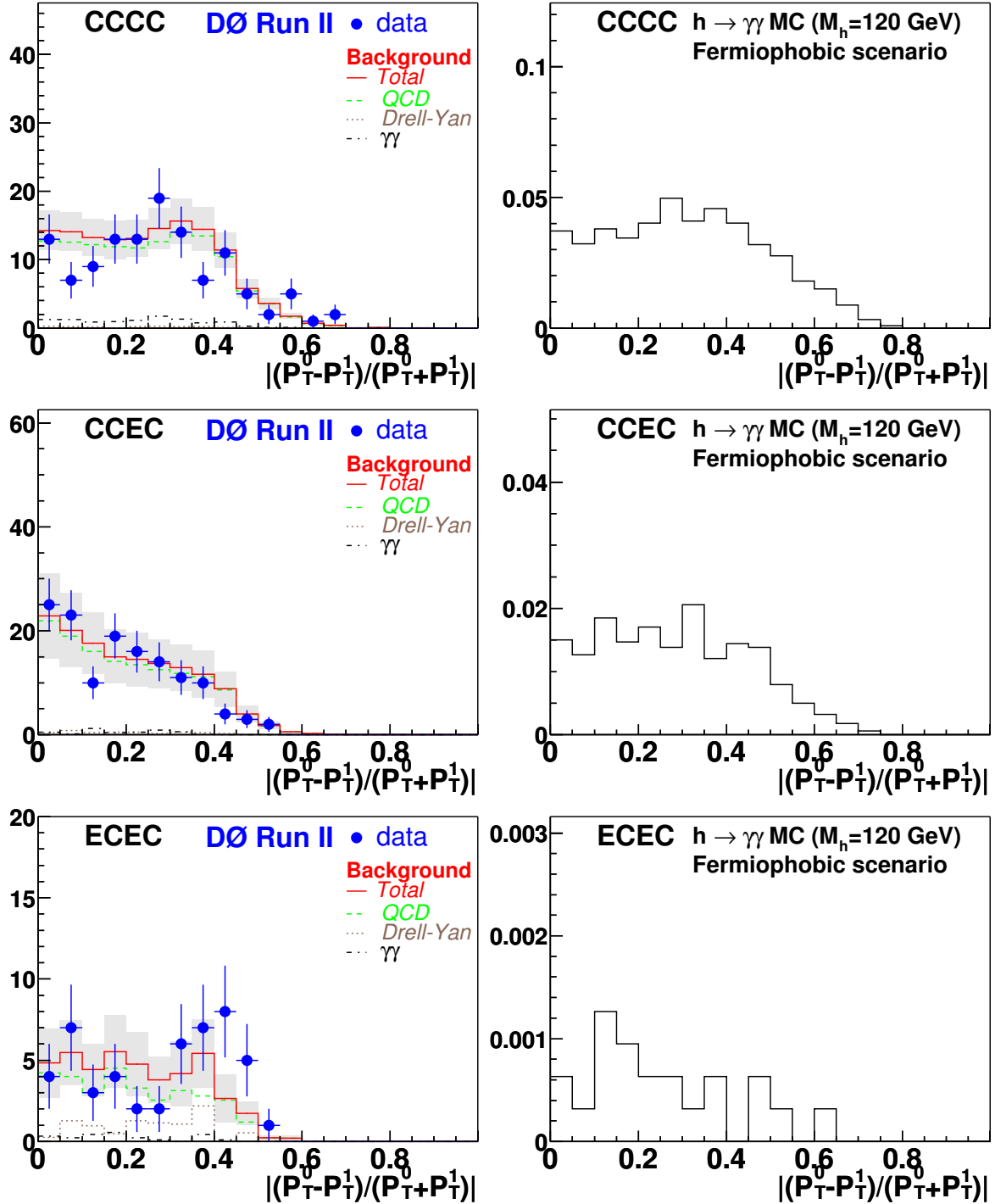


Figure 23: p_T -asymmetry between two photons ($((P_T^0 - P_T^1)/(P_T^0 + P_T^1))$). Left: data and estimated background, points – data, solid (red) line – total SM background with systematic errors shown with gray rectangles, dashed (green) line – QCD background, dotted (brown) line – Drell-Yan background, dot-dashed (black) line – direct diphoton background. Right: 120 GeV Fermiophobic Higgs (vertical scale corresponds to the number of expected $h \rightarrow \gamma\gamma$ events for $\approx 270 \text{ pb}^{-1}$)

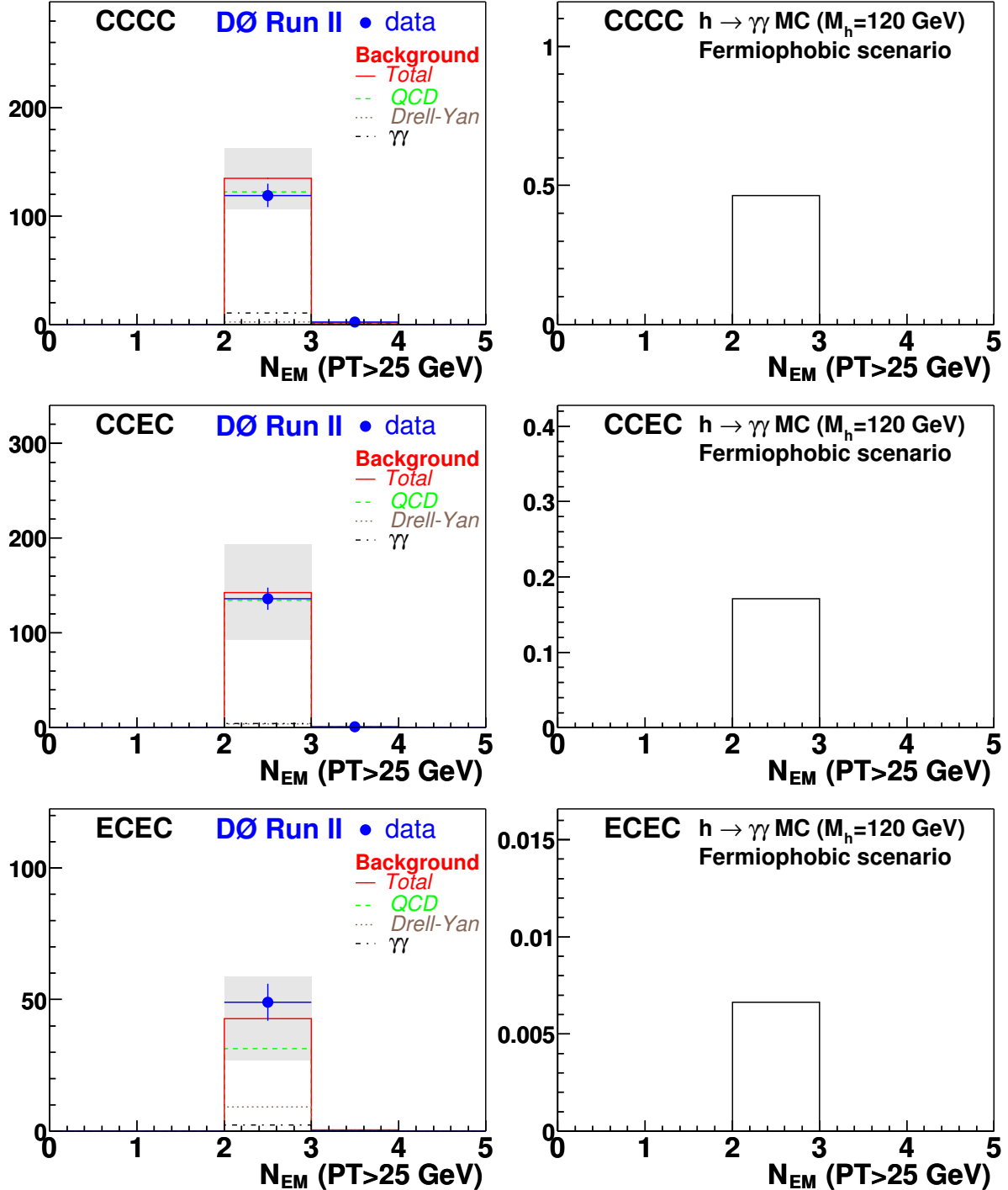


Figure 24: Number of Loose EM objects ($p_T > 25$ GeV). Left: data and estimated background, points – data, solid (red) line – total SM background with systematic errors shown with gray rectangles, dashed (green) line – QCD background, dotted (brown) line – Drell-Yan background, dot-dashed (black) line – direct diphoton background. Right: 120 GeV Fermiophobic Higgs (vertical scale corresponds to the number of expected $h \rightarrow \gamma\gamma$ events for $\approx 270 \text{ pb}^{-1}$)

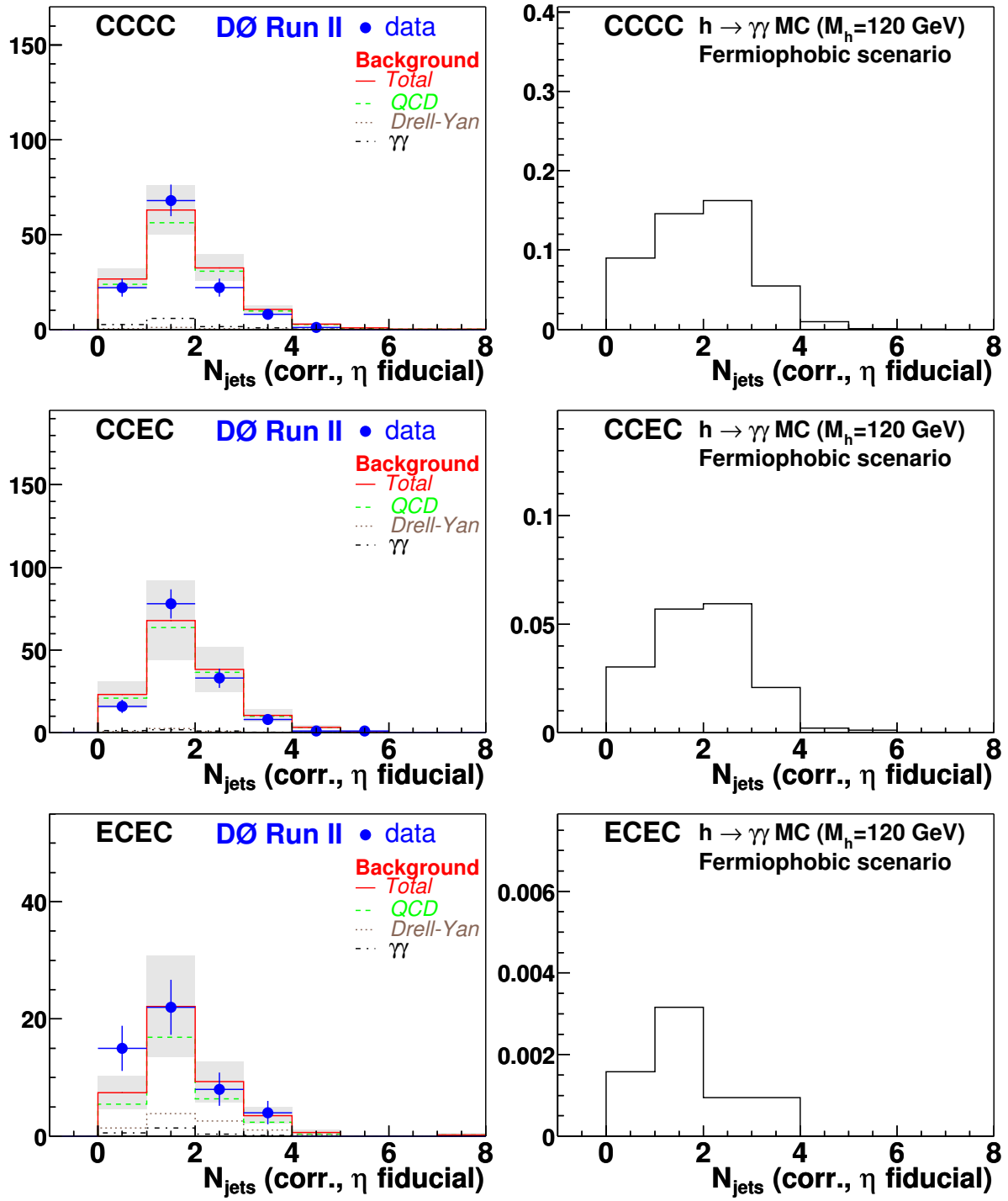


Figure 25: Number of corrected jets (“corrJCCB”) inside the EM-object η -fiducial region (CC and EC up to $|\eta| < 2.4$). Left: data and estimated background, points – data, solid (red) line – total SM background with systematic errors shown with gray rectangles, dashed (green) line – QCD background, dotted (brown) line – Drell-Yan background, dot-dashed (black) line – direct diphoton background. Right: 120 GeV Fermiophobic Higgs (vertical scale corresponds to the number of expected $h \rightarrow \gamma\gamma$ events for $\approx 270 \text{ pb}^{-1}$)

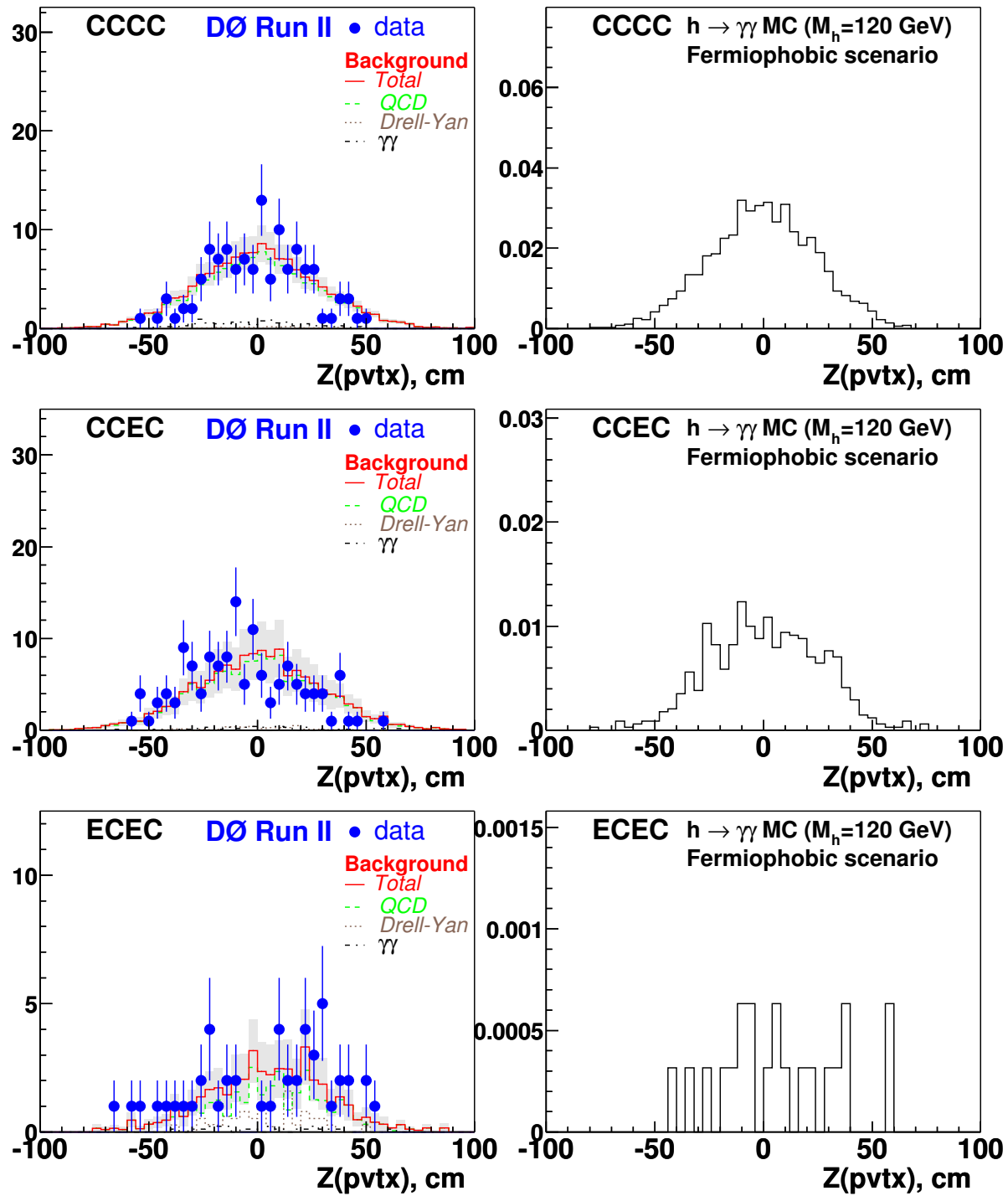


Figure 26: Z position of the reconstructed primary vertex. Left: data and estimated background, points – data, solid (red) line – total SM background with systematic errors shown with gray rectangles, dashed (green) line – QCD background, dotted (brown) line – Drell-Yan background, dot-dashed (black) line – direct diphoton background. Right: 120 GeV Fermiophobic Higgs (vertical scale corresponds to the number of expected $h \rightarrow \gamma\gamma$ events for $\approx 270 \text{ pb}^{-1}$)

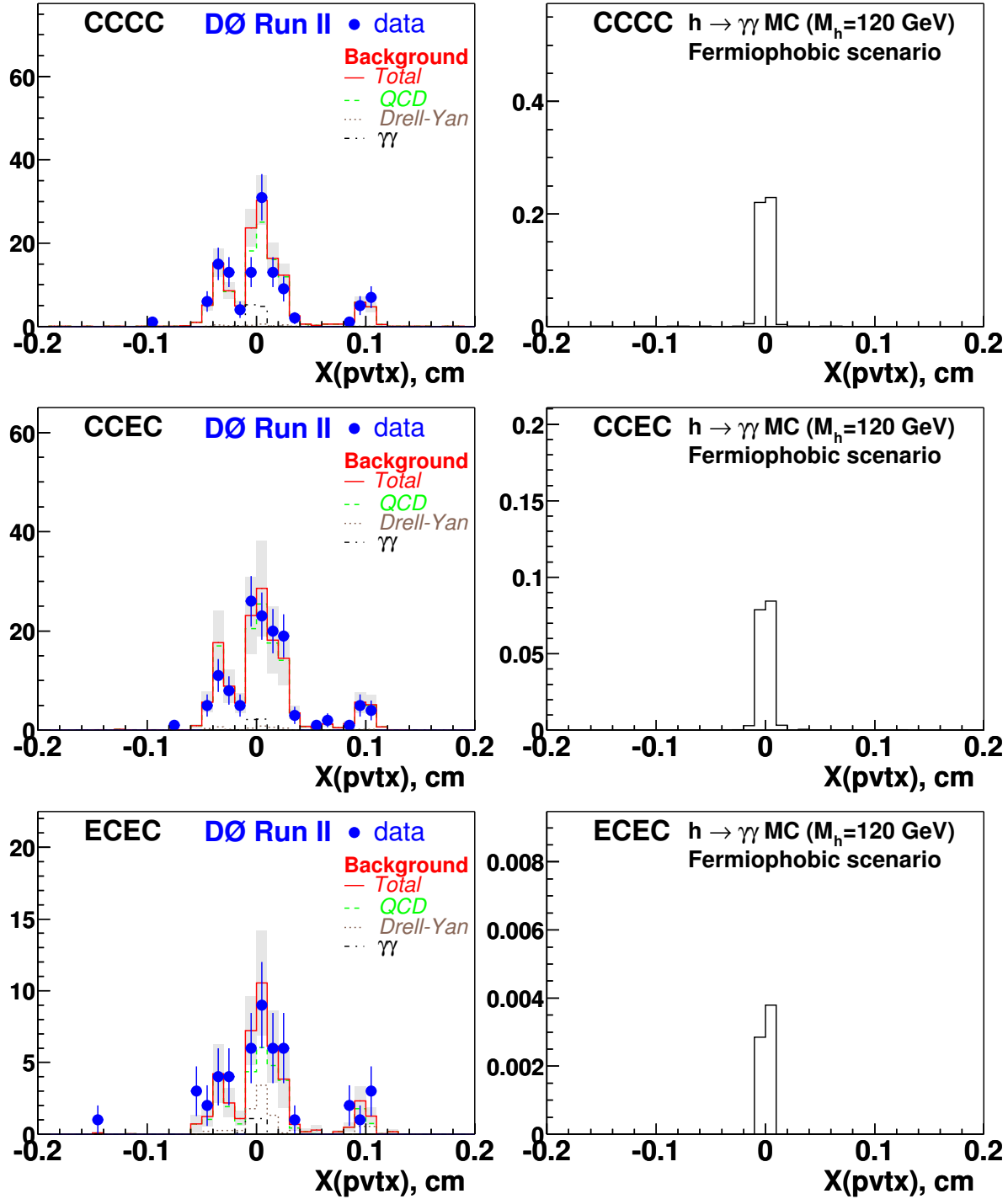


Figure 27: X position of the reconstructed primary vertex. Left: data and estimated background, points – data, solid (red) line – total SM background with systematic errors shown with gray rectangles, dashed (green) line – QCD background, dotted (brown) line – Drell-Yan background, dot-dashed (black) line – direct diphoton background. Right: 120 GeV Fermiophobic Higgs (vertical scale corresponds to the number of expected $h \rightarrow \gamma\gamma$ events for $\approx 270 \text{ pb}^{-1}$)

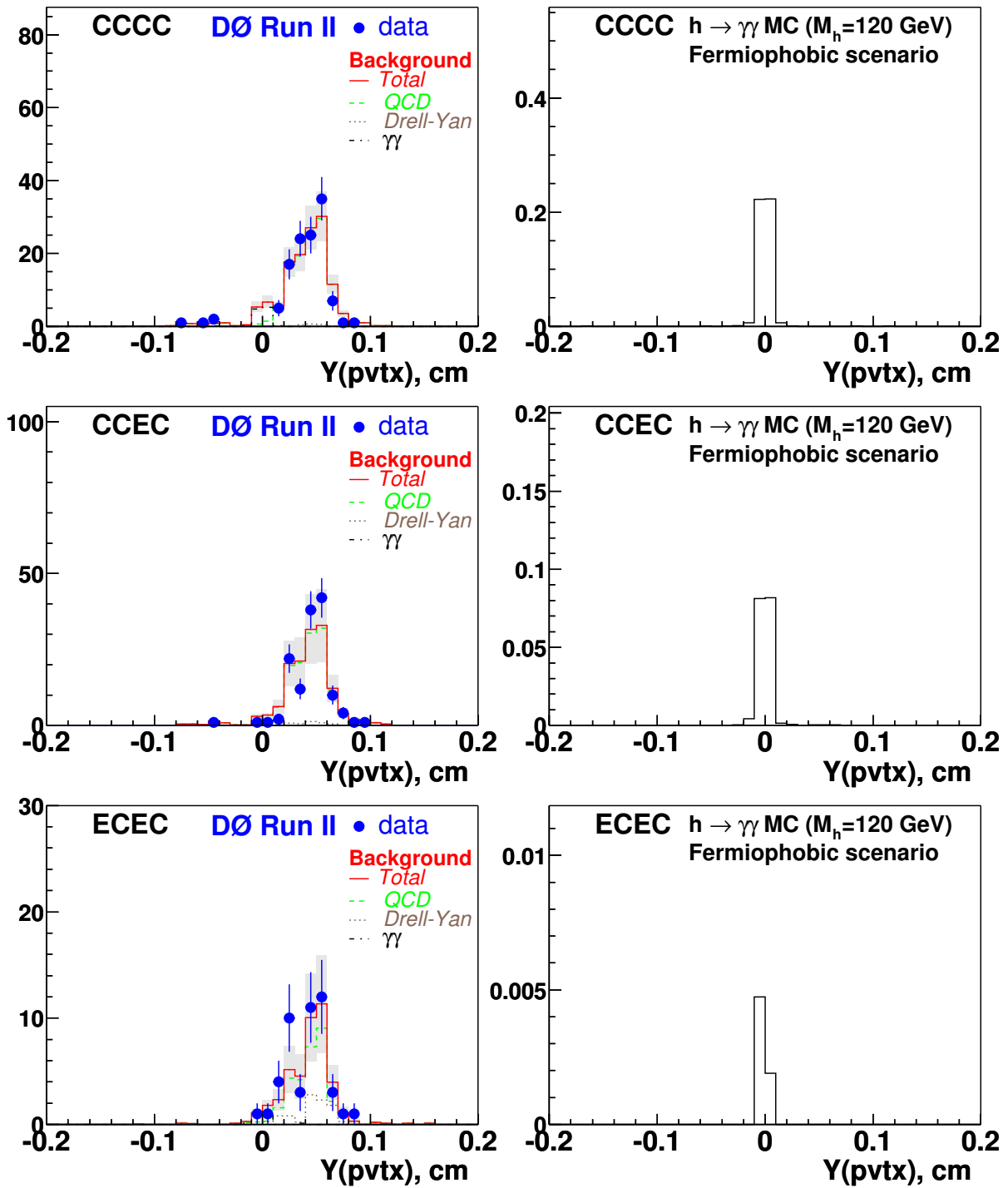


Figure 28: Y position of the reconstructed primary vertex. Left: data and estimated background, points – data, solid (red) line – total SM background with systematic errors shown with gray rectangles, dashed (green) line – QCD background, dotted (brown) line – Drell-Yan background, dot-dashed (black) line – direct diphoton background. Right: 120 GeV Fermiophobic Higgs (vertical scale corresponds to the number of expected $h \rightarrow \gamma\gamma$ events for $\approx 270 \text{ pb}^{-1}$)

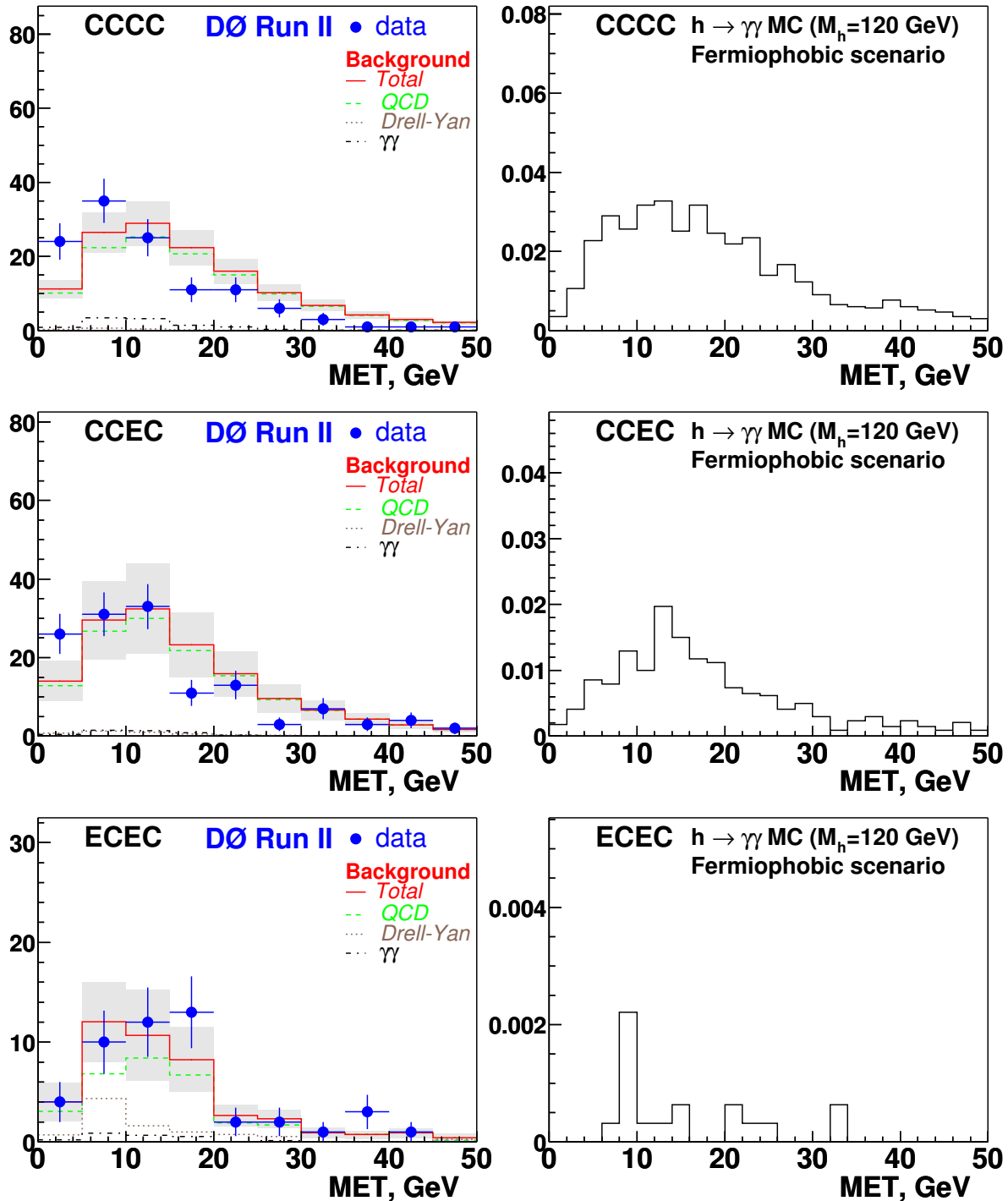


Figure 29: Missing E_T distributions. Left: data and estimated background, points – data, solid (red) line – total SM background with systematic errors shown with gray rectangles, dashed (green) line – QCD background, dotted (brown) line – Drell-Yan background, dot-dashed (black) line – direct diphoton background. Right: 120 GeV Fermiophobic Higgs (vertical scale corresponds to the number of expected $h \rightarrow \gamma\gamma$ events for $\approx 270 \text{ pb}^{-1}$)

This is for MonteCarlo. Start with comparing photon and electron MC efficiencies. Then fitted Higgs mass peak and derived width (also comparing natural and recod mass peak)

To compare electron and photon efficiencies in Monte Carlo we use $Z \rightarrow ee$ and $h \rightarrow \gamma\gamma$ MC samples. We use gluon fusion production $h \rightarrow \gamma\gamma$ sample with $M=90$ GeV, since this sample should be most similar kinematically to the $Z \rightarrow ee$ sample. Slight differences may be expected in angular distributions of photons and electrons, due to spin (vector boson decaying to fermions vs. scalar decaying into vector bosons). Also since Higgs is produced via gluon fusion and Z is produced at the tree level by quark-antiquark annihilation more jets can be expected in $h \rightarrow \gamma\gamma$ events. This is shown in Figure 30

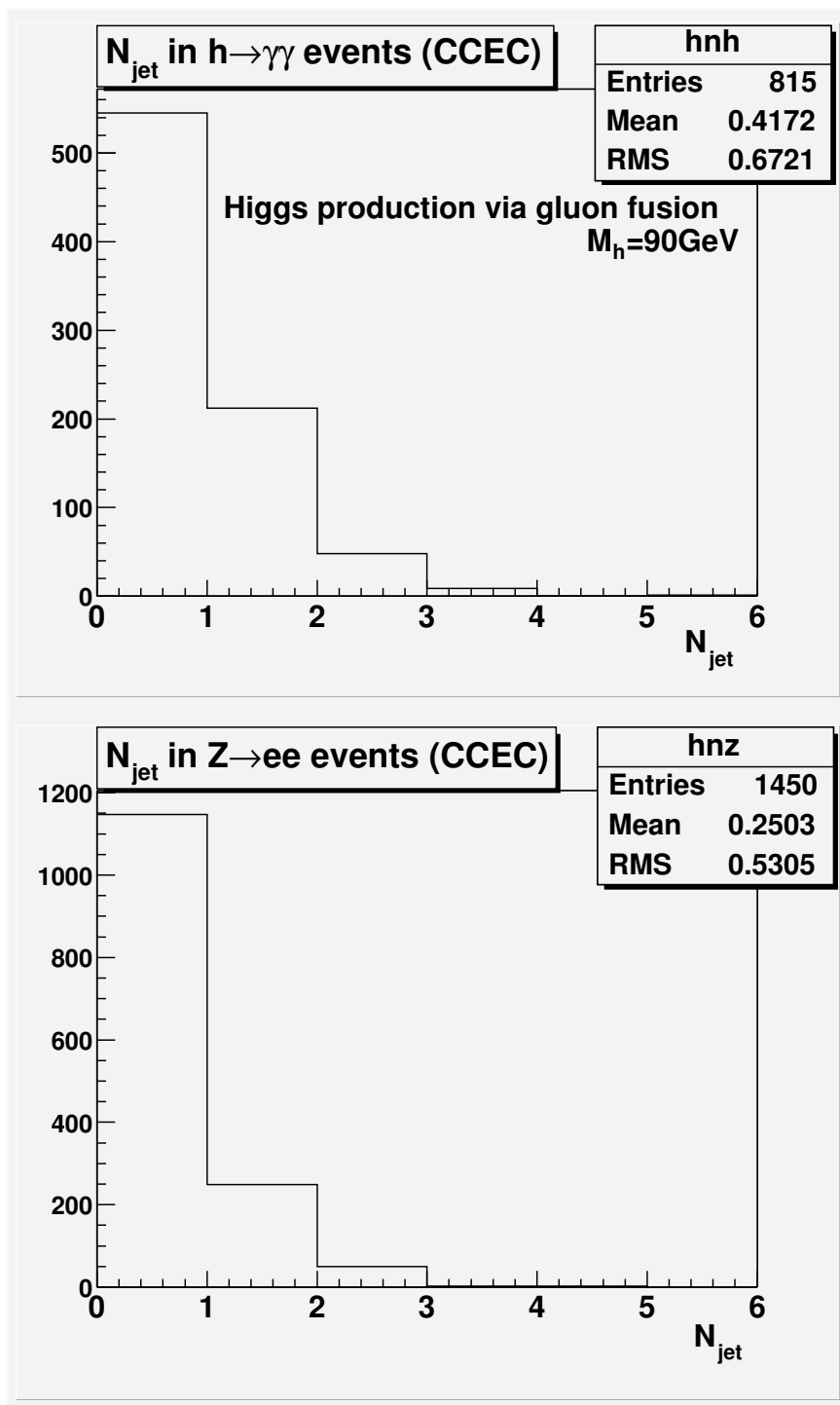


Figure 30: Comparison of jet multiplicity for $h \rightarrow \gamma\gamma$ $Z \rightarrow ee$ events (CCEC). Top – $h \rightarrow \gamma\gamma$. Bottom – $Z \rightarrow$. $h \rightarrow \gamma\gamma$ sample is gluon fusion production, $M=90 \text{ GeV}$.

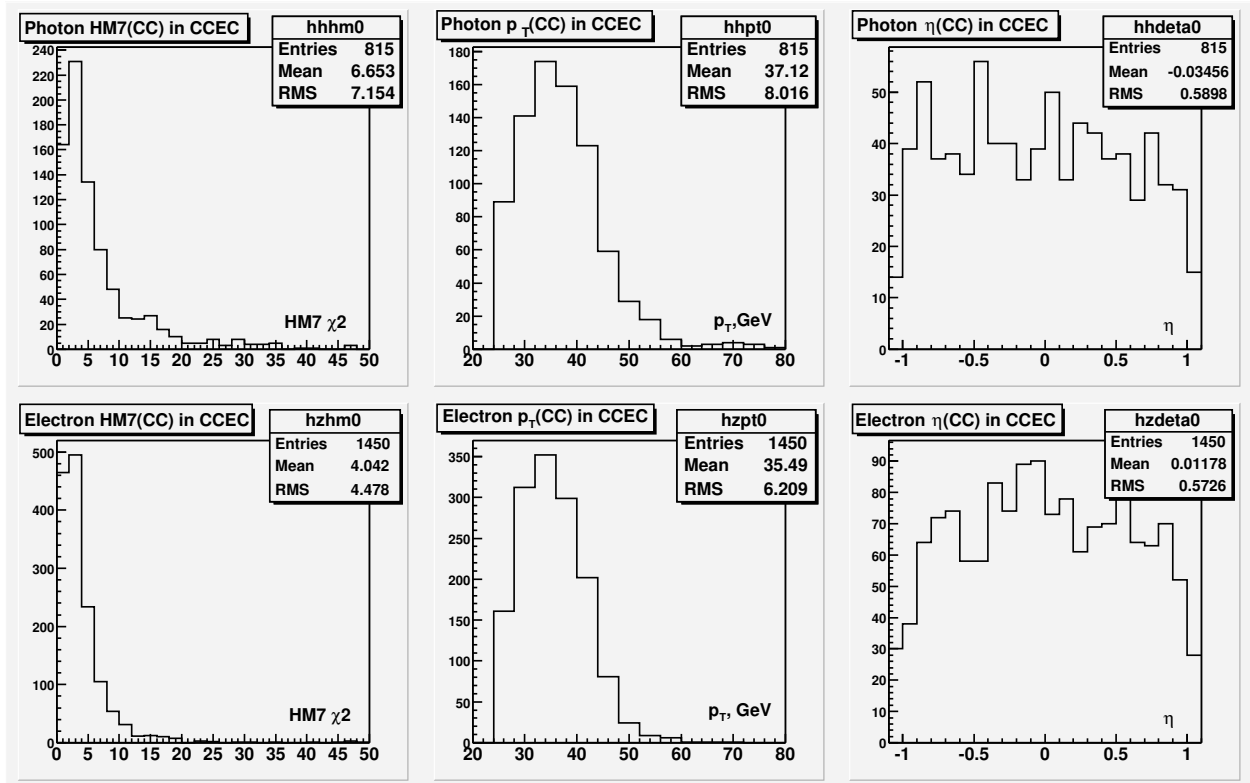


Figure 31: Comparsion of HMatrix χ^2 distributions for $h \rightarrow \gamma\gamma$ MC photons and $Z \rightarrow ee$ MC electrons in CC (in CCEC events). Top row – MC photons. Bottom row – MC electrons. Left column – HMatrix7 χ^2 distributions. Middle column – p_T distributions. Right column – detector η distributions.

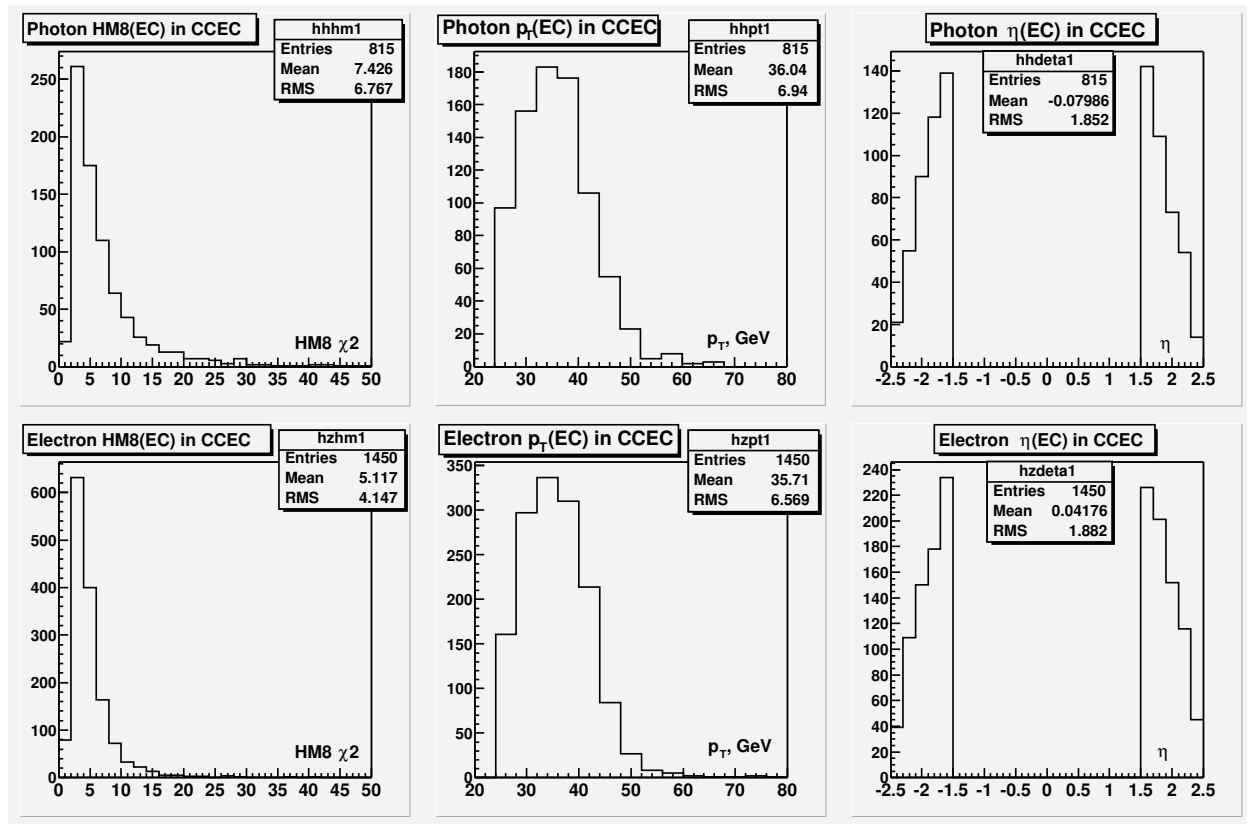


Figure 32: Comparison of HMatrix χ^2 distributions for $h \rightarrow \gamma\gamma$ MC photons and $Z \rightarrow ee$ MC electrons in EC (in CCEC events). Top row – MC photons. Bottom row – MC electrons. Left column – HMatrix8 χ^2 distributions. Middle column – p_T distributions. Right column – detector η distributions.

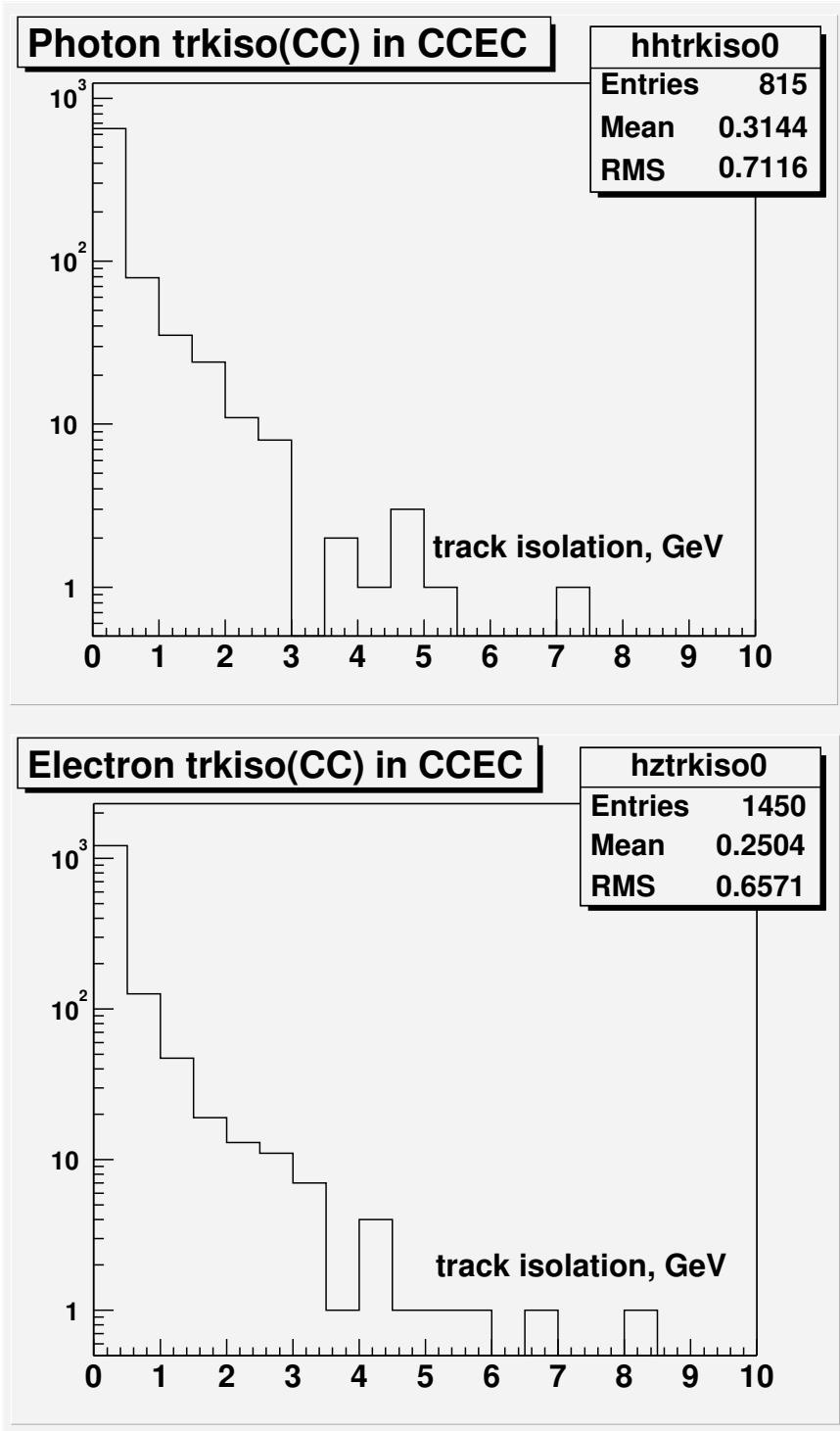


Figure 33: Comparsion of track isolation for $h \rightarrow \gamma\gamma$ photons and $Z \rightarrow ee$ electrons in CC (in CCEC events). Top – MC photons. Bottom – MC electrons.

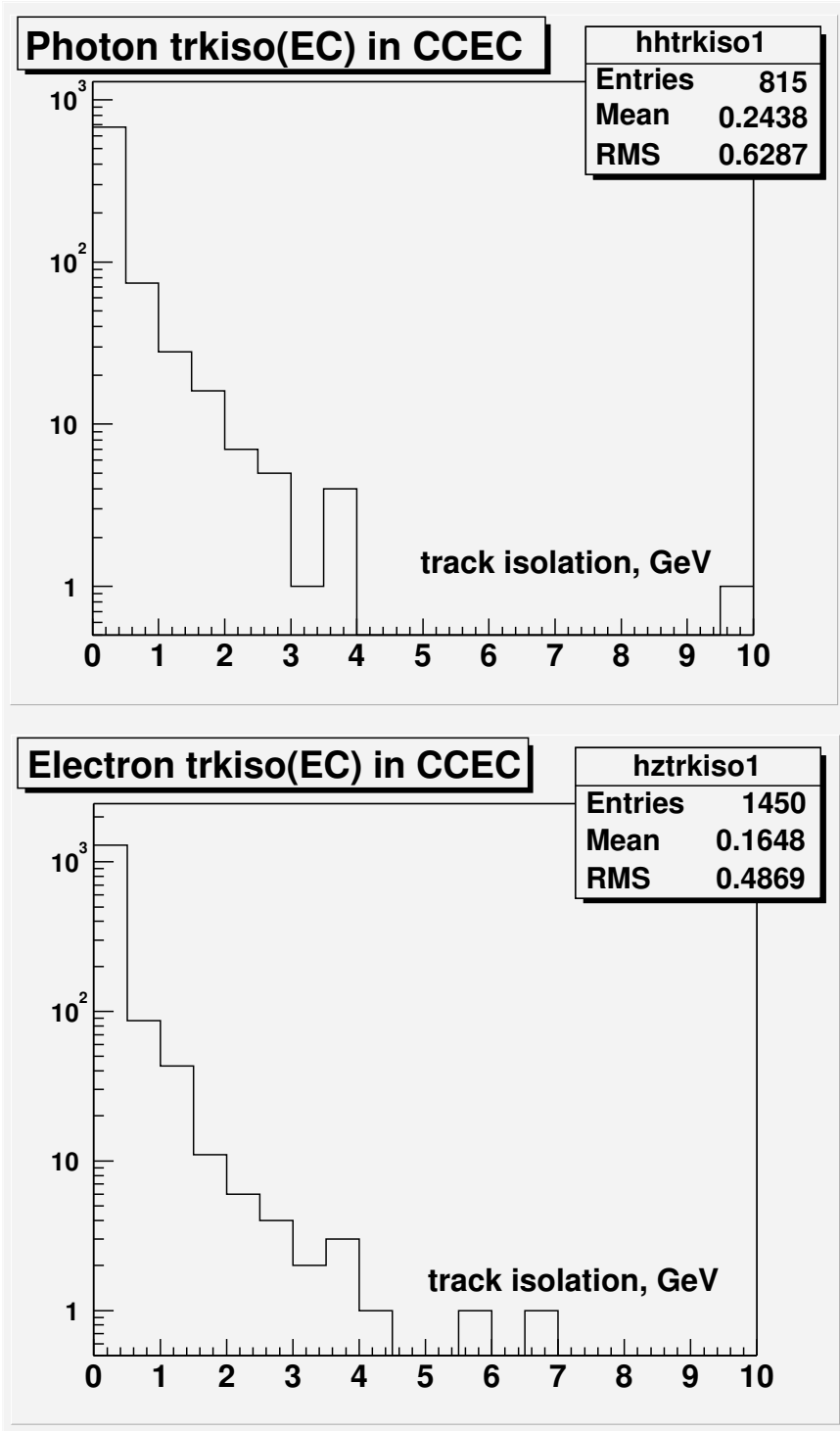


Figure 34: Comparsion of track isolation for $h \rightarrow \gamma\gamma$ photons and $Z \rightarrow ee$ electrons in EC (in CCEC events). Top – MC photons. Bottom – MC electrons.

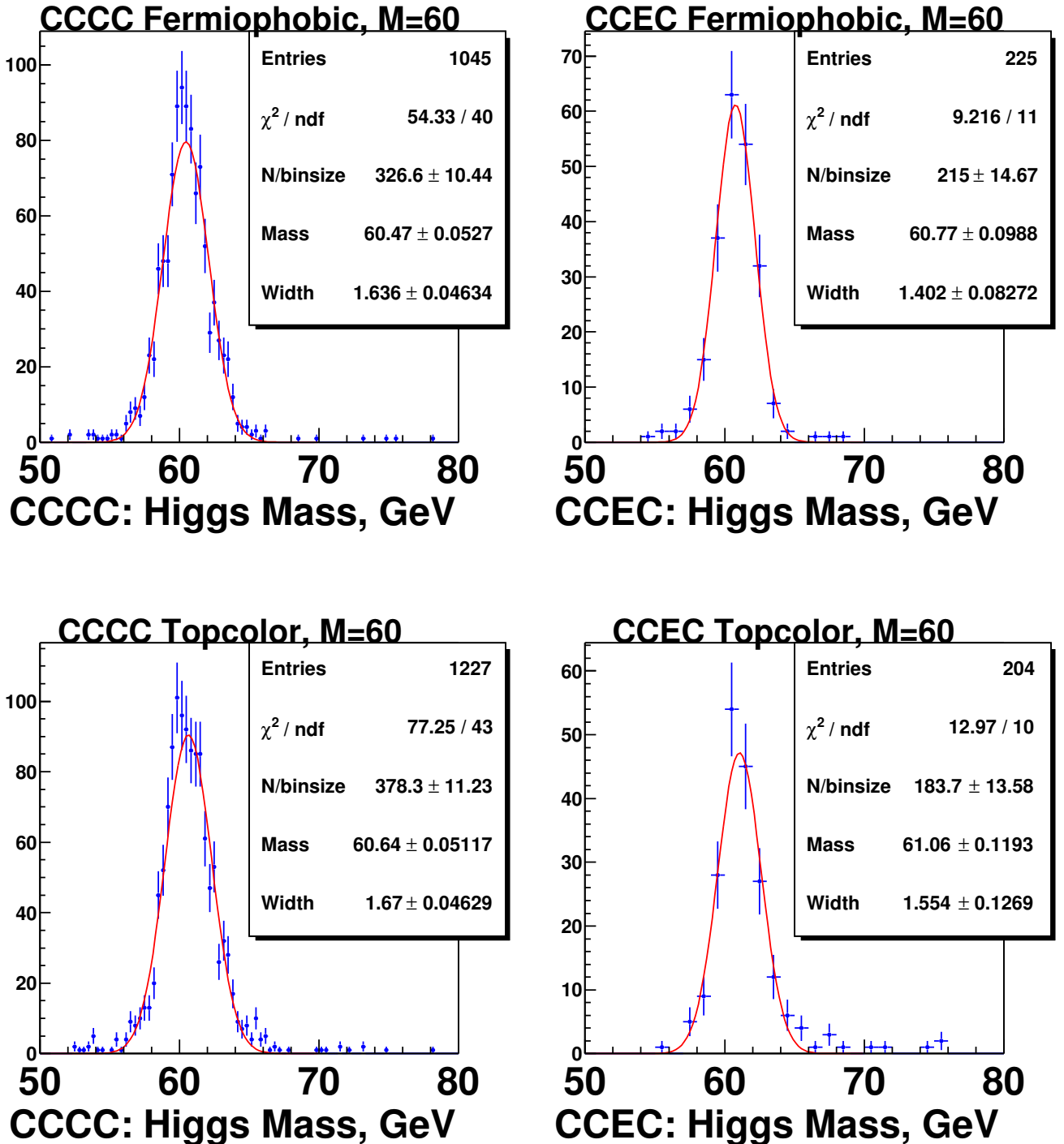


Figure 35: Fitted Higgs mass and width for $M_h = 60$ GeV.

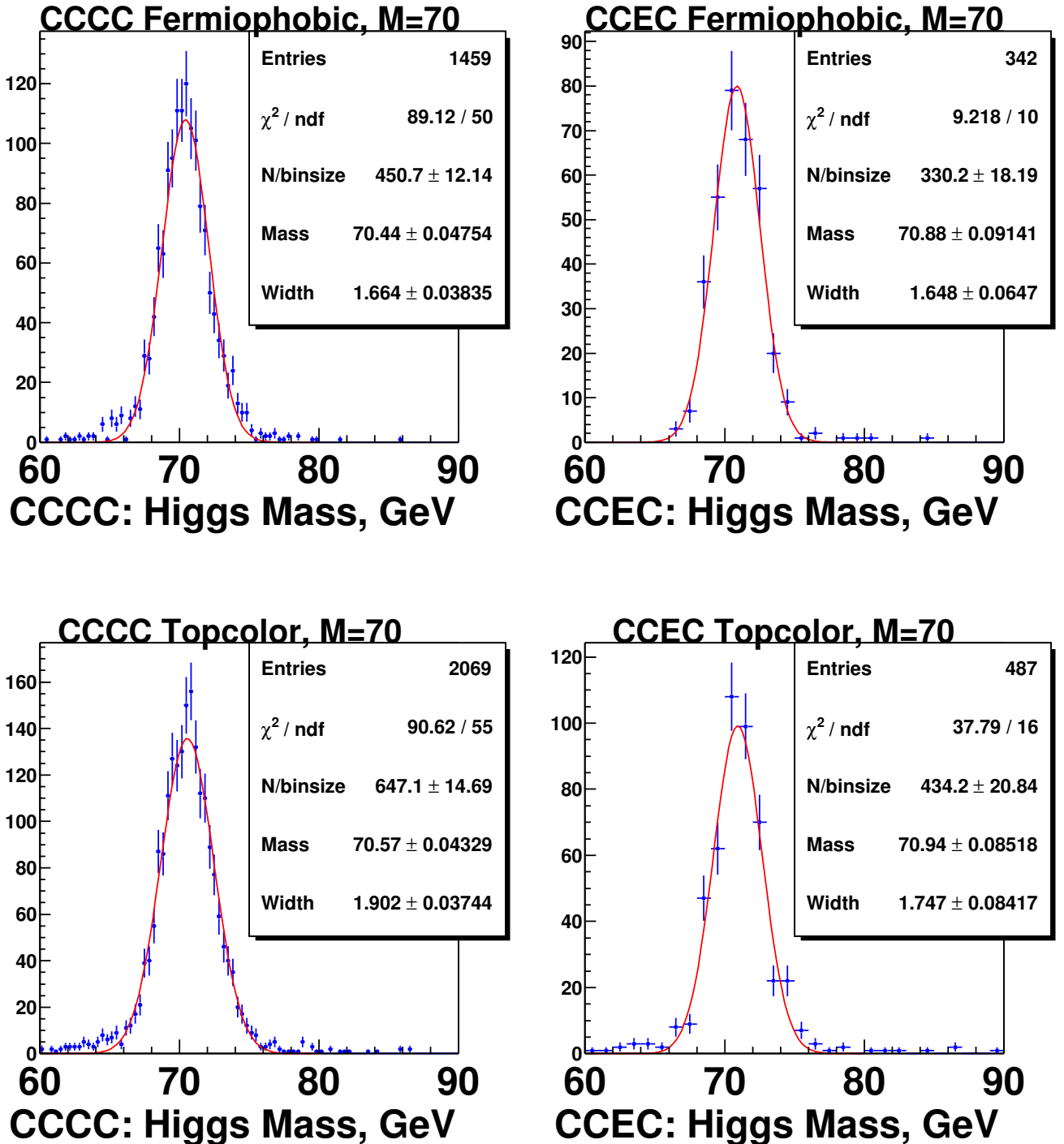


Figure 36: Fitted Higgs mass and width for $M_h = 70$ GeV.

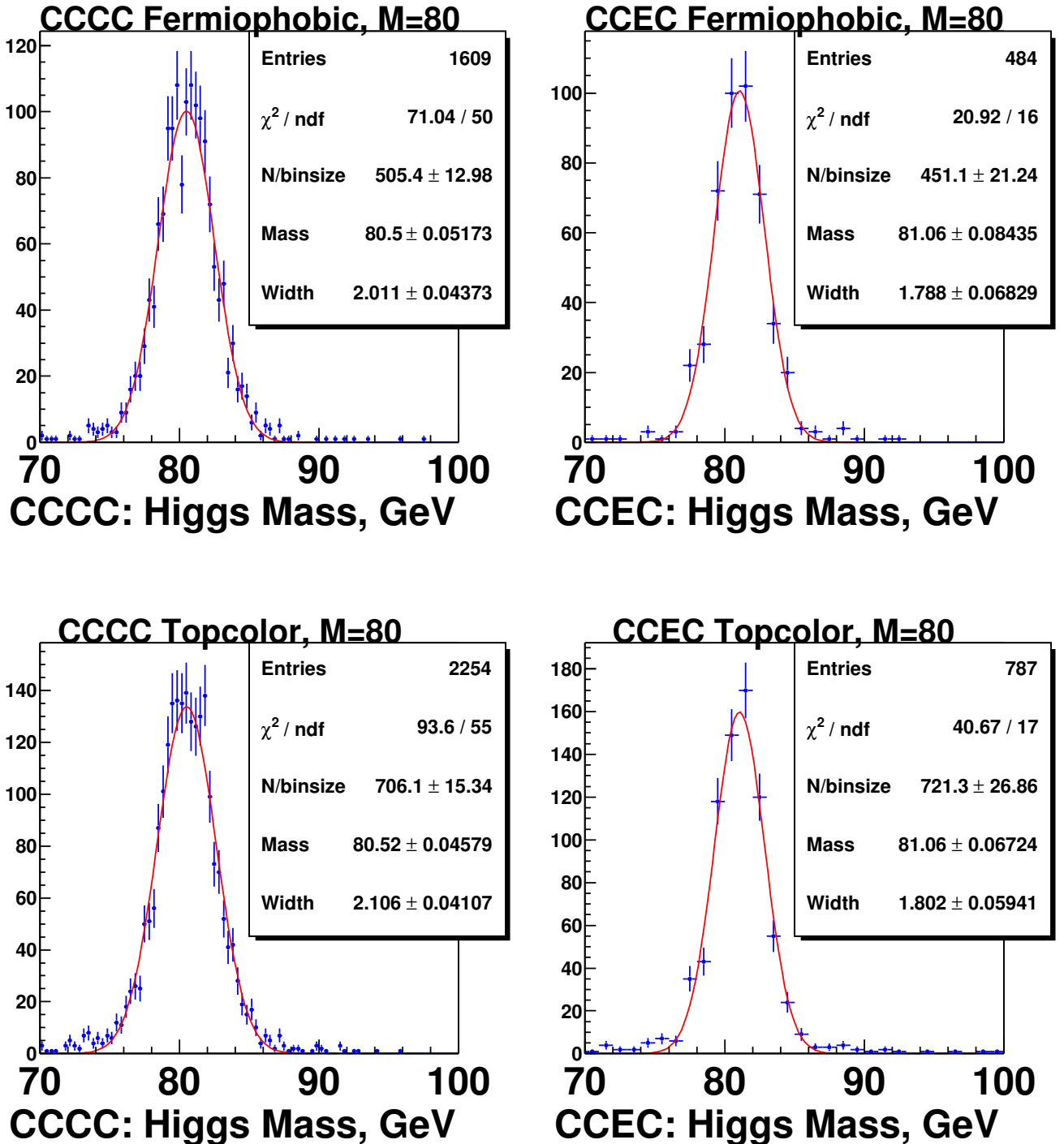


Figure 37: Fitted Higgs mass and width for $M_h = 80$ GeV.

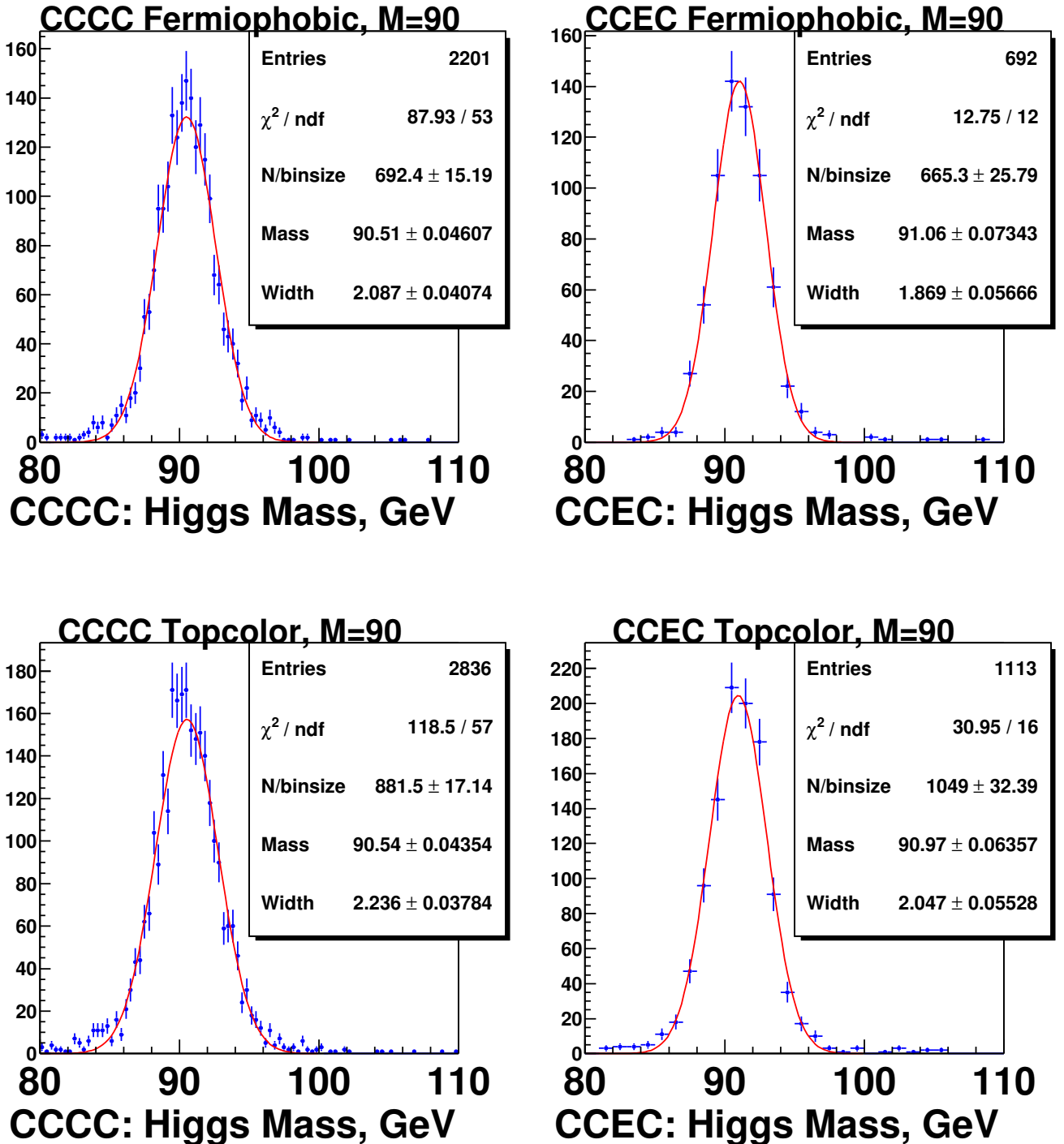


Figure 38: Fitted Higgs mass and width for $M_h = 90$ GeV.

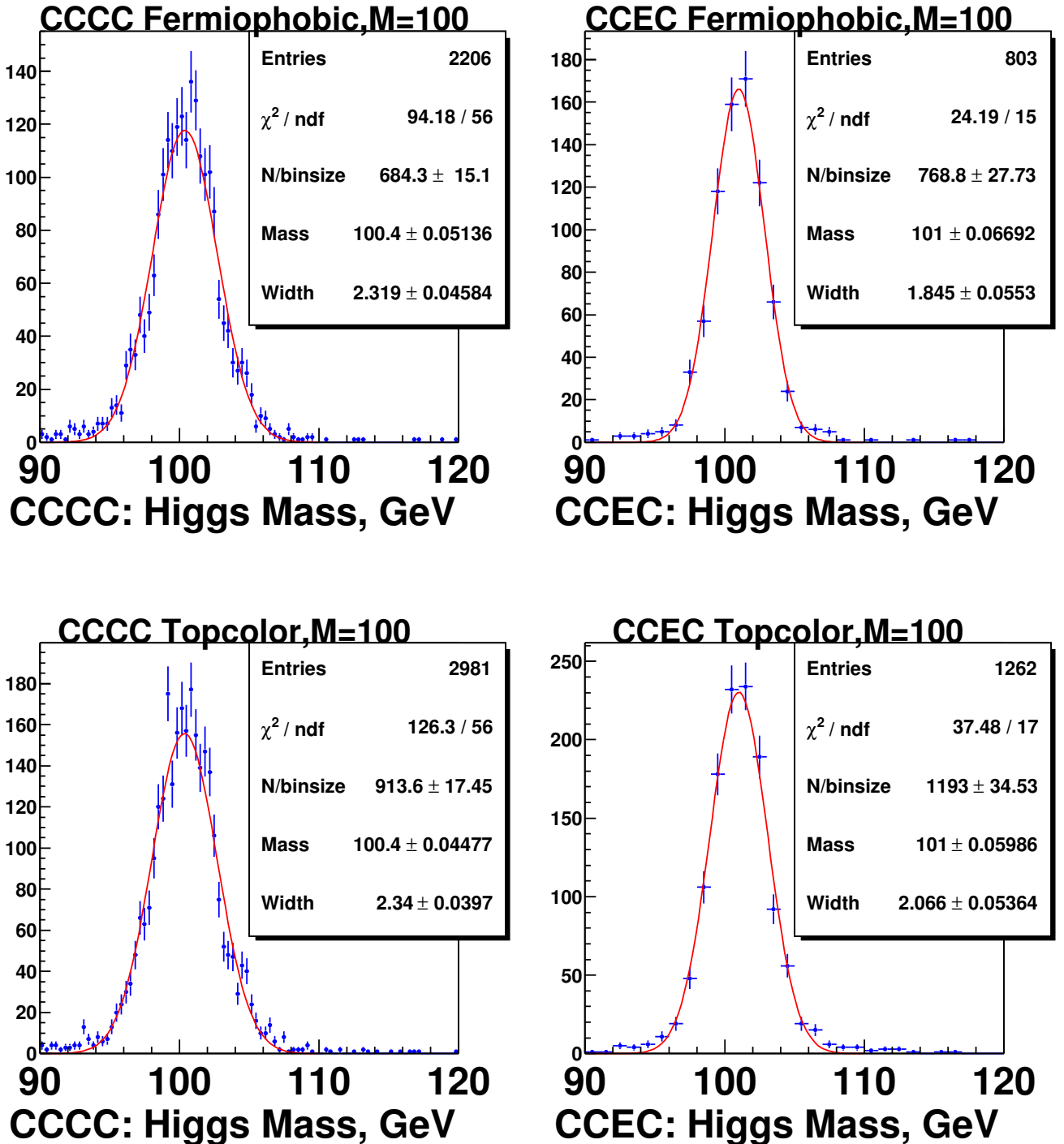


Figure 39: Fitted Higgs mass and width for $M_h = 100$ GeV.

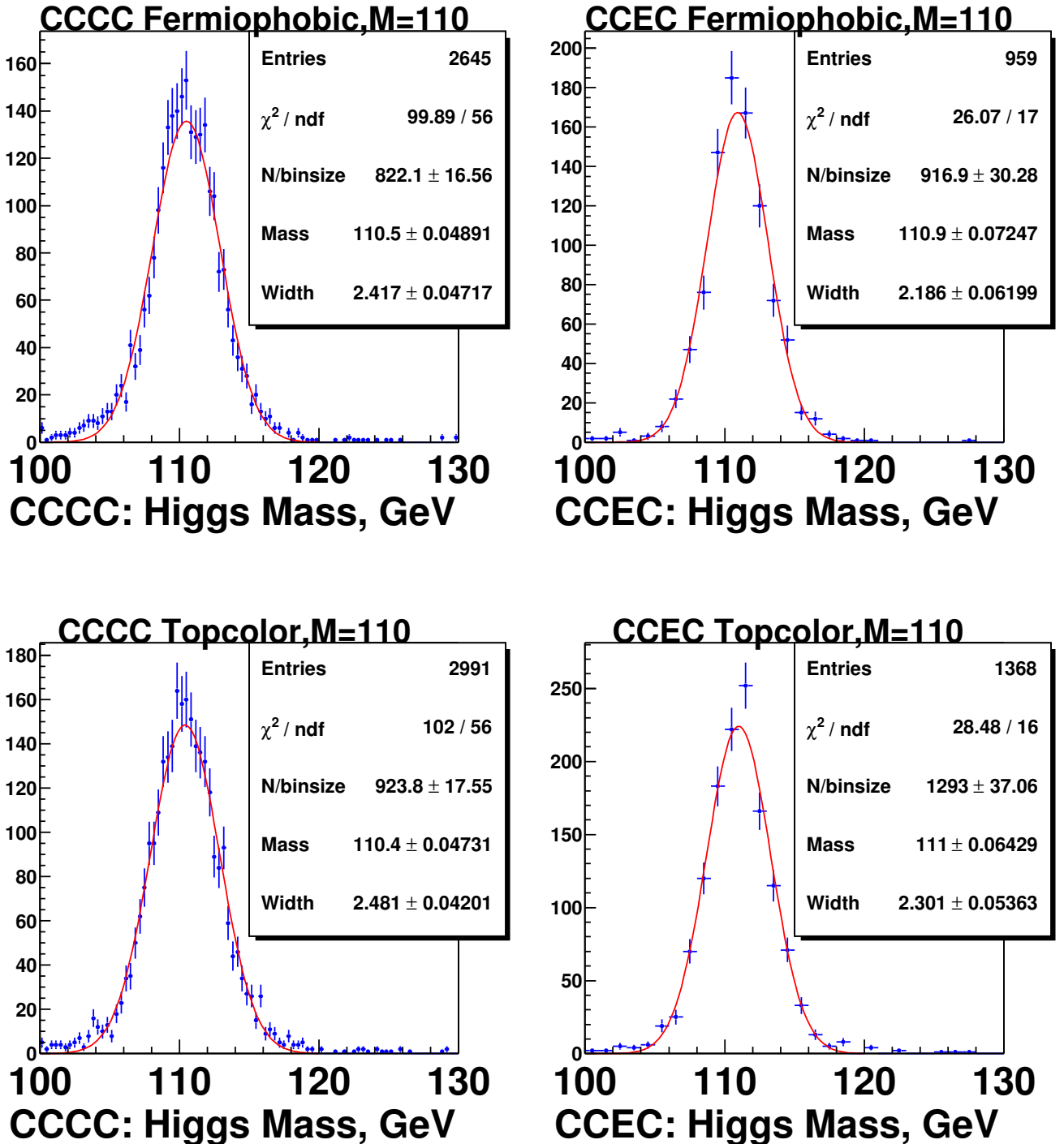


Figure 40: Fitted Higgs mass and width for $M_h = 110$ GeV.

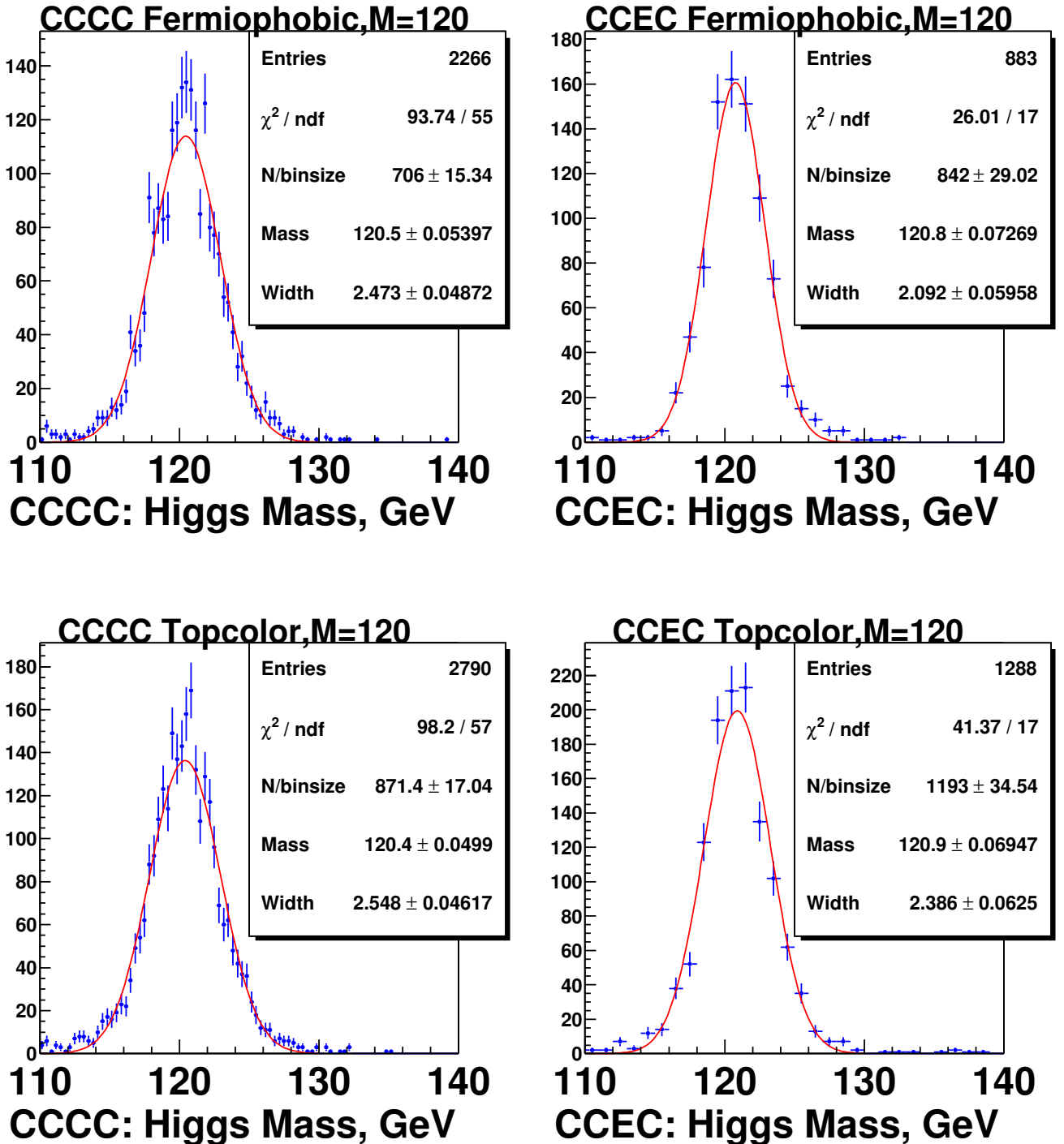


Figure 41: Fitted Higgs mass and width for $M_h = 120$ GeV.

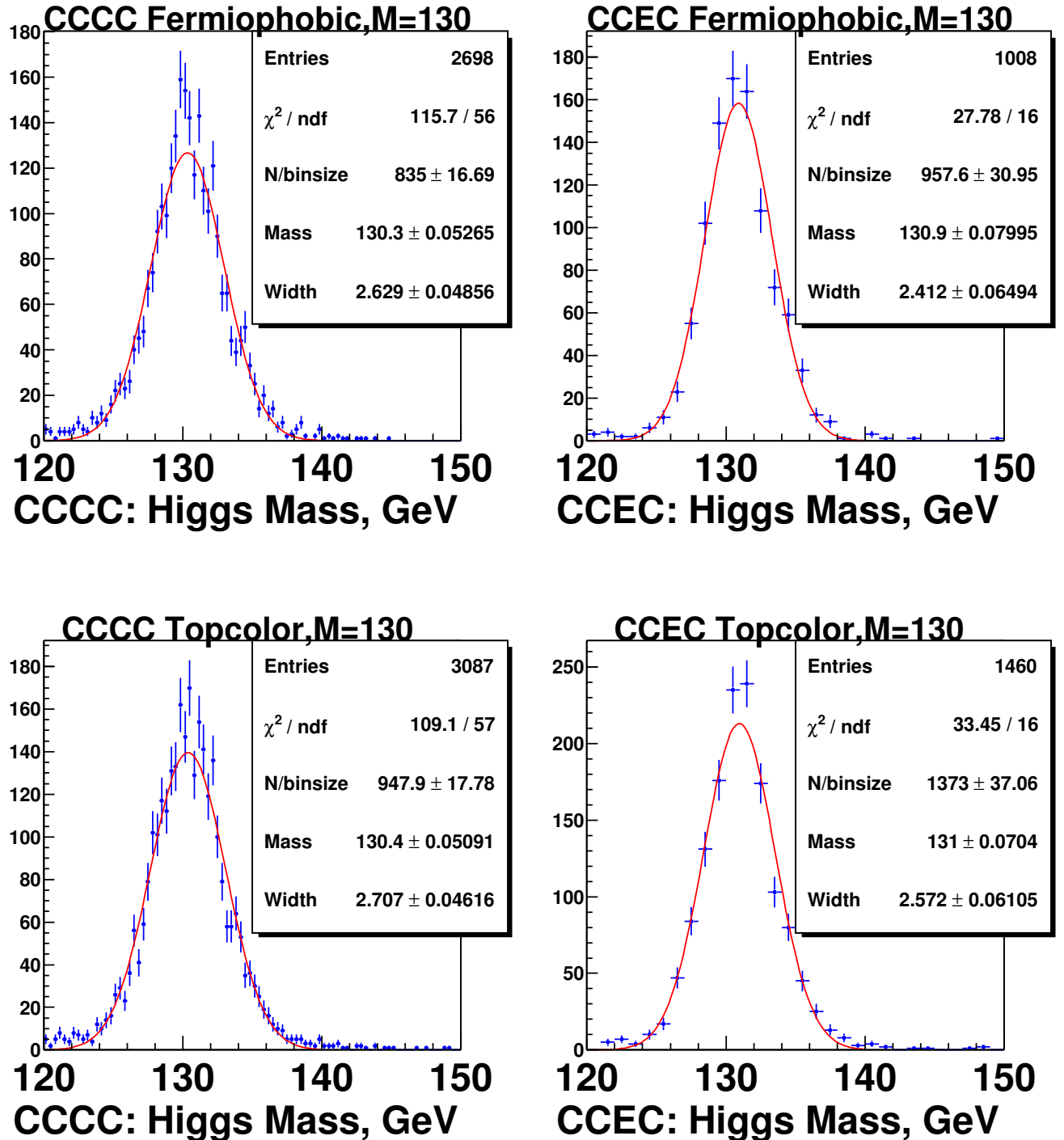


Figure 42: Fitted Higgs mass and width for $M_h = 130$ GeV.

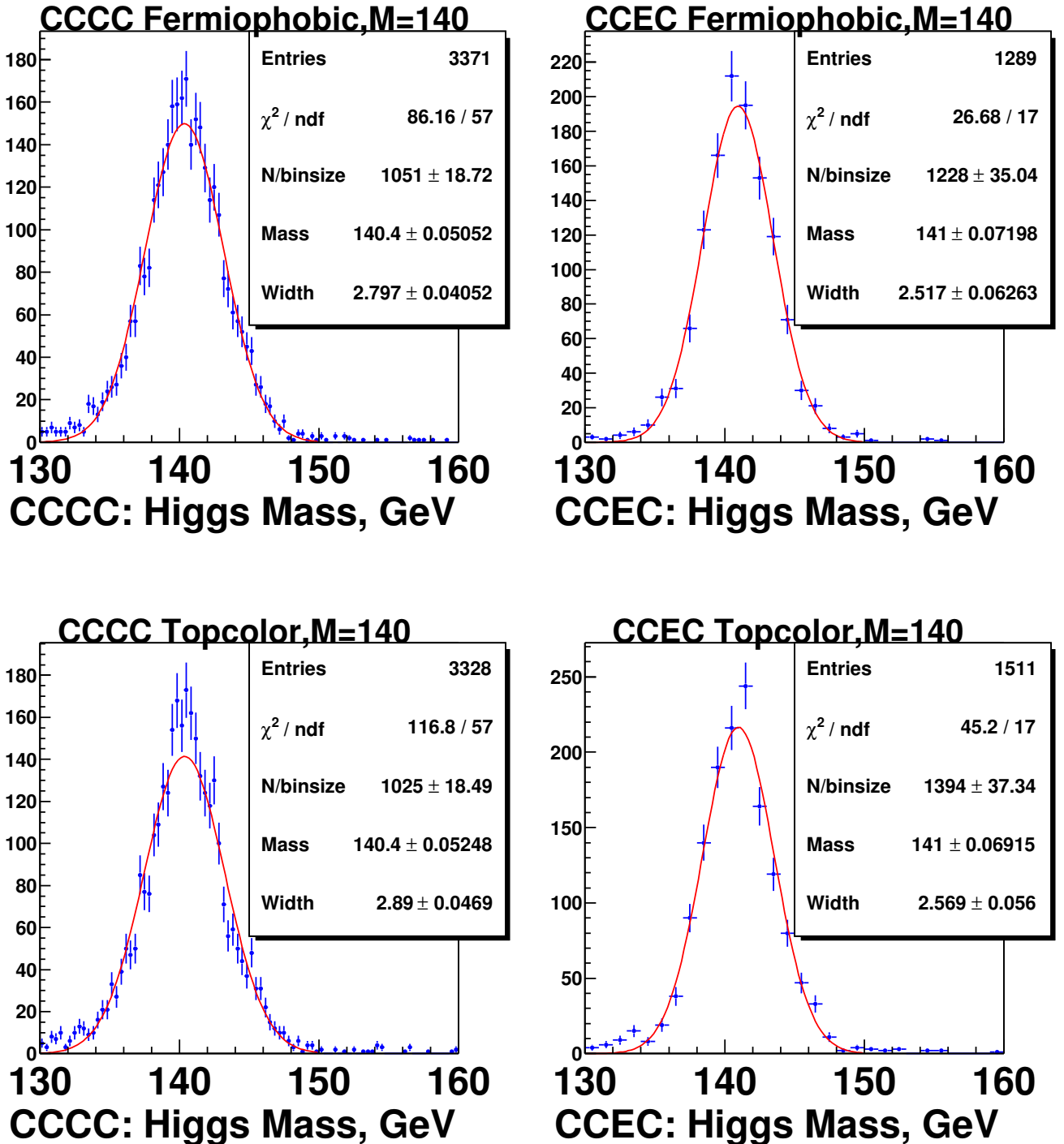


Figure 43: Fitted Higgs mass and width for $M_h = 140$ GeV.

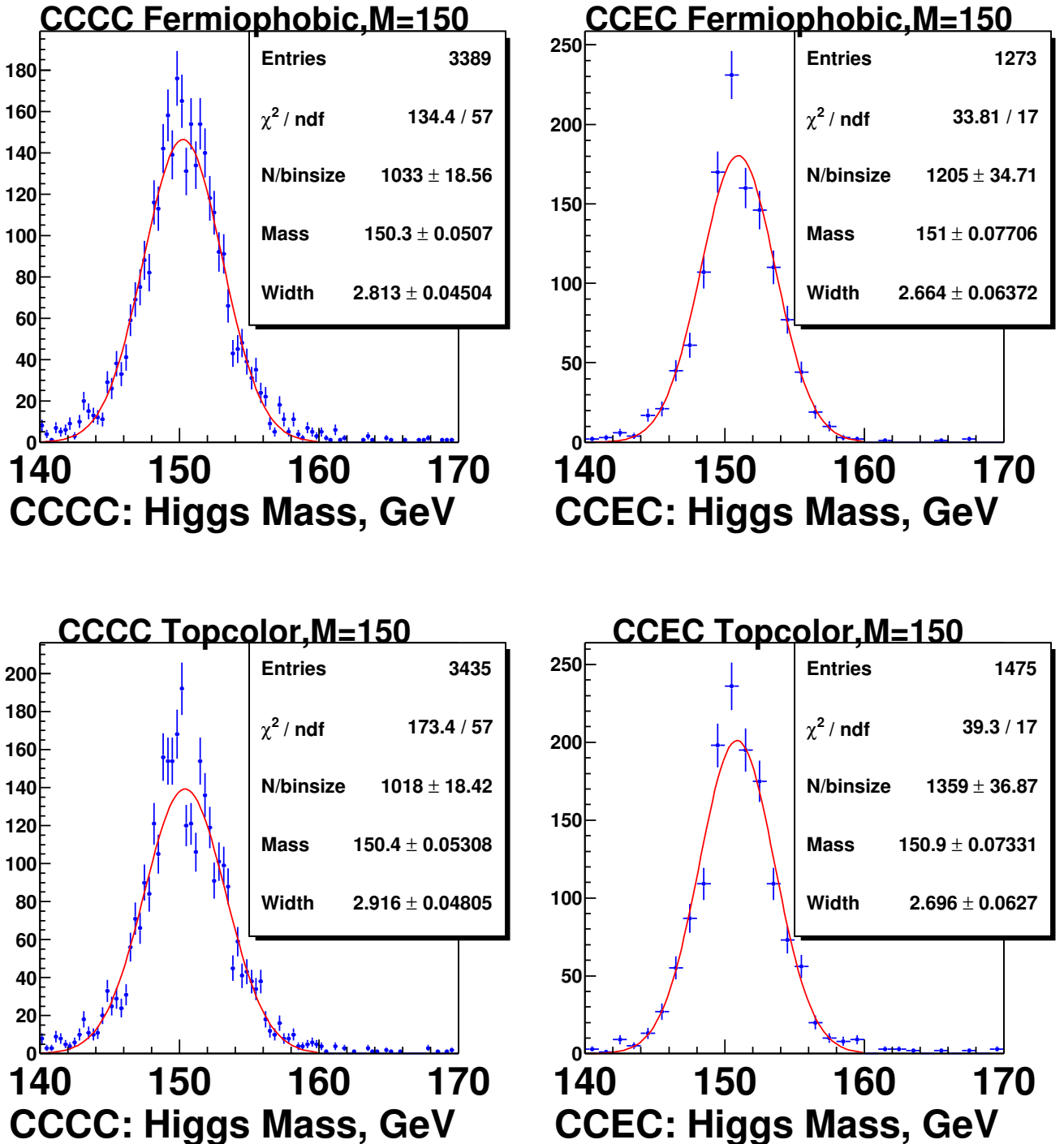


Figure 44: Fitted Higgs mass and width for $M_h = 150$ GeV.

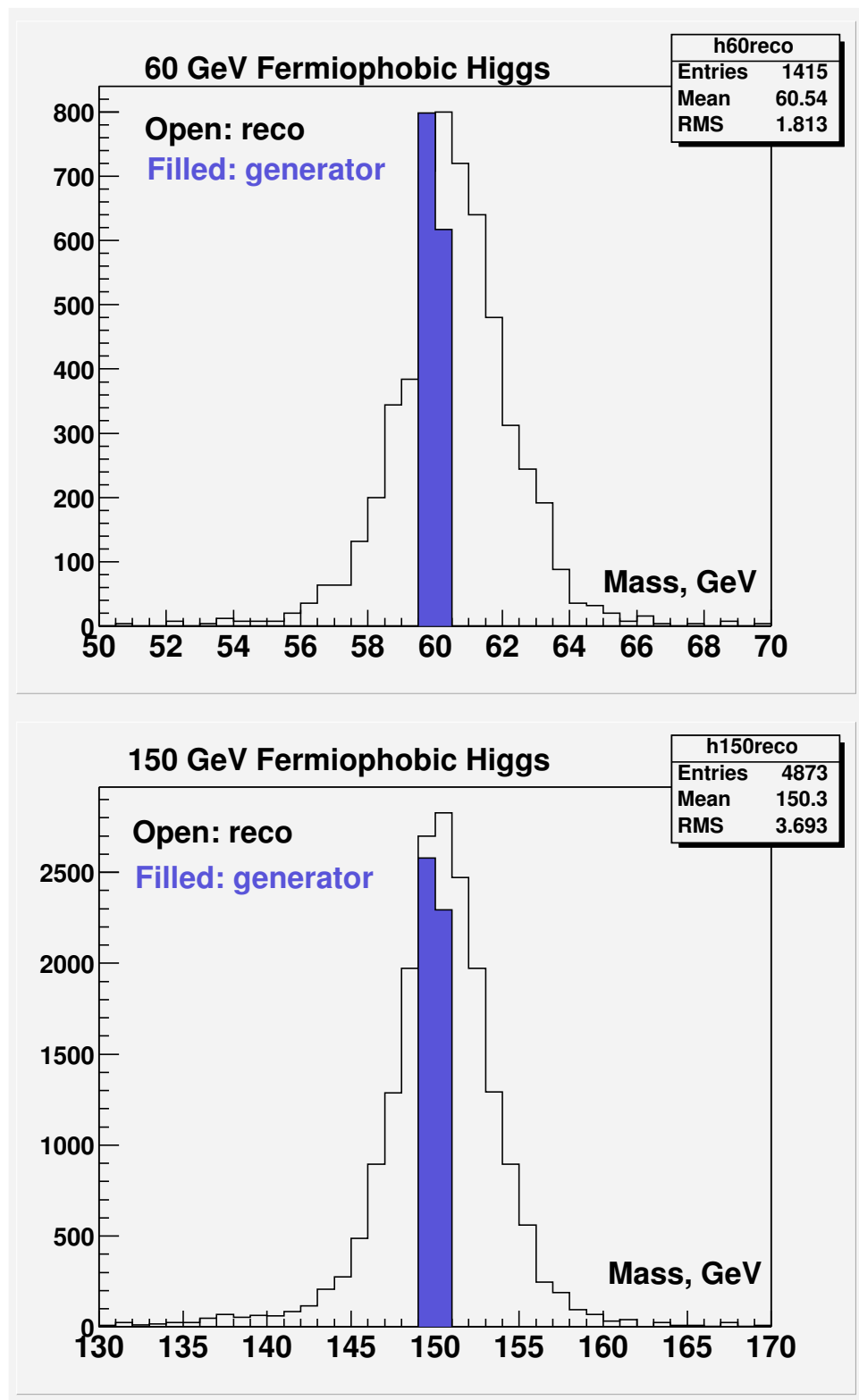


Figure 45: $h \rightarrow \gamma\gamma$ mass peak. Top: 60 GeV fermiophobic Higgs. Bottom: 150 GeV fermiophobic Higgs Filled Histogram – natural width. Open histogram – reconstructed width.

This is for Appendix on $Z(\text{pvtx})$

This appendix describes the studies of asymmetry in Z location of the primary vertex (pvtx). As shown in Figure 26 of section XXXXXXXXXXXXXXXXXXXXXXXXXXXXXXXXX there seems to be an excess of diphoton events with negative Z(pvtx) relative to positive Z(pvtx) events in CCEC. At the same time, ECEC events show excess of positive Z(pvtx). Figure 26 also shows (solid red line) that for the diLooseEM sample (of 1000 times larger statistics) the Z(pvtx) distributions are symmetric. Our goal is to make sure that such asymmetries in diphoton events result from fluctuations, the significance of which would lessen if we do not split the sample in three topology-based subsamples (or find a definite statistics-unrelated cause which would be expected to generate asymmetries for CCEC and ECEC events in opposite directions)

First of all we make sure that the observed patterns in the Z location of the primary vertex (pvtx) are not produced(enhanced) by "bad" data quality runs. Z(pvtx) distributions with bad runs included/removed are shown in Figs. 46, 47, and 48:

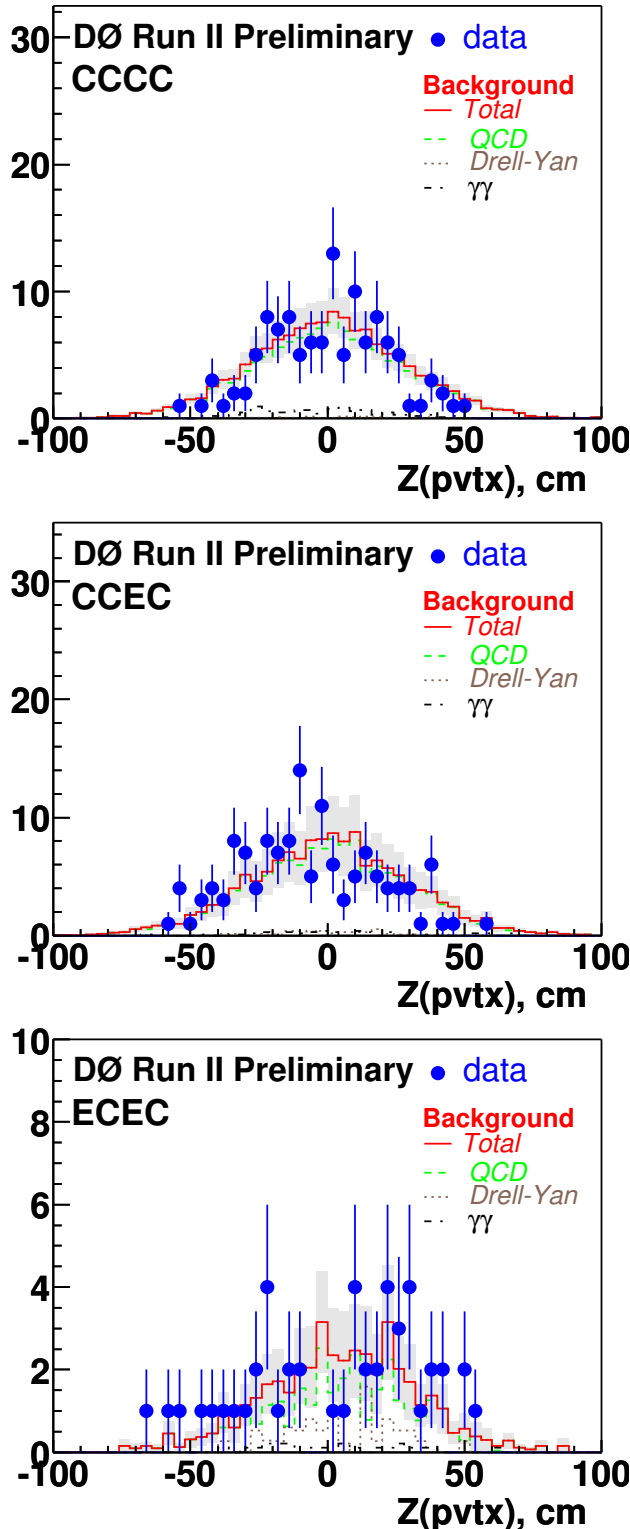
- bad CFT and bad SMT runs are removed – Figure 46;
- bad CFT, SMT, Calorimeter, and Jet/MET runs(lbns) are removed – Figure 47;
- full data sample (same plots as in Figure 26) – Figure 48.

All of the three run selections show the same asymmetry pattern. Therefore it is not related to bad runs.

Next, we look at η location of both photons and that of a leading jet. We do this separately for events with positive Z(pvtx) and negative Z(pvtx). Figures and show η distribution for events with positive Z(pvtx) for leading and second photon respectively. Figures and show η distribution for events with negative Z(pvtx) for leading and second photon respectively. Figure show leading jet η distributions for events with positive Z(pvtx). Figure show leading jet η distributions for events with negative Z(pvtx). Within statistics, the objects (both photons and jets) tend to be on the side of the primary vertex location. No anomalies in object η distributions are observed.

Then we look at some of the track properties. We would like to make sure that there is no difference in the properties of tracks that originate on the positive side of the tracker in comparison with those that originate on the negative side. Figure 55 shows track p_T distributions while Figure 56 shows track Z, η , and 2D Z vs. η distributions. No anomalies are observed.

Finally, we look at the Z(pvtx) distribution as a function of run number (Figure 57). In particular, we are interested in comparing Z(pvtx) distributions for pre- and post(Fall 2003)-shutdown data. For the post-shutdown data the CCEC asymmetry is stronger pronounced. At the same time ECEC asymmetry in the opposite direction is stronger pronounced as well, and CCCC distribution is symmetric. Having not found a cause for Z(pvtx) asymmetries related to object topologies, run number dependence, data quality, or properties we conclude that the observed asymmetries arise from statistical fluctuations.

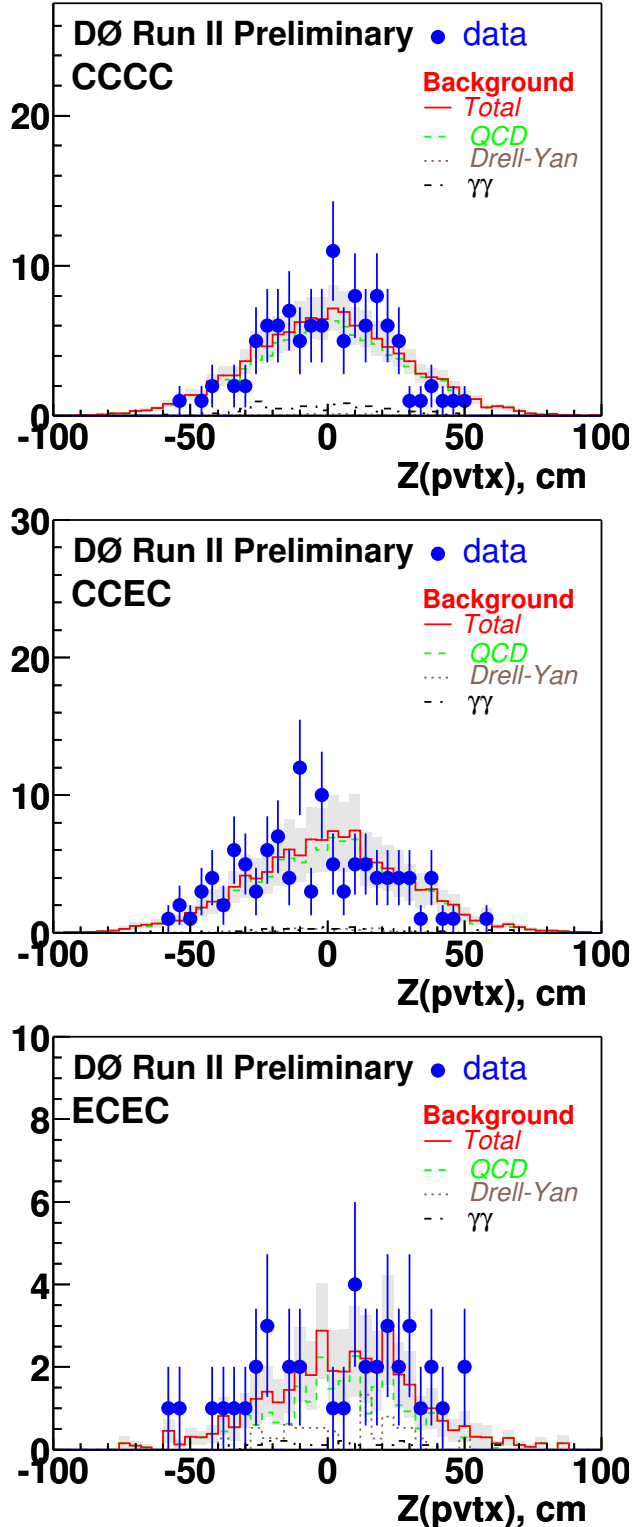


data = 117.0
bkgd = 133.9 +- 27.8
QCD = 121.4 +- 27.5
DY = 1.9 +- 1.8
 $\gamma\gamma$ = 10.6 +- 3.2

data = 136.0
bkgd = 141.8 +- 50.0
QCD = 133.0 +- 49.8
DY = 4.3 +- 4.3
 $\gamma\gamma$ = 4.5 +- 1.3

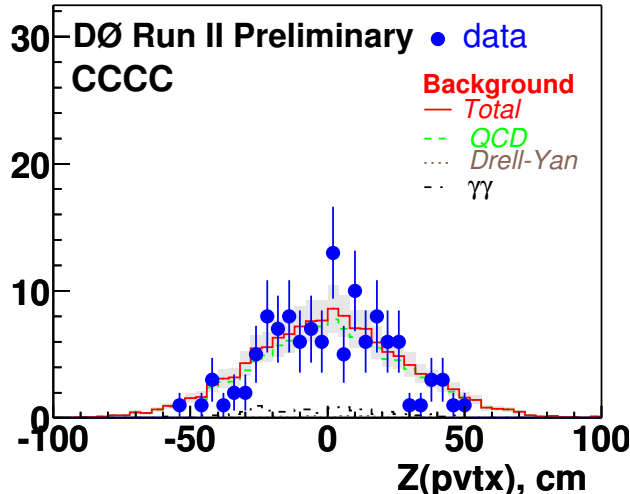
data = 48.0
bkgd = 42.8 +- 15.8
QCD = 31.2 +- 15.3
DY = 9.2 +- 4.1
 $\gamma\gamma$ = 2.4 +- 0.6

Figure 46: Z position of the reconstructed primary vertex for the case when bad (CFT, SMT) runs are removed. Points – $\gamma\gamma$ spectrum observed in data, solid (red) line – total SM background with systematic errors shown with gray rectangles, dashed (green) line – QCD background, dotted (brown) line – Drell-Yan background, dot-dashed (black) line – direct diphoton background.

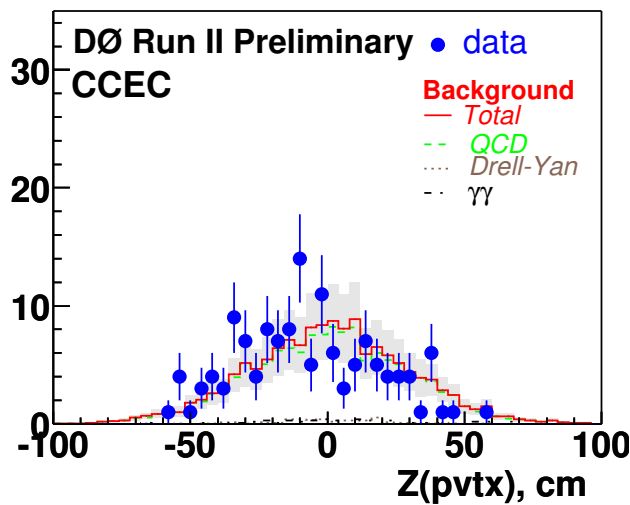


data = 105.0	
bkgd = 115.7 +/- 23.8	
QCD = 103.7 +/- 23.6	
DY = 1.5 +/- 1.5	
$\gamma\gamma$ = 10.6 +/- 3.2	
data = 111.0	
bkgd = 120.4 +/- 42.2	
QCD = 112.3 +/- 42.0	
DY = 3.6 +/- 3.7	
$\gamma\gamma$ = 4.5 +/- 1.3	
data = 39.0	
bkgd = 37.9 +/- 14.1	
QCD = 27.6 +/- 13.7	
DY = 8.0 +/- 3.5	
$\gamma\gamma$ = 2.4 +/- 0.6	

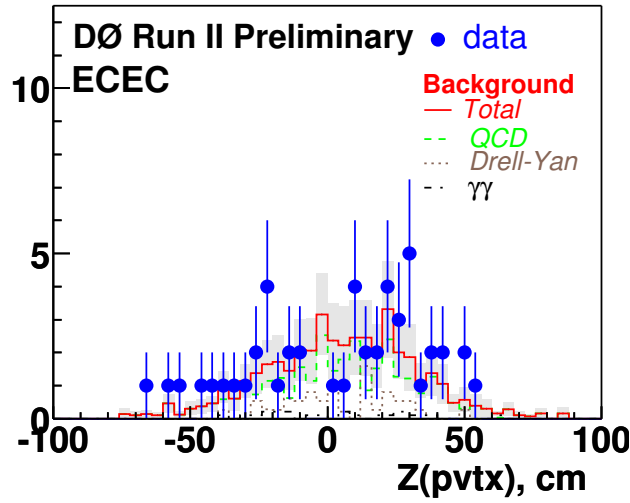
Figure 47: Z position of the reconstructed primary vertex for the case when bad (CFT, SMT, Calorimeter, Jet/MET) runs(lbns) are removed. Points – $\gamma\gamma$ spectrum observed in data, solid (red) line – total SM background with systematic errors shown with gray rectangles, dashed (green) line – QCD background, dotted (brown) line – Drell-Yan background, dot-dashed (black) line – direct diphoton background.



data = 121.0
bkgd = 135.9 +- 28.3
QCD = 123.4 +- 28.0
DY = 2.0 +- 1.9
 $\gamma\gamma$ = 10.6 +- 3.2

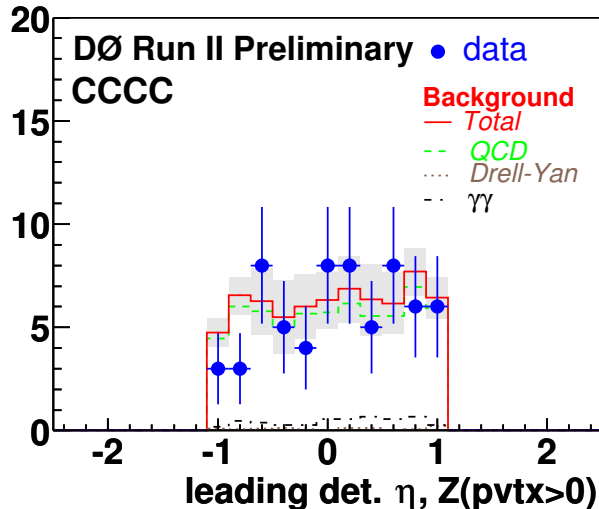


data = 137.0
bkgd = 143.7 +- 50.7
QCD = 135.0 +- 50.5
DY = 4.3 +- 4.3
 $\gamma\gamma$ = 4.5 +- 1.3

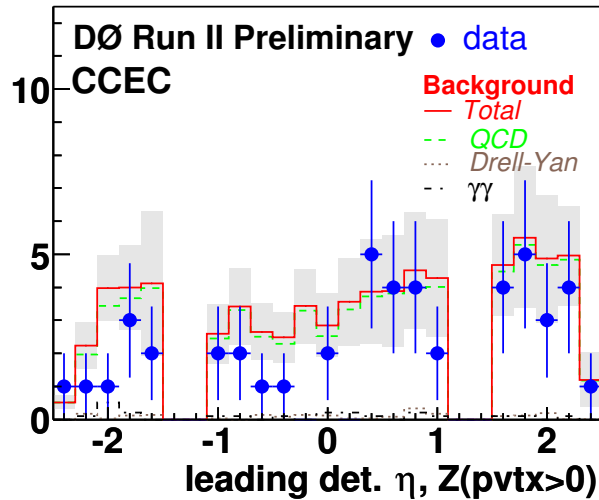


data = 49.0
bkgd = 43.3 +- 16.0
QCD = 31.7 +- 15.5
DY = 9.2 +- 4.1
 $\gamma\gamma$ = 2.4 +- 0.6

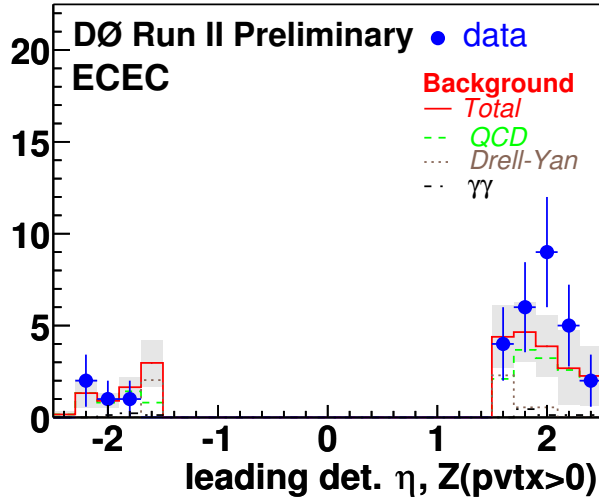
Figure 48: Z position of the reconstructed primary vertex for the whole data sample (no bad detector/ID quality runs removed). The plots in this figure are the same ones that are shown in the left column of Figure 26. Points – $\gamma\gamma$ spectrum observed in data, solid (red) line – total SM background with systematic errors shown with gray rectangles, dashed (green) line – QCD background, dotted (brown) line – Drell-Yan background, dot-dashed (black) line – direct diphoton background.



data = 64.0
bkgd = 68.9 +- 14.3
QCD = 62.8 +- 14.2
DY = 1.1 +- 1.0
γγ = 4.9 +- 1.5

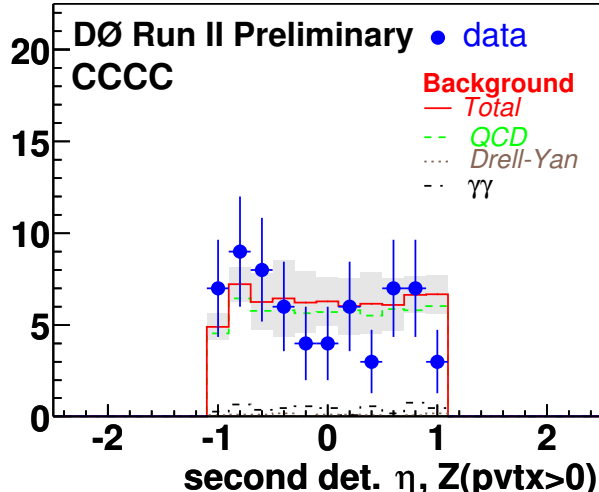


data = 48.0
bkgd = 73.6 +- 26.1
QCD = 69.2 +- 26.1
DY = 2.1 +- 2.0
γγ = 2.2 +- 0.6

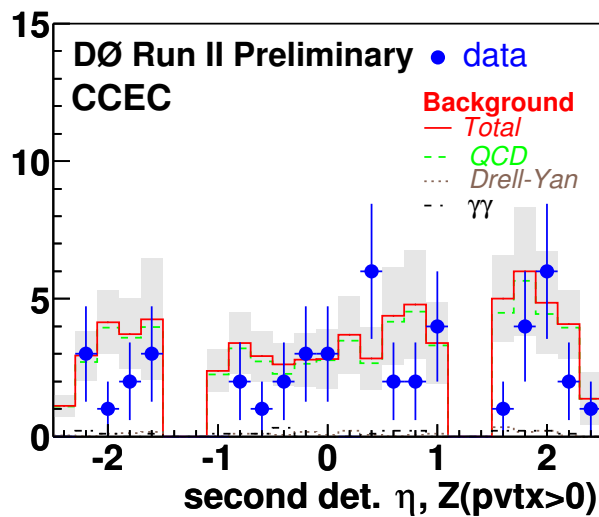


data = 30.0
bkgd = 24.8 +- 9.8
QCD = 18.2 +- 9.5
DY = 5.4 +- 2.5
γγ = 1.2 +- 0.3

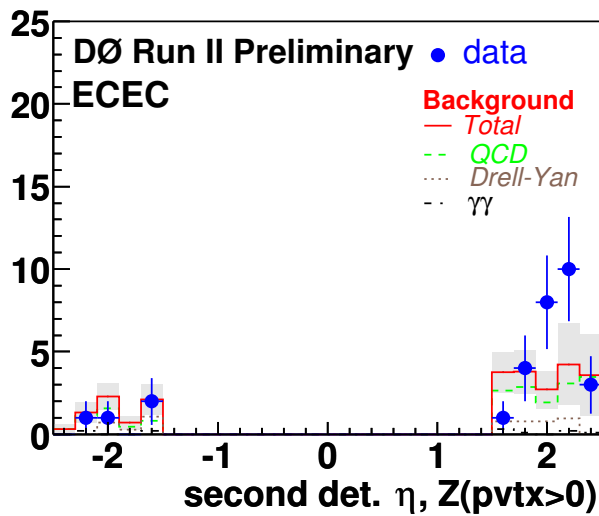
Figure 49: Leading photon detector η distributions for the case of positive $Z(\text{Primary Vertex})$ Points – $\gamma\gamma$ spectrum observed in data, solid (red) line – total SM background with systematic errors shown with gray rectangles, dashed (green) line – QCD background, dotted (brown) line – Drell-Yan background, dot-dashed (black) line – direct diphoton background.



data = 64.0
bkgd = 68.9 ± 14.3
QCD = 62.8 ± 14.2
DY = 1.1 ± 1.0
 $\gamma\gamma = 4.9 \pm 1.5$

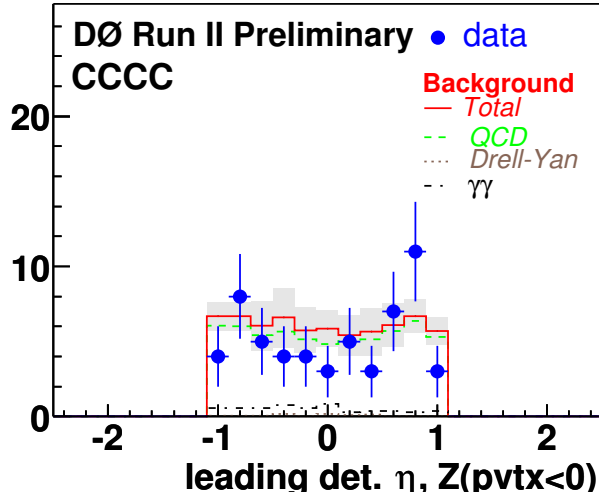


data = 48.0
bkgd = 73.6 ± 26.1
QCD = 69.2 ± 26.1
DY = 2.1 ± 2.0
 $\gamma\gamma = 2.2 \pm 0.6$

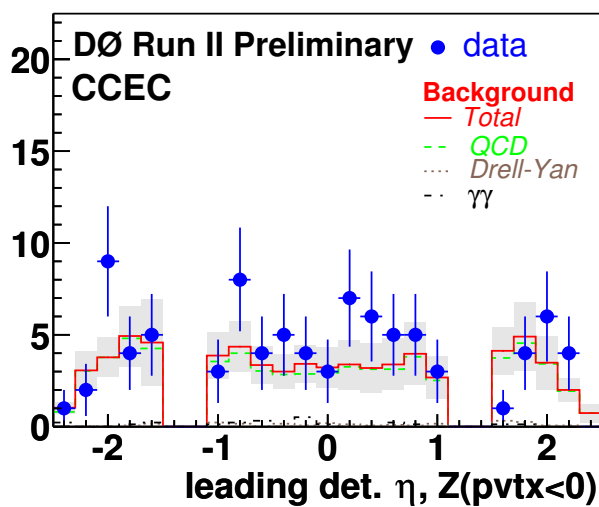


data = 30.0
bkgd = 24.8 ± 9.8
QCD = 18.2 ± 9.5
DY = 5.4 ± 2.5
 $\gamma\gamma = 1.2 \pm 0.3$

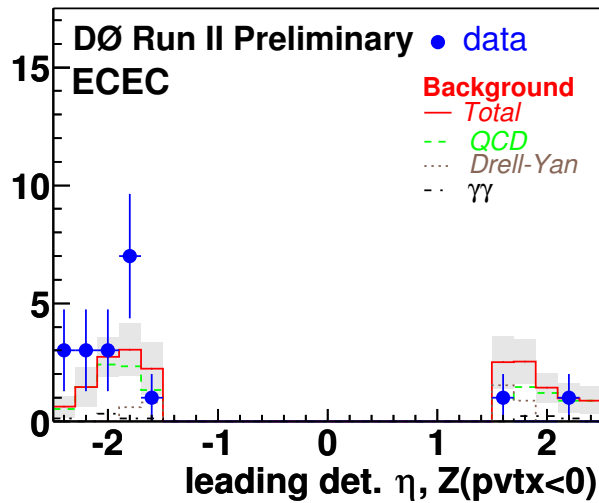
Figure 50: Second photon detector η distributions for the case of positive $Z(\text{Primary Vertex})$ Points – $\gamma\gamma$ spectrum observed in data, solid (red) line – total SM background with systematic errors shown with gray rectangles, dashed (green) line – QCD background, dotted (brown) line – Drell-Yan background, dot-dashed (black) line – direct diphoton background.



data = 57.0
bkgd = 67.2 ± 14.0
QCD = 60.7 ± 13.9
DY = 0.9 ± 0.9
 $\gamma\gamma = 5.6 \pm 1.7$

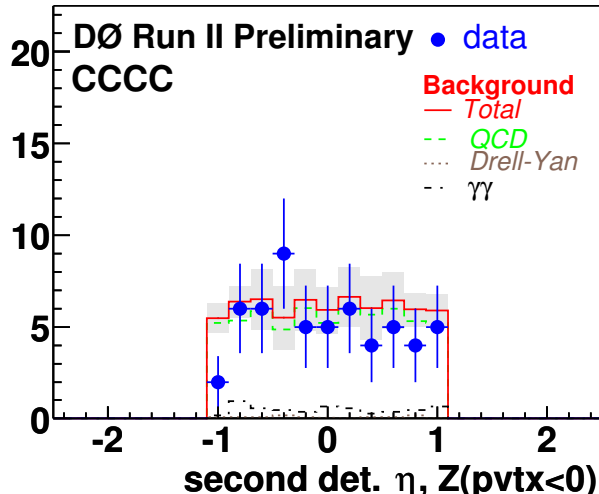


data = 89.0
bkgd = 70.4 ± 24.7
QCD = 65.9 ± 24.6
DY = 2.2 ± 2.3
 $\gamma\gamma = 2.2 \pm 0.6$

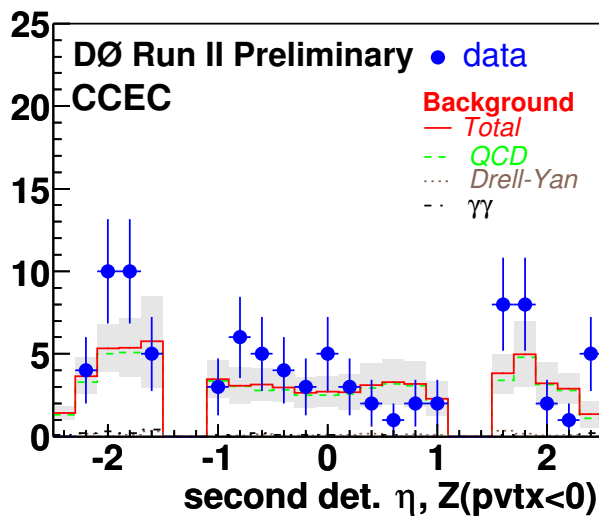


data = 19.0
bkgd = 18.4 ± 6.4
QCD = 13.4 ± 6.1
DY = 3.8 ± 1.8
 $\gamma\gamma = 1.2 \pm 0.3$

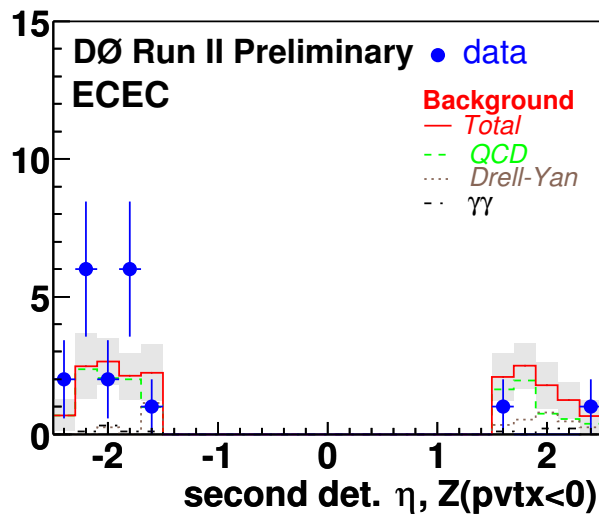
Figure 51: Leading photon detector η distributions for the case of negative $Z(\text{Primary Vertex})$ Points – $\gamma\gamma$ spectrum observed in data, solid (red) line – total SM background with systematic errors shown with gray rectangles, dashed (green) line – QCD background, dotted (brown) line – Drell-Yan background, dot-dashed (black) line – direct diphoton background.



data = 57.0
bkgd = 67.2 ± 14.0
QCD = 60.7 ± 13.9
DY = 0.9 ± 0.9
 $\gamma\gamma = 5.6 \pm 1.7$

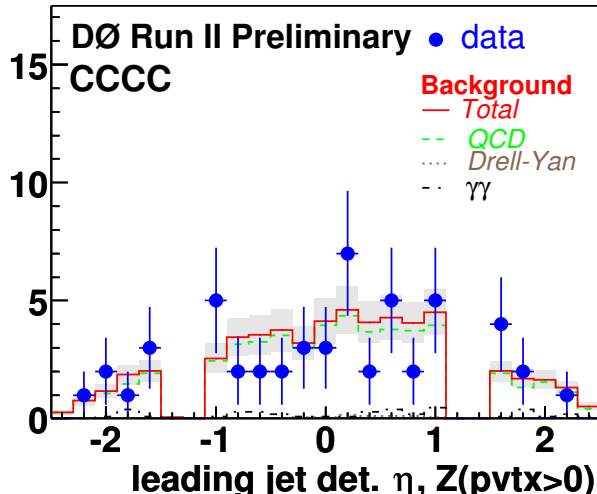


data = 89.0
bkgd = 70.4 ± 24.7
QCD = 65.9 ± 24.6
DY = 2.2 ± 2.3
 $\gamma\gamma = 2.2 \pm 0.6$

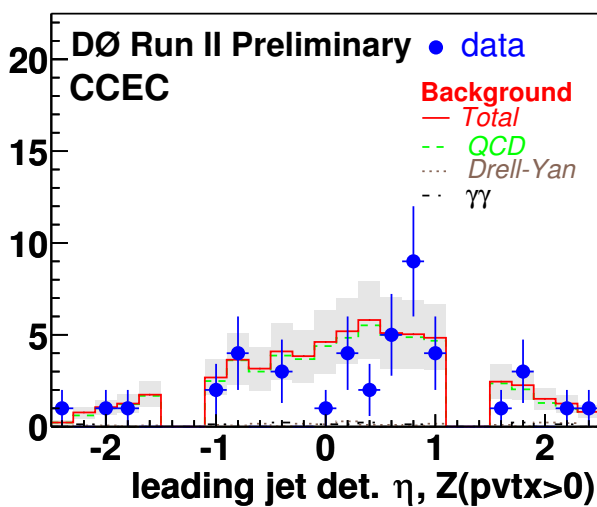


data = 19.0
bkgd = 18.4 ± 6.4
QCD = 13.4 ± 6.1
DY = 3.8 ± 1.8
 $\gamma\gamma = 1.2 \pm 0.3$

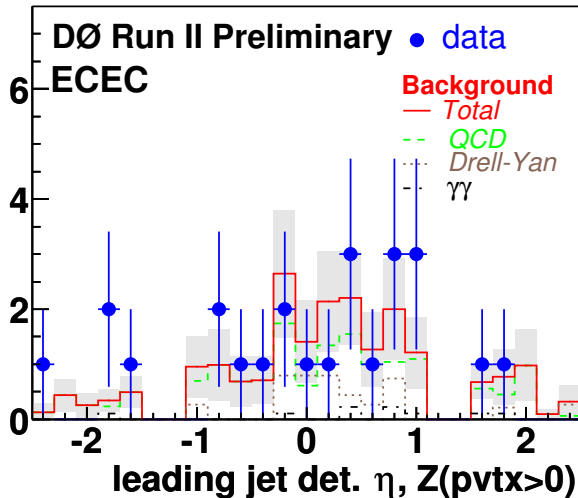
Figure 52: Second photon detector η distributions for the case of negative $Z(\text{Primary Vertex})$ Points – $\gamma\gamma$ spectrum observed in data, solid (red) line – total SM background with systematic errors shown with gray rectangles, dashed (green) line – QCD background, dotted (brown) line – Drell-Yan background, dot-dashed (black) line – direct diphoton background.



data = 52.0
bkgd = 55.4 ± 11.5
QCD = 50.7 ± 11.4
DY = 0.8 ± 0.8
 $\gamma\gamma = 3.9 \pm 1.2$

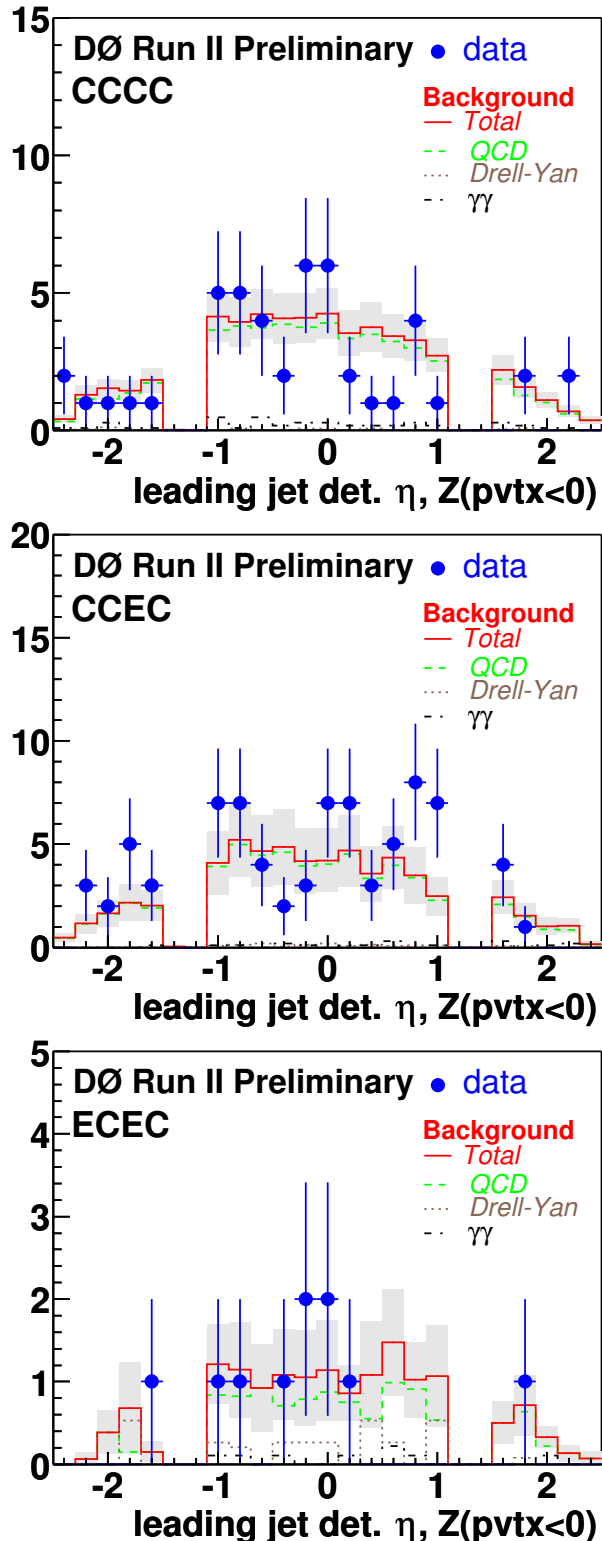


data = 43.0
bkgd = 61.1 ± 21.8
QCD = 58.0 ± 21.7
DY = 1.9 ± 1.9
 $\gamma\gamma = 1.2 \pm 0.3$



data = 24.0
bkgd = 20.7 ± 8.2
QCD = 15.2 ± 8.0
DY = 4.6 ± 2.2
 $\gamma\gamma = 1.0 \pm 0.3$

Figure 53: Leading jet detector η distributions for the case of positive $Z(\text{Primary Vertex})$. Points – $\gamma\gamma$ spectrum observed in data, solid (red) line – total SM background with systematic errors shown with gray rectangles, dashed (green) line – QCD background, dotted (brown) line – Drell-Yan background, dot-dashed (black) line – direct diphoton background.



data = 47.0	
bkgd = 54.0 +/- 11.4	
QCD = 49.1 +/- 11.3	
DY = 0.7 +/- 0.7	
$\gamma\gamma = 4.2 +/- 1.3$	
data = 78.0	
bkgd = 59.6 +/- 21.2	
QCD = 56.1 +/- 21.1	
DY = 1.6 +/- 1.8	
$\gamma\gamma = 1.8 +/- 0.5$	
data = 10.0	
bkgd = 15.1 +/- 5.3	
QCD = 11.0 +/- 5.0	
DY = 3.2 +/- 1.6	
$\gamma\gamma = 0.9 +/- 0.2$	

Figure 54: Leading jet detector η distributions for the case of negative $Z(\text{Primary Vertex})$. Points – $\gamma\gamma$ spectrum observed in data, solid (red) line – total SM background with systematic errors shown with gray rectangles, dashed (green) line – QCD background, dotted (brown) line – Drell-Yan background, dot-dashed (black) line – direct diphoton background.

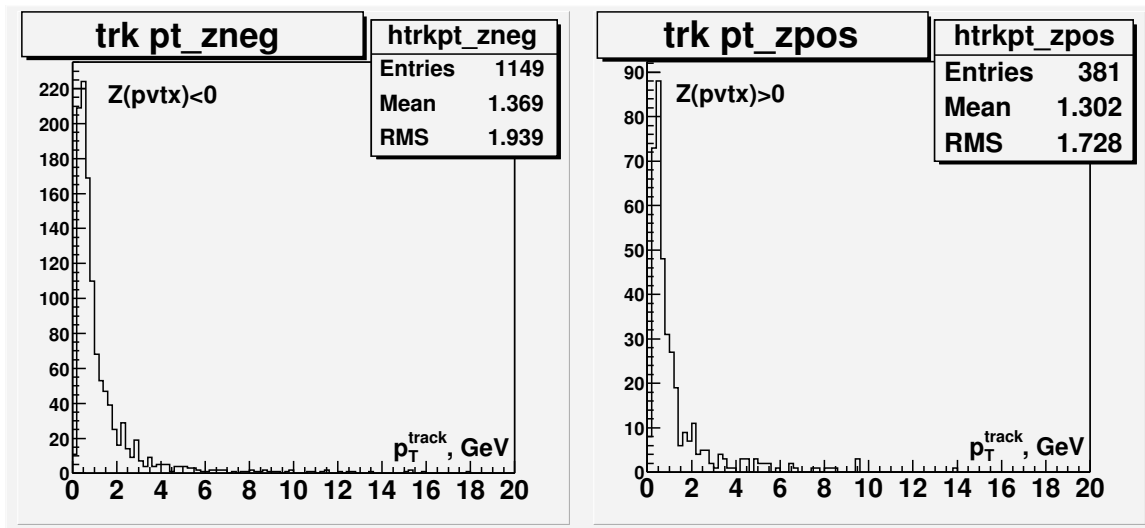


Figure 55: track p_T distributions for reduced subsample of (91 of 137) CCEC events. Left – events with negative $Z(\text{Primary Vertex})$. Right – events with positive $Z(\text{Primary Vertex})$. (91 events were picked for intermediate studies that are not included in this note, and then later the plots shown in this figure were made out of that picked sample).

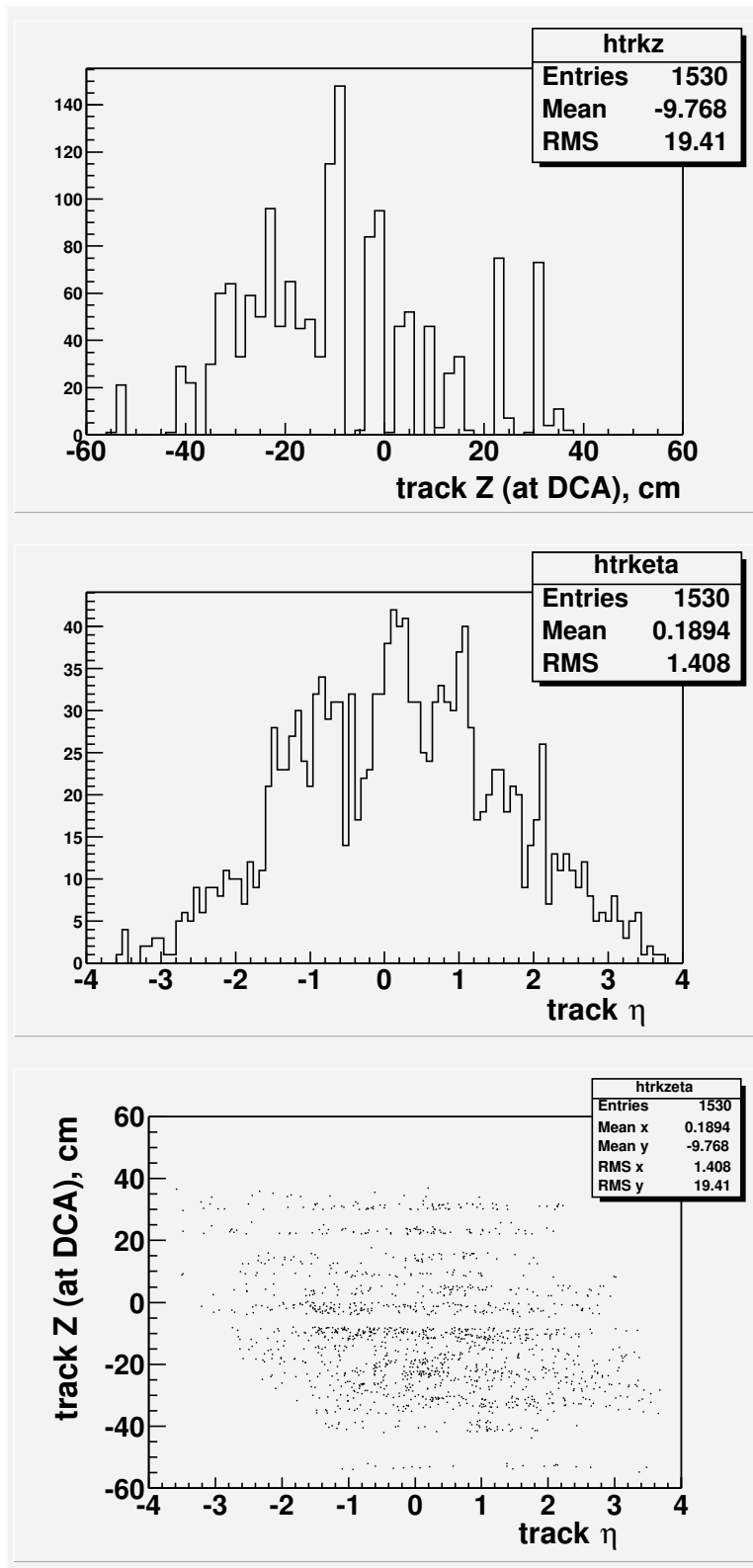


Figure 56: track Z(at DCA) (top), η (middle), and Z(at DCA) vs. η (bottom) for sub-sample of (91 of 137) CCEC events. (91 events were picked for intermediate studies that are not included in this note, and then later the plots shown in this figure were made out of that picked sample).

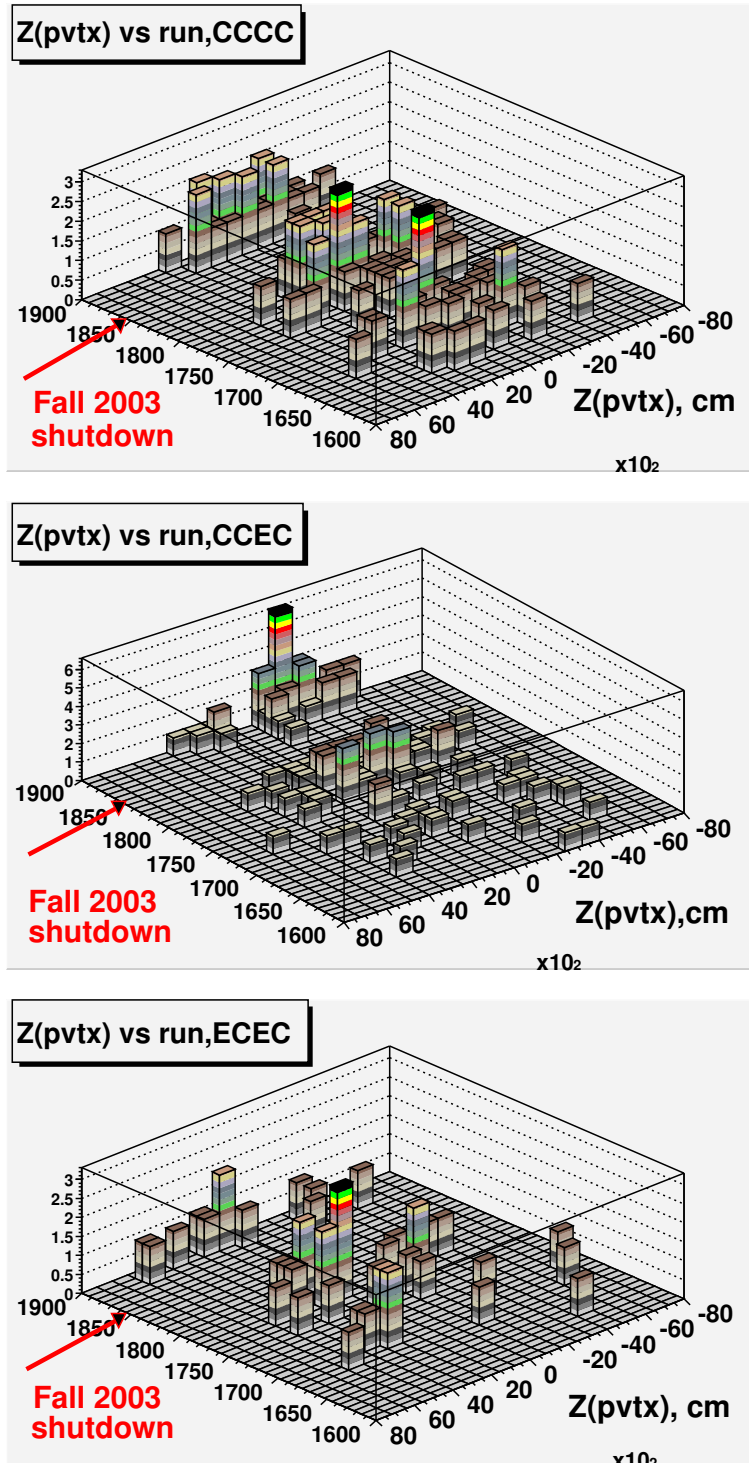


Figure 57: $Z(\text{Primary Vertex})$ vs. Run number. Red arrow indicates the division between pre- and post(Fall 2003)-shutdown data

Limits !!!

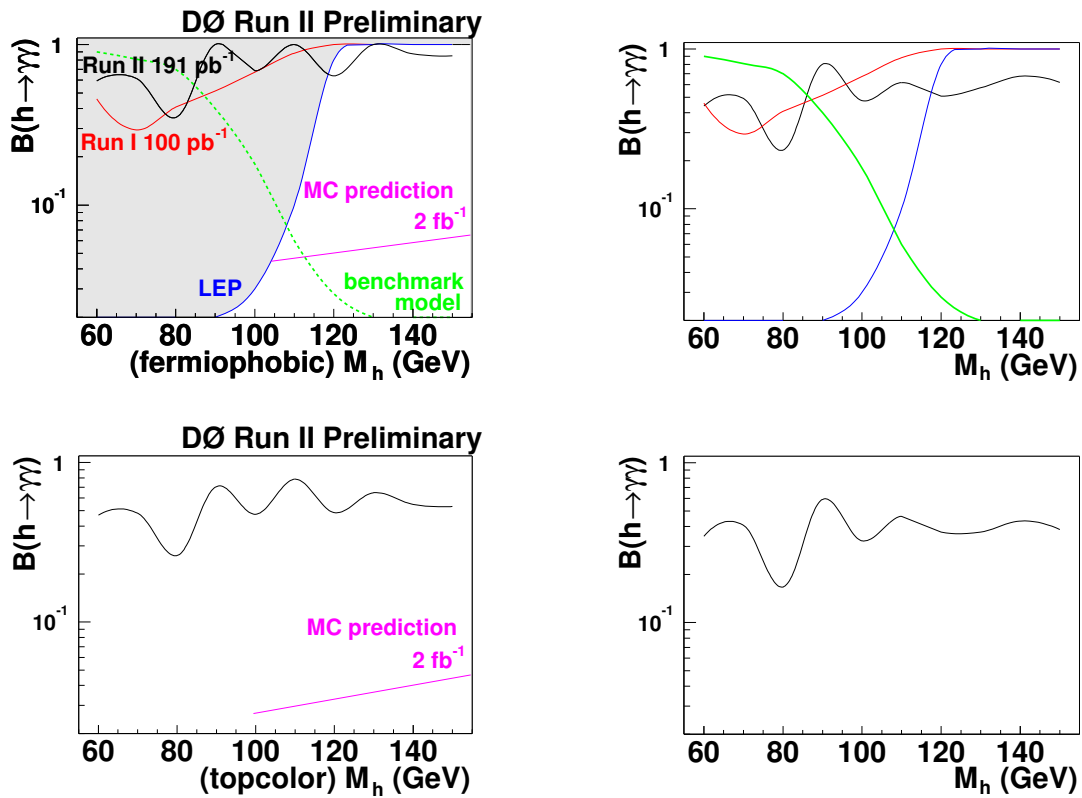


Figure 58: Limits. Left: Moriond 2004. Right: current (June 2004).